Response to the interactive comment by Referee #1:

We thank referee #1 for his or her thoughtful comments and feedback. Please find below our responses and suggestions for the manuscript revision, with the referee comments in black, our answers in red, and suggested changes and/or additions to the manuscript in blue.

This study shows the seasonal cycle of immersion-mode ice nucleating particles (INPs) in boreal forests in Finland. Since few studies have reported the seasonal cycle of atmospheric INPs in a forested site based on year-round measurements, the INP datasets presented here are unique and will be valuable for atmospheric science communities. This study also suggests that the seasonal cycle of INPs would be attributable to biogenic aerosol particles and provides two new INP parameterizations related to ambient temperature and ice nucleation active site (INAS) approach. However, since evidences to support these points are insufficient, the authors should conduct an indeep discussion based on other available datasets (e.g., meteorological data, WIBS and L-RoF-AMS data) to quantify the possible contributions of biogenic aerosol particles to INP populations. I would like to support the publication if the authors can answer the following requests/comments.

Major Comments:

1) Further detailed discussion is necessary to investigate a possible relationship between INPs and primary biological aerosol particles (PBAPs). For example, this study uses ambient temperature data as a proxy of changes of the season. As illustrated in Figure 4, it seems that the variation of INPs active at given temperatures are somewhat related to that of ambient temperatures. On the other hand, the comparison with other meteorological parameters is not performed, despite the fact that many earlier studies (e.g., Heald and Spracklen, GRL 2009; Hoose et al., ERL 2010; Huffman et al., ACP 2013; Wright et al., Aerosol Sci. Technol. 2014) have suggested that humidity would be a key factor influencing the release of PBAPs and/or INPs. In addition, as cited in the Introduction section of this paper, rain events might also be an important factor. The authors should conduct further comparison with other meteorological parameters.

We agree to the referee that correlations to other parameters may be worth considering. In fact we have already explored more than shown in the first manuscript version, but did not find strong correlations. Nevertheless, we have followed the referees suggestion and extended Figure 4 (in the new version, this is Figure 5) by including three additional panels showing the time series of relative humidity (Fig. 5c), wind speed (Fig. 5d) and precipitation (Fig. 5e) and ajusted the description accordingly. We included the following section in the manuscript:

Figure 5c shows the comparison of the INP time series with the time series of relative humidity (RH) measured 35 m above ground. Over the entire time period, no clear relationship between RH and INP concentrations is observed. For a shorter time period from June 2018 to September 2018, there seems to be some correlation of the INP concentration with the RH, during which the peaks in INP concentration in June corresponds to a RH peak. In Figure 5d, we compare the time series of INP concentrations with the time series of wind speed measured 34 m above the ground, which is also above the forest canopy. A relationship between measured INP concentrations and wind speed is not observed. In Figure 5e, the time series of INP concentration is compared to the occurrence of precipitation. Although other studies like Prenni et al. (2013), Huffman et al. (2013) and Iwata et al. (2019) report increasing INP concentrations during and after rain events in forested sites, we do not consistently observe this behavior. In this respect, increased INP concentrations are observed only during two of the strongest precipitation events in June and September 2018. However, it should be noted that in the cited studies INP concentrations were measured with higher time resolutions from minutes to hours. Huffman et al. (2013) reported increased INP and biological particle concentrations during rain events and up to one day after rain events. With our sampling (and therefore averaging)

time of 24 hours or more, rain-induced enhancements of INP concentrations may have been missed. Therefore, this type of sampling strategy may not be appropriate to deterministically link INP concentrations with rain events.

We do not exclude that the INP concentrations measured in the boreal forest are influenced by precipitation events for the whole year. However, our sampling set up is not appropriate to investigate the relationship more precisely.

2) In addition to the meteorological parameters and snow coverage/depth, the authors might need to check indicators showing the seasonal cycle of vegetation in/around the monitoring site (if available). For example, some earlier studies have used leaf are index (LAI) data as a measure of vegetation density (e.g., Heald and Spracklen, GRL 2009; Hoose et al., ERL 2010).

For our measurement site at SMEARII, the vegetation indexes NDVI (Normalized Difference Vegetation Index) and PRI (Photochemical Reflectance Index) are available, but only from 11 March 2018 to 11 September 2018. The NDVI and PRI data and the following interpretation is provided by Jon Atherton and Pasi Kolari from University of Helsinki (personal communication, October, 2020). For both vegetation indices, we calculated daily average values, which are averaged between 12:00 and 13:00 Finnish time, because the solar angle plays an important role for these indices. Unfortunately, LAI is not available. NDVI mainly tracks the development and loss of green leaf material including overstory trees and understory shrubs. We observe a trend in NDVI over the seasonal transition as the canopy slowly greens from winter to summer. During summer, when the color of the canopy does not change significantly, the NDVI remains relatively constant. The increase in NDVI in the transition period from winter to summer is observed some days later than the increase in INP concentrations. The increase in INP concentrations is nicely represented by increasing air temperature and melting snow in early April 2018 (see Figure 4), whereas a strong increase in NDVI is observed in the second half of April. It has to be considered, that the NDVI is affected by snow resulting in smaller NDVI values. The PRI measures the abundance of photoprotective pigments called carotenoids, which help the tree to deal with excess light, which is potentially harmful. We observed a PRI increase in May, which indicates a carotenoid change of the trees. A relationship to the increasing INP concentrations in April is not observed.

We do not think that these comparisons are of great benefit to the story outlined within the manuscript and have decided not to include the comparison in the paper. However, we are glad it can be made available in this publicly accessible discussion and gratefully acknowledge the support of Jon Atherton and Pasi Kolari by providing and interpreting the NDVI and PRI data.

3) After checking the points described in the above Comments 1 and 2, I would like to suggest reconsidering the INP parameterization related to ambient temperature (equation 1). I admit that this parameterization seems to successfully reproduce the INP number concentrations at this site as compared with other existing parameterizations. However, it is skeptical if this parameterization is scientifically meaningful, while it may be technically useful for reproducing only INP number concentrations near the ground level of this site. Given that this study emphasizes the possible contribution of PBAPs to INP populations, the development of parameterizations related to PBAPs and/or factors influencing the release of PBAPs would be more scientifically valuable. For example, given that previous model studies have used humidity and LAI to simulate the release of PBAPs, it might be interesting to evaluate if these parameters would also be useful for developing new INP parameterizations.

As the time series of vegetation indices available for SMEAR II do not show the same pattern as the time series of INP concentrations, and RH only correlates with INP concentrations in summer months, we do not get a better parameterization of INP concentrations using these parameters. Moreover, ground-level ambient air temperature represents the variability in measured INP concentrations better than other meteorological parameters or the vegetation indices. We are aware, that a physical mechanism that could explain this behavior remains unclear and that this parameterization is only empirical. We report this relationship simply as an observation and provide a description that technically describes INP concentrations quite well in this environment. We also see this result as a motivation for further studies and measurements regarding these findings.

4) As for the datasets during the HyICE-2018 campaign, the WIBS data would be potentially powerful, because these data might be useful as an indicator of biogenic aerosol particles. Unfortunately, however, the explanations and discussion on these data are insufficient. The authors should add detailed explanations and discussion regarding the WIBS data. For example, the WIBS has multiple channels as illustrated in Figure A2, but I could not find any detailed explanations and discussion about these data in the main text. I assume the categorization, such as FL1, FL2, and FL3, is based on Savage et al. (AMT, 2017). If so, the authors should clarify the source of this definition and then clearly explain the characteristics of each channel provided in Figure A2 (for example, what materials are expected to be detected using FL1, FL2, FL3, and their combinations?). In addition, the authors may need to discuss what channel was most sensitive to the variations of INPs.

Thanks for this comment. We agree that a more detailed description of the WIBS instrument and a more thorough discussion of the WIBS data is important to underpin the results of this study. Therefore, we have added a more detailed description of the WIBS instrument to Section 2.3. "Additional Instrumentation at SMEARII", which addresses the question and suggestion about the WIBS and also addresses the associated comments of the other referees.

The WIBS-NEO (Droplet Measurement Technologies, Longmont, CO, USA) is a bioaerosol sensor that provides information on the fluorescence properties, size and asphericity ratio of individual aerosol particles. It operates with an inlet flow of 0.3 l min^{-1} and detects particles with diameters between 500 nm and 30 µm. From 11 March 2018 to 2 April 2018, the WIBS was located about 50m from the aerosol filter sampling line used for the INP analysis. There, it was attached to a total aerosol inlet, which is characterized in Vogel (2018). On 3 April 2018, the WIBS was moved and installed directly next to the filter sampling line and attached to a PM10 inlet, which is described in Schmale et al. (2017). For the WIBS data analysis, particles from 0.5 µm to 10 µm were considered. To analyse the fluorescence of the particles, the WIBS sensor utilizes two xenon flashlamps as excitation light sources (optically filtered at wavelengths of 280 nm and 370 nm) and two emission detection channels (wavelength bands 310 – 400 nm and 420 – 650 nm). Optical size information is acquired utilizing elastic scattering from a continuous wave laser with a wavelength of 635 nm and a photomultiplier tube located orthogonally with respect to the laser. The excitation pulses are fired into the sample volume at different times and both detection channels record the emission(s) from both excitations, leading to three distinguishable excitation-emission combinations (the 370 nm light saturates the 310 – 400 nm detection channel and therefore does not provide any information). Thus, the fluorescence can be divided into 7 unique fluorescence groups based on the excitation-emission wavelength pairs and their combinations, after Perring et al. (2015) and Savage et al. (2017): A (only FL1: excitation 280 nm, emission 310 – 400 nm), B (only FL2: excitation 280 nm, emission 420 – 650 nm), C (only FL3: excitation 370 nm, emission 420 – 650 nm), AB (FL1 + FL2), BC (FL2 + FL3), AC (FL1 + FL3) and ABC (FL1 + FL2 + FL3).

The WIBS performs an empty-chamber background signal check every 8 hours, during which the excitation pulses are fired into the optical chamber without any present particles. The background check collects a multitude of emission intensities that form a baseline for particle fluorescence. In this study, a particle is considered fluorescent, if the associated emission peak intensity is larger than $FT + 9\sigma$. FT is the mean value of the forced trigger intensities and σ is their standard deviation.

A more commonly used method would be to compare the emission peak intensity to $FT + 3\sigma$. However, some non-biological particle types such as wood smoke, African dust and black carbon are weakly fluorescent and therefore might satisfy the lower threshold value, leading to an overestimation of biological particle concentration. Furthermore, the stricter threshold only marginally affects the detection efficiency of biological particles, because they tend to have stronger fluorescence (Savage et al., 2017). More detailed descriptions on the WIBS are also available in Savage et al. (2017) and Perring et al. (2015).

We also added the following text to the description on Figure 4 (old Figure 3b) to Section 3.2 Comparison to meteorology and aerosol properties to explain the characteristic of the different excitation-emission wavelengths pairs:

The time series of the number concentration of particles with a fluorescence signal in other fluorescence groups is shown in the Appendix in Fig. A2. In this Figure, the strongest seasonal increase in the transition period from winter to summer is observed in the group ABC. Consequently, this fluorescent group correlates best with the measured INP concentrations (see Figure 4). The characteristics of each fluorescence group are comprehensively investigated and reported in Savage et al. (2017), who examined the fluorescence emissions of different types of pollen, fungi, bacteria, biofluorophores, dust, HULIS (humic-like substances), PAH (polycyclic aromatic hydrocarbons), soot and brown carbon. Using the $FT + 9\sigma$ threshold for defining a particle as fluorescent, nearly all dust and HULIS types show no fluorescence signal at all. Some of the soot and brown carbon types only show weak signals in A, and B, BC and A, respectively. Nearly all of the bacteria types show fluorescence only in group A. The fluorescence of fungal spores are also mainly detected in group A, but also in AB and ABC. The investigated biofluorophores show mainly fluorescence in the groups BC (Riboflavin, NAD), A (Pyridoxamine), AB (Tryptophan) and ABC (Ergosterol). PAHs show fluorescence mostly in groups ABC and A. Finally, most pollen types show fluorescence in groups ABC and AB. Some pollen types also show a fluorescence signal in groups A and B.

We have also modified the discussion on the comparison of WIBS data to INP in the same Section as follows:

Such a correlation is also supported by the peaks of pollen and PBAP concentrations observed in snow-free periods in spring and in autumn, and by the increases of the organic aerosol mass concentration and fluorescent particle numbers of group ABC observed in spring. According to the study of Savage et al. (2017), we assume particles of fluorescence group ABC to be mainly pollen, particles containing PAH or Ergosterol, or fungal spores. ~~Fluorescent particles are expected to be primarily of biological origin except for a few percent, which could arise from non-biological materials (Pöhlker et al., 2012; Savage et al., 2017).~~

As was suggested by Savage et al. (2017), we have also introduced the categorization of fluorescence groups using A, B, C, AB, BC, AC, ABC instead of FL1, DL2, FL3, FL1+FL2, FL2+FL3, FL1+FL3, FL1+FL2+FL3, as this appeared to be less confusing. We changed the legend of Fig. A2 accordingly.

5) The explanations on the L-RoF-AMS data are also insufficient. The authors should briefly explain what kinds of organics were measured using the L-RoF-AMS and how they obtained organic mass concentrations presented in Figure 3.

Thanks for the comment. We agree that the description and discussion of the L-Tof-AMS needs to be more detailed and precise. We have added a more detailed description of the L-ToF-AMS instrument to Section 2.3. "Additional Instrumentation at SMEARII", which addresses this comment and also the associated comments regarding the L-Tof-AMS description from other referees:

The size-resolved chemical composition of ambient aerosol was measured with the L-ToF-AMS. Its application in the same campaign has been described in Paramonov et al. (2020). It builds on the functionality and characteristics of the high-resolution ToF-AMS (DeCarlo et al., 2006). However, due to the longer time-of-flight chamber, the L-ToF-AMS, has a better resolution (8000 M/ΔM) than the standard ToF-AMS (2000 M/ΔM in V-mode). Detailed descriptions of the instrument, measurements and data processing are available in other publications (Canagaratna et al., 2007; DeCarlo et al., 2006). In general, the L-ToF-AMS measures the size-resolved, non-refractory composition of submicron aerosols, including organic, sulfate, nitrate, ammonium and chloride. The aerodynamic lens has a 100% transmission range of 75-650 nm (in vacuum aerodynamic diameter; Liu et al. (2007)) and focuses particles into a narrow beam that impacts the surface of a porous tungsten vaporizer heated to 600°C, followed by ionization by a 70eV electron source. Ions are detected by a long time-of-flight mass analyzer (Tofwerk AG). The sample flow of 0.09 l min^{-1} is extracted from an extra suction flow (3 l min^{-1}) that is used to avoid aerosol losses in the inlet line. A PM2.5 cyclone mounted at the inlet removes large particles to avoid clogging the critical orifice (100µm), and before entering the L-ToF-AMS, the samples are dried by a Nafion dryer to keep the RH below 30%.

The L-ToF-AMS data were analyzed using standard ToF-AMS data analysis toolkits (Squirrel V1.61B and PIKA1.21B) using Igor Pro software (V6.37, WaveMetrics Inc.). To calculate mass concentrations an ionization efficiency (IE) was determined using 300 nm, size-selected, dry ammonium nitrate particles, and a relative ionization efficiency (RIE) for ammonium of 3.7 was determined. The default relative ionization efficiency (RIE) values of 1.1, 1.2, 1.3 and 1.4 for nitrate, sulfate, chloride and organics, respectively, were applied. A composition-dependent collection efficiency (CE) was applied based on the principles proposed by Middlebrook et al. (2012).

We have also added the following text to the discussion of Figure 4 (old Figure 3b) in Section 3.2 "Comparison to meteorology and aerosol properties."

The non-refractory organic components measured by the AMS include the commonly observed primary organic aerosol (POA) and oxygenated organic aerosol (OOA).

Specific Comments:

6) I could not find any descriptions of the objective of this study in the Introduction section. I thought that most sentences in the first paragraph of the Methods section (Lines 75-88) should be included in the Introduction section.

We agree that the manuscript would benefit from a stronger definition of the objectives of this study – thanks for this comment. We add the following text to the introduction:

The main objective of this study is to investigate and describe the variability and seasonal trends in INP concentrations and INP temperature spectra in a boreal forest environment. The absence of anthropogenic and/or dust aerosol sources in the boreal region motivates the additional

investigation of biogenic ice nucleation activity and reveals the relevance of boreal forest areas as an important INP source. The comprehensive instrumentation provided at the measurement site at the SMEARII station allows comparisons between INP measurements with simultaneous measurements of many meteorological variables. These measurements are complemented by measurements characterizing the sampled aerosol number concentrations, size distributions and chemical compositions in order to elucidate the potential origin and nature of the INPs. Heat treatments of the suspensions prior to INP analysis also help identifying the nature of INPs. We aim to improve the parameterizations describing atmospheric INP concentrations in the boreal forest by considering seasonal dependences in the formulations. Finally, this study provides motivation for further continuous long-term studies of INP in different environments across the globe.

In addition, we have shifted the description of the SMEARII station from the Methods to the Introduction, as the referee suggested.

7) Sections 2.1: What is the top height of the inlet? It is also important to provide the information on vegetation of the SMEARII site (e.g., tree canopy heights, dominant vegetation types) and the difference of the heights between the inlet and canopy.

For the top height of the inlet of the aerosol sampling line, we added the following sentence to Section 2.1 "Aerosol filter sampling":

The inlet height is approximately 4.6 m above ground and therefore approximately 17.2 m below the forest canopy.

Concerning the dominant vegetation species and canopy height, we have added the following information to the introduction into the description of the SMEARII station:

The boreal forest around the SMEARII station is dominated by Scots pine trees (Hari and Kulmala, 2005). In summer 2018, the canopy height of pines at SMEARII was determined to be 21.8 m.

8) Line 189 (and Figure 3): What is the definition of snow coverage? Where and how was the snow coverage measured?

We have added the following explanation to Section 3.2 "Comparison to meteorology and aerosol properties" to explain the definition of snow coverage applied here:

We have defined snow coverage as measured snow depth > 1 cm, where snow depth was measured by a Jenoptik SHM30 snow depth sensor, which is based on an opto-electronic laser distance sensor, in open field about 500 m southeast of the aerosol collection area of SMEARII.

9) Line 190: The authors would need to briefly explain about how pollen and other PBAPs reported by Manninen et al. (2014) have been measured at the SMEARII site.

We have added the following explanation to Section 3.2 "Comparison to meteorology and aerosol properties" to explain the measurements of PBAP in Manninen et al, 2014:

Manninen et al. (2014) collected aerosol samples in a Hirst-type volumetric spore trap (Burkard Manufacturing Co. Ltd.; Hirst, 1952), located at SMEARII 3 m above the forest canopy. The trap is driven by a clockwork and collects aerosol particles larger than approximately 3 µm on an adhesive, transparent, plastic tape with a sampling flow rate of approximately 10 l min^{-1}. The analysis of the collected particles was performed according to standard methodology adopted by the Finnish pollen

information network and following the principles of the European Aeroallergen Network (www.polleninfo.org/) and Rantio-Lehtimäki et al. (1994).

10) Line 208 (and Figure 4b): What is the definition of snow depth? Where and how was the snow depth measured?

See answer to Comment 8.

11) Figure 1: The size of numbers in x-axis and y-axis are too small.

We have increased the size of the axis description in Figure 1.

12) Figure 3a: What is the unit of y-axis? As for pollen and PBAP data, since pollen is a kind of PBAPs, I think these should be treated as "pollen" and "other PBAPs". Also, since the pollen and other PBAP data were obtained in 2003/2004, these data should not be included in Figure 3a. I would like to suggest making another figure if they want to show the pollen and other PBAP data in 2003/2004.

We thank the referee for this suggestion. The units for PBAP and INP concentrations has been added (m^{-2} and std l^{-1}, respectively). The fraction of NPF event days has no unit. The legend was changed from "PBAP" to "other PBAP". To improve the comparison of data measured in different years, the x-axis labels were adjusted by removing the year(s) and instead the corresponding years are shown in the legend. Now, the presentation of pollen and PBAP data from 2003/2004 together with INP, NPF and snow data from 2018-2019 should be improved. We think it is useful to have this data in one panel, as we focus on general seasonal trends and not on quantitative values measured in specific years. Other improvements to this Figure has been done considering other referee comments.

13) Figure 3b: What is the unit of y-axis? What is the source of fluorescent particles in this figure? I guessed that it would be the same as "all" in Figure A2 according to a description "all three lase-channel combinations of WIBS" in the main text (lines 205- 206). However, these curves in Figures 3b and Figure A2 seems to be quite different. Please clarify this point (see also Comment 4).

We did not use "all", but "FL1+FL2+FL3" (group ABC), which agrees with the curve in Figure A2. We have now completely modified the Figure. For details see answer to comment 14) below. A complete comparison, including aerosol number concentration and surface concentration is too much for a single panel, and thus we prepared a separate Figure including several panels showing INP concentrations compared to ABC fluorescent particle concentration, mass concentrations of organics, PM10 number concentration and PM10 surface concentration (see new Figure 4). We have added corresponding units to the axis labels, where they were missing.

14) Figure 3b: I would like to suggest including the data on the number and/or surface area concentrations in PM10 (the data in Figure A1) during the HyICE period in this figure. Then, the authors should discuss if the variations of INPs are indeed related to organics and fluorescent particles, rather than PM10 particles.

Thanks for this suggestion. Continuing from above in the new Figure 4 panel (a) shows a comparison of INP concentrations to ABC fluorescent particles, panel (b) to organic mass concentrations, panel (c) to PM10 number concentrations and panel (d) to PM10 surface concentrations.
We have added additional description to Section 3.2. "Comparison to meteorology and aerosol properties:"

Both, the organic aerosol mass concentration measured by the L-ToF-AMS and the number concentration of fluorescent particles measured by WIBS, tend to increase during the transition

period from winter to summer (Fig. 4a and b). The number concentration of atmospheric PM10 aerosol presented in Fig. 4c does not show this trend. However, a slight seasonal trend is visible in the PM10 surface concentration (Fig. 4d).

We have also added a short discussion of the previous observation later to the same Section:

As the surface concentration of PM10 particles is more sensitive to larger particles, the increase in PM10 surface concentration (see Fig. 4d) indicates that the observed seasonal increase may be due to larger particles, which are expected to be mainly of biogenic origin.

15) Figure 6d: How did the authors apply the parameterization by Ullrich et al. (2017)? Did they measure the surface area concentrations of mineral dust particles at this site? Or did they simply apply this parameterization to the measured total aerosol surface area concentrations in PM10? Please clarify this point.

The parameterization of Ullrich et al. (2017) for the INAS density of mineral dust is only temperature dependent. Therefore, for the application of this parameterization, we only used the activation temperatures in the Ullrich et al. (2017) formulation. When we established a new parameterization for the INAS densities of the measured boreal forest INPs (see Eq. (2)), we used the same exponential relation of INAS density and activation temperature as suggested in Ullrich et al. (2017). For calculating the INAS densities used to establish this new parameterization, the PM10 surface area concentrations measured by APS/DMPS including all atmospheric aerosol particles were used.

16) Figure A1a: I could not understand how to see this figure. What do the authors mean by "percentage deviation"? Please clearly explain the meaning of this word.

Thanks for this comment. The old Figure A1a was meant to explain and show the difference in percent between the number/surface concentration of total aerosol and PM10 aerosol. As the Figure seems to be more confusing, we decided to remove this Figure and just describe in the text that the difference between total aerosol and PM10 aerosol is lower than 1% (line 151, revised manuscript). The old Figure A1b was separated into two panels and compared to INP concentration at 257 K in the same way as meteorological parameters are compared to INPs and are now the new Figure A1.

We referred to the new Figure in Section 3.2 “Comparison to meteorology and aerosol properties,” as follows:

The number and surface concentration of PM10 atmospheric aerosol for the entire time period from March 2018 to May 2019 is shown in the Appendix in Fig. A1.

17) What are the valid temperature ranges of equations 1 and 2? Did you apply these equations to all available INP data or INP data in a specific temperature range when you made Figure 7?

Regarding equation 1, it is mentioned in line 494 that INP-T-spectra between 250-265 K are used. Therefore, the parameterization is valid for this temperature range. Also, for the INAS density parameterization in equation 2, the spectra in the full T range (250-265 K) was used and is therefore valid in the same temperature range.

References:

Canagaratna, M. R., Jayne, J. T., Jimenez, J. L., Allan, J. D., Alfarra, M. R., Zhang, Q., Onasch, T. B., Drewnick, F., Coe, H., Middlebrook, A., Delia, A., Williams, L. R., Trimborn, A. M., Northway, M. J., DeCarlo, P. F., Kolb, C. E., Davidovits, P. and Worsnop, D. R.: Chemical and microphysical characterization of ambient aerosols with the aerodyne aerosol mass spectrometer, Mass Spectrom. Rev., 26(2), 185–222, doi:10.1002/mas.20115, 2007.

DeCarlo, P. F., Kimmel, J. R., Trimborn, A., Northway, M. J., Jayne, J. T., Aiken, A. C., Gonin, M., Fuhrer, K., Horvath, T., Docherty, K. S., Worsnop, D. R. and Jimenez, J. L.: Field-deployable, high-resolution, time-of-flight aerosol mass spectrometer, Anal. Chem., 78(24), 8281–8289, doi:10.1021/ac061249n, 2006.

Hari, P. and Kulmala, M.: Station for measuring ecosystem-atmosphere relations (SMEARII), Boreal Environ. Res., 10(October), 315–322, doi:10.1007/978-94-007-5603-8_9, 2005.

Heald, C. L. and Spracklen, D. V.: Atmospheric budget of primary biological aerosol particles from fungal spores, Geophys. Res. Lett., 36(9), doi:10.1029/2009GL037493, 2009.

Hirst, J. M.: An automatic volumetric spore trap, Ann. Appl. Biol., 39(2), 257–265, doi:10.1111/j.1744-7348.1952.tb00904.x, 1952.

Hoose, C., Kristjánsson, J. E. and Burrows, S. M.: How important is biological ice nucleation in clouds on a global scale?, Environ. Res. Lett., 5(2), 1–7, doi:10.1088/1748-9326/5/2/024009, 2010.

Huffman, J. A., Prenni, A. J., Demott, P. J., Mason, R. H., Huffman, J. A., Prenni, A. J., Demott, P. J., Pöhlker, C., Mason, R. H., Robinson, N. H., Fröhlich-Nowoisky, J., Tobo, Y., Després, V. R., Garcia, E., Gochis, D. J., Harris, E., M ¨ Uller-Germann, I., Ruzene, C., Schmer, B., Sinha, B., Day, D. A., Andreae, M. O., Jimenez, J. L., Gallagher, M., Kreidenweis, S. M., Bertram, A. K. and Pöschl, U.: High concentrations of biological aerosol particles and ice nuclei during and after rain, Atmos. Chem. Phys, 13, 6151–6164, doi:10.5194/acp-13-6151-2013, 2013.

Iwata, A., Imura, M., Hama, M., Maki, T., Tsuchiya, N., Kunihisa, R. and Matsuki, A.: Release of highly active ice nucleating biological particles associated with rain, Atmosphere (Basel)., 10(10), 1–13, doi:10.3390/atmos10100605, 2019.

Liu, P. S. K., Deng, R., Smith, K. A., Williams, L. R., Jayne, J. T., Canagaratna, M. R., Moore, K., Onasch, T. B., Worsnop, D. R. and Deshler, T.: Transmission Efficiency of an Aerodynamic Focusing Lens System: Comparison of Model Calculations and Laboratory Measurements for the Aerodyne Aerosol Mass Spectrometer, Aerosol Sci. Technol., 41(8), 721–733, doi:10.1080/02786820701422278, 2007.

Manninen, H. E., Sihto-Nissilä, S. L., Hiltunen, V., Aalto, P. P., Kulmala, M., Petäjä, T., Manninen, H. E., Bäck, J., Hari, P., Huffman, J. A., Huffman, J. A., Saarto, A., Pessi, A. M. and Hidalgo, P. J.: Patterns in airborne pollen and other primary biological aerosol particles (PBAP), and their contribution to aerosol mass and number in a boreal forest, Boreal Environ. Res., 19(September), 383–405, 2014.

Middlebrook, A. M., Bahreini, R., Jimenez, J. L. and Canagaratna, M. R.: Evaluation of composition-dependent collection efficiencies for the Aerodyne aerosol mass spectrometer using field data, Aerosol Sci. Technol., 46(3), 258–271, doi:10.1080/02786826.2011.620041, 2012.

Paramonov, M., Drossaart Van Dusseldorp, S., Gute, E., Abbatt, J. P. D., Heikkilä, P., Keskinen, J., Chen, X., Luoma, K., Heikkinen, L., Hao, L., Petäjä, T. and Kanji, Z. A.: Condensation/immersion mode ice-nucleating particles in a boreal environment, Atmos. Chem. Phys, 20, 6687–6706, doi:10.5194/acp-20-6687-2020, 2020.

Perring, A. E., Schwarz, J. P., Baumgardner, D., Hernandez, M. T., Spracklen, D. V., Heald, C. L., Gao, R. S., Kok, G., McMeeking, G. R., McQuaid, J. B. and Fahey, D. W.: Airborne observations of regional variation in fluorescent aerosol across the United States, J. Geophys. Res. Atmos., 120(3), 1153–1170,

doi:10.1002/2014JD022495, 2015.

Prenni, A. J., Tobo, Y., Garcia, E., DeMott, P. J., Huffman, J. A., McCluskey, C. S., Kreidenweis, S. M., Prenni, J. E., Pöhlker, C. and Pöschl, U.: The impact of rain on ice nuclei populations at a forested site in Colorado, Geophys. Res. Lett., 40(1), 227–231, doi:10.1029/2012GL053953, 2013.

Rantio-Lehtimäki, A., Viander, M. and Koivikko, A.: Airborne birch pollen antigens in different particle sizes, Clin. Exp. Allergy, 24(1), 23–28, doi:10.1111/j.1365-2222.1994.tb00912.x, 1994.

Savage, N., Krentz, C., Könemann, T., Han, T. T., Mainelis, G., Pöhlker, C. and Huffman, J. A.: Systematic characterization and fluorescence threshold strategies for the Wideband Integrated Bioaerosol Sensor (WIBS) using size resolved biological and interfering particles, Atmos. Meas. Tech. Discuss., 10, 4279–4302, 2017.

Schmale, J., Henning, S., Henzing, B., Keskinen, H., Sellegri, K., Ovadnevaite, J., Bougiatioti, A., Kalivitis, N., Stavroulas, I., Jefferson, A., Park, M., Schlag, P., Kristensson, A., Iwamoto, Y., Pringle, K., Reddington, C., Aalto, P., Äijälä, M., Baltensperger, U., Bialek, J., Birmili, W., Bukowiecki, N., Ehn, M., Fjæraa, A. M., Fiebig, M., Frank, G., Fröhlich, R., Frumau, A., Furuya, M., Hammer, E., Heikkinen, L., Herrmann, E., Holzinger, R., Hyono, H., Kanakidou, M., Kiendler-Scharr, A., Kinouchi, K., Kos, G., Kulmala, M., Mihalopoulos, N., Motos, G., Nenes, A., O'Dowd, C., Paramonov, M., Petäjä, T., Picard, D., Poulain, L., Prévôt, A. S. H., Slowik, J., Sonntag, A., Swietlicki, E., Svenningsson, B., Tsurumaru, H., Wiedensohler, A., Wittbom, C., Ogren, J. A., Matsuki, A., Yum, S. S., Myhre, C. L., Carslaw, K., Stratmann, F. and Gysel, M.: Collocated observations of cloud condensation nuclei, particle size distributions, and chemical composition, Sci. Data, 4(1), 1–27, doi:10.1038/sdata.2017.3, 2017.

Ullrich, R., Hoose, C., Möhler, O., Niemand, M., Wagner, R., Höhler, K., Hiranuma, N., Saathoff, H. and Leisner, T.: A new ice nucleation active site parameterization for desert dust and soot, J. Atmos. Sci., 74(3), 699–717, doi:10.1175/JAS-D-16-0074.1, 2017.

Vogel, F.: First field application of a mobile expansion chamber to measure ice nucleating particles, Karlsruhe Insitute of Technology, Karlsruhe, Germany, 2018.

Wright, T. P., Hader, J. D., McMeeking, G. R. and Petters, M. D.: High relative humidity as a trigger for widespread release of ice nuclei, Aerosol Sci. Technol., 48(11), i–v, doi:10.1080/02786826.2014.968244, 2014.

Response to the interactive comment by Referee #2:

We thank referee #2 for his or her thoughtful comments and feedback. Please find below our responses and suggestions for the manuscript revision, with the referee comments in black, our answers in red, and suggested changes or additions to the manuscript in blue.

Schneider et al. present a well-written, succinct manuscript describing results from a full year of INP measurements in a boreal forest region. The study involves assessment of INP biogenic sources in addition to development of a new parameterization for boreal forest INPs. While I find the results and new parameterization valuable, there are a few issues with the manuscript that need to be addressed prior to publication.

While there are indeed very few year-long INP measurements at one location, there are several that report such measurements over an inter-seasonal scale (e.g. Šantl-Temkiv et al., 2019; Stopelli et al., 2015, 2016, and 2017). These studies are worth describing in the introduction. Additionally, it would be useful for the authors to report main findings from previous analogous studies to clearly demonstrate a comparison between those previous and the current results. The introduction is very short and could be beefed up by providing more details on these studies, including their limitations to promote the motivation for the current work.

Šantl-Temkiv, T., Lange, R., Beddows, D., Rauter, U., Pilgaard, S., Dall'Osto, M., Gunde-Cimerman, N., Massling, A., and Wex, H.: Biogenic Sources of Ice Nucleating Particles at the High Arctic Site Villum Research Station, Environ Sci Technol, 53, 10580-10590, 10.1021/acs.est.9b00991, 2019.
Stopelli, E., Conen, F., Morris, C. et al. Ice nucleation active particles are efficiently removed by precipitating clouds. Sci Rep 5, 16433 (2015). https://doi.org/10.1038/srep16433
Stopelli, E., Conen, F., Morris, C. E., Herrmann, E., Henne, S., Steinbacher, M., and Alewell, C.: Predicting abundance and variability of ice nucleating particles in precipitation at the high-altitude observatory Jungfraujoch, Atmos. Chem. Phys., 16, 8341–8351, https://doi.org/10.5194/acp-16-8341-2016, 2016.
Stopelli, E., Conen, F., Guilbaud, C., Zopfi, J., Alewell, C., and Morris, C. E.: Ice nucleators, bacterial cells and Pseudomonas syringae in precipitation at Jungfraujoch, Biogeosciences, 14, 1189–1196, https://doi.org/10.5194/bg-14-1189-2017, 2017.

Thanks for this suggestion. We agree that the introduction should be more comprehensive and precise. Therefore, we described previous studies, which could be compared to our study, in more detail within the introduction focusing on the presented seasonal cycle, the considered time period, the continuity of measurements and the measurement locations. We also included the suggested publications Santl-Temkiv et al. (2019) and Stopelli et al. (2015, 2016), as those also show seasonal trends in their INP data sets. Stopelli et al. (2017) and Stopelli et al. (2016) have been added as references when discussing the relation between INP concentrations and precipitation (lines 44-45, revised manuscript).

We have included the following section to the introduction:

Hartmann et al. (2019) report INP concentrations from the past 500 years derived from ice core samples collected at two Arctic sites. These measurements do not show a long-term trend of INP concentrations over their multiyear period, but the variability within a year is observed to be large. They do suggest indications that biological INPs contribute to Arctic INP populations throughout the past centuries, for example, the general shape of the INP spectra and high INP concentrations at relatively high temperatures are typically associated with biological materials. Although they did not find a statistically significant seasonal variation, they assume that it is likely that the strength of local biological particle sources is enhanced during a particular time of the year influencing the INP

variability. However, due to the time resolution and dating uncertainty a seasonal relation could not be explicitly shown. Tobo et al. (2019) also report INP concentrations measured at an Arctic station in Svalbard in July 2016 and March 2017, which show seasonal changes with enhanced values in summertime. Tobo et al. (2019) link these enhanced concentrations to the emission of high-latitude dust from glacial outwash plains. Šantl-Temkiv et al. (2019) report INP measurements from the Arctic in spring 2015 and spring and summer 2016 and also show higher INP concentrations in summer than in spring, which they also associate with biological aerosol and biogenic compounds. In another study of pan-Arctic INP, Wex et al. (2019) report INP concentrations from four Arctic stations for different time periods and time resolutions measured between 2012 and 2016. At all locations, the highest observed INP concentrations are recorded in the summer months from June to September. The nature of the INPs was not explicitly determined, but high INP concentrations observed at high activation temperatures indicate a contribution from biogenic material. Wex et al. (2019) suggest potential INP source regions mainly on open land and open water. Stopelli et al. (2015) presents INP concentrations measured from snow samples collected at the Jungfraujoch on a few days per month in the period from December 2012 to September 2013. Here, INP concentrations are again higher in the summer months. Based on this dataset, a model to predict INP concentrations at the Jungfraujoch was established by Stopelli et al. (2016) and validated using several precipitation samples collected between May and October 2014. The dataset from 2014 shows a completely different seasonal pattern than the 2012/2013 dataset with the lowest values during summer and maxima in May and October. The authors suggest these maxima are related to a Saharan dust event and a cold front passage. Schrod et al. (2020) describe a global network of four INP sampling stations, at a range of northern hemisphere latitudes, where atmospheric aerosol samples were collected on substrates for two years from September 2014. The substrates were analysed for deposition and condensation mode INPs using the FRIDGE isothermal static diffusion chamber (Schrod et al., 2020). The Schrod et al. (2020) results do not yield a clear seasonality but instead show that short-term variability overwhelms long-term trends. However, that observation may not represent the full picture of INP in those locations. The short sampling times (low volumes, 1 hour per day) and/or colder activation temperatures may serve to maximize sampling variability and mask any potential biological signal (Schrod et al. 2020). To date these studies present the first observations and indications of the seasonal variability of INP concentrations, addressing the need for more long-term INP observations. None of these studies presents a comprehensive analysis of continuously recorded INP data for a full seasonal cycle at one location without interruptions. Moreover, the focus of most of the previous studies except for the Schrod et al. (2020) study was especially at Arctic INPs.

In regard to the very short introduction, perhaps more time could be spent on: (1) the motivation and objectives of the study itself (i.e. SMEAR II) and (2) more details on current parameterizations and modelling efforts for bioaerosols and biological INPs, which often are conflicting and based on a very limited subset of INP observations. This would inherently provide a clear motivator for developing the boreal INP parameterization.

Explanations of the objectives and motivation for this study have been added to the introduction. We have also extended the discussion of studies, which report about biological INPs and bioaerosols and included a discussion of the difficulties related to investigating and parameterizing these particles.

Text added to the introduction describing motivation:

The main objective of this study is to investigate and describe the variability and seasonal trends in INP concentrations and INP temperature spectra in a boreal forest environment. The absence of anthropogenic and/or dust aerosol sources in the boreal region motivates the additional investigation of biogenic ice nucleation activity and reveals the relevance of boreal forest areas as an important INP source. The comprehensive instrumentation provided at the measurement site at the

SMEARII station allows comparisons between INP measurements with simultaneous measurements of many meteorological variables. These measurements are complemented by measurements characterizing the sampled aerosol number concentrations, size distributions and chemical compositions in order to elucidate the potential origin and nature of the INPs. Heat treatments of the suspensions prior to INP analysis also help identifying the nature of INPs. We aim to improve the parameterizations describing atmospheric INP concentrations in the boreal forest by considering seasonal dependences in the formulations. Finally, this study provides motivation for further continuous long-term studies of INP in different environments across the globe.

Text added to the introduction discussing studies on bioaerosols and biological INP:

Several biogenic aerosol types have been shown to have atmospherically relevant ice-nucleating abilities (Augustin et al., 2013; Creamean et al., 2013; Hader et al., 2014; Möhler et al., 2007; Morris et al., 2004; O'Sullivan et al., 2015, 2018; Pratt et al., 2009; Schnell and Vali, 1973) especially at temperatures above -15°C (Christner et al., 2008; Murray et al., 2012). Although the contribution of biogenic INPs to the total global INP abundance is thought to be rather low (Hoose et al., 2010), biogenic aerosol may contribute substantially at regional scales where biological aerosol sources are important. For example, Tobo et al. (2013), Prenni et al. (2009) and O'Sullivan et al. (2018) have observed biogenic aerosol in the INP populations of the forested environments in Colorado, in the Amazon basin and in rural areas in Northern Europe. Furthermore, Pratt et al. (2009) and Creamean et al. (2013) showed that biological particles were frequently present in ice crystal and precipitation residues measured over the western United States and suggested that these particles play a key role in cloud ice formation. In a study about Swedish and Czech birch pollen, Augustin et al. (2013) reported the ice-nucleation activity of sampled macromolecules and formulated new parameterizations for the heterogeneous nucleation rates of two different ice-active macromolecules. However, in general, measuring and parameterizing the IN ability of biogenic particles has proven to be difficult for several reasons. For accurate biogenic INP model simulations, it is critical to understand the global distribution of biogenic INP, their source strength and their aerosolization and atmospheric transport mechanisms (O'Sullivan et al., 2018). It remains unresolved how the microphysical and chemical properties of biogenic aerosol may change during transport processes in the atmosphere. In field studies, which attempt to address these deficiencies, it remains difficult to identify biogenic aerosol particles and to separate them from non-biogenic particles (Möhler et al., 2007). Moreover, there are many biogenic species with a range of properties, which complicate comparisons and generalized parameterizations.

The snow cover information is useful and corroborates the INP concentration cycle, but what about the transition between melt and full growth of vegetation? Showing some sort of vegetation index and/or type information would be useful, particularly for the inter-seasonal transitions.

For our measurement site at SMEARII, the vegetation indexes NDVI (Normalized Difference Vegetation Index) and PRI (Photochemical Reflectance Index) are available, but only from 11 March 2018 to 11 September 2018. The NDVI and PRI data and the following interpretation is provided by Jon Atherton and Pasi Kolari from University of Helsinki (personal communication, October, 2020). For both vegetation indices, we calculated daily average values, which are averaged between 12:00 and 13:00 Finnish time, because the solar angle plays an important role for these indices. NDVI mainly tracks the development and loss of green leaf material including overstory trees and understory shrubs. We observe a trend in NDVI over the seasonal transition as the canopy slowly

greens from winter to summer. During summer, when the color of the canopy does not change significantly, the NDVI remains relatively constant. The increase in NDVI in the transition period from winter to summer is observed some days later than the increase in INP concentrations. The increase in INP concentrations is nicely represented by increasing air temperature and melting snow in early April 2018 (see Figure 4), whereas a strong increase in NDVI is observed in the second half of April. It has to be considered, that the NDVI is affected by snow resulting in smaller NDVI values. The PRI measures the abundance of photoprotective pigments called carotenoids, which help the tree to deal with excess light, which is potentially harmful. We observed a PRI increase in May, which indicates a carotenoid change of the trees. A relationship to the increasing INP concentrations in April is not observed.

We do not think that these comparisons are of great benefit to the story outlined within the manuscript and have decided not to include the comparison in the paper. However, we are glad it can be made available in this publicly accessible discussion and gratefully acknowledge the support of Jon Atherton and Pasi Kolari by providing and interpreting the NDVI and PRI data.

The methodology on the WIBS and L-ToF-AMS is incredibly limited. Because data from these methods are presented in the paper, the methods should include sufficient descriptions on each instrument, their operating parameters during SMEAR II, and data analysis and interpretation. Even though the L-ToF-AMS is presented in detail in Paramonov et al. (2020), there should still be a brief description of the instrument and data produced here.

Thanks for this comment. We agree that a more detailed explanation of these measurements is needed to support the results of this study. We have added a more detailed description of the WIBS instrument to Section 2.3. “Additional Instrumentation at SMEARII”. As the other referees also asked further questions about the details on the WIBS and L-ToF-AMS, the added description addresses the comments of all the referees regarding this topic:

The WIBS-NEO (Droplet Measurement Technologies, Longmont, CO, USA) is a bioaerosol sensor that provides information on the fluorescence properties, size and asphericity ratio of individual aerosol particles. It operates with an inlet flow of 0.3 l min^{-1} and detects particles with diameters between 500 nm and 30 µm. From 11 March 2018 to 2 April 2018, the WIBS was located about 50m from the aerosol filter sampling line used for the INP analysis. There, it was attached to a total aerosol inlet, which is characterized in Vogel (2018). On 3 April 2018, the WIBS was moved and installed directly next to the filter sampling line and attached to a PM10 inlet, which is described in Schmale et al. (2017). For the WIBS data analysis, particles from 0.5 µm to 10 µm were considered. To analyse the fluorescence of the particles, the WIBS sensor utilizes two xenon flashlamps as excitation light sources (optically filtered at wavelengths of 280 nm and 370 nm) and two emission detection channels (wavelength bands 310 – 400 nm and 420 – 650 nm). Optical size information is acquired utilizing elastic scattering from a continuous wave laser with a wavelength of 635 nm and a photomultiplier tube located orthogonally with respect to the laser. The excitation pulses are fired into the sample volume at different times and both detection channels record the emission(s) from both excitations, leading to three distinguishable excitation-emission combinations (the 370 nm light saturates the 310 – 400 nm detection channel and therefore does not provide any information). Thus, the fluorescence can be divided into 7 unique fluorescence groups based on the excitation-emission wavelength pairs and their combinations, after Perring et al. (2015) and Savage et al. (2017): A (only FL1: excitation 280 nm, emission 310 – 400 nm), B (only FL2: excitation 280 nm, emission 420 – 650 nm), C (only FL3: excitation 370 nm, emission 420 – 650 nm), AB (FL1 + FL2), BC (FL2 + FL3), AC (FL1 + FL3) and ABC (FL1 + FL2 + FL3).

The WIBS performs an empty-chamber background signal check every 8 hours, during which the excitation pulses are fired into the optical chamber without any present particles. The background check collects a multitude of emission intensities that form a baseline for particle fluorescence. In this study, a particle is considered fluorescent, if the associated emission peak intensity is larger than $FT + 9\sigma$. FT is the mean value of the forced trigger intensities and σ is their standard deviation.

A more commonly used method would be to compare the emission peak intensity to $FT + 3\sigma$. However, some non-biological particle types such as wood smoke, African dust and black carbon are weakly fluorescent and therefore might satisfy the lower threshold value, leading to an overestimation of biological particle concentration. Furthermore, the stricter threshold only marginally affects the detection efficiency of biological particles, because they tend to have stronger fluorescence (Savage et al., 2017). More detailed descriptions on the WIBS are also available in Savage et al. (2017) and Perring et al. (2015).

We also added the following text to the description on Figure 4 (old Figure 3b) to Section 3.2 "Comparison to meteorology and aerosol properties" to explain the characteristic of the different excitation-emission wavelengths pairs:

The time series of the number concentration of particles with a fluorescence signal in other fluorescence groups is shown in the Appendix in Fig. A2. In this Figure, the strongest seasonal increase in the transition period from winter to summer is observed in the group ABC. Consequently, this fluorescent group correlates best with the measured INP concentrations (see Figure 4). The characteristics of each fluorescence group are comprehensively investigated and reported in Savage et al. (2017), who examined the fluorescence emissions of different types of pollen, fungi, bacteria, biofluorophores, dust, HULIS (humic-like substances), PAH (polycyclic aromatic hydrocarbons), soot and brown carbon. Using the $FT + 9\sigma$ threshold for defining a particle as fluorescent, nearly all dust and HULIS types show no fluorescence signal at all. Some of the soot and brown carbon types only show weak signals in A, and B, BC and A, respectively. Nearly all of the bacteria types show fluorescence only in group A. The fluorescence of fungal spores are also mainly detected in group A, but also in AB and ABC. The investigated biofluorophores show mainly fluorescence in the groups BC (Riboflavin, NAD), A (Pyridoxamine), AB (Tryptophan) and ABC (Ergosterol). PAHs show fluorescence mostly in groups ABC and A. Finally, most pollen types show fluorescence in groups ABC and AB. Some pollen types also show a fluorescence signal in groups A and B.

We also adjusted the discussion on the comparison of WIBS data to INP in the same Section as follows:

Such a correlation is also supported by the peaks of pollen and PBAP concentrations observed in snow-free periods in spring and in autumn, and by the increases of the organic aerosol mass concentration and fluorescent particle numbers of group ABC observed in spring. According to the study of Savage et al. (2017), we assume particles of fluorescence group ABC to be mainly pollen, particles containing PAH or Ergosterol, or fungal spores. ~~Fluorescent particles are expected to be primarily of biological origin except for a few percent, which could arise from non-biological materials (Pöhlker et al., 2012; Savage et al., 2017).~~

We also added a more detailed description on the L-ToF-AMS instrument to Section 2.3." Additional Instrumentation at SMEARII":

The size-resolved chemical composition of ambient aerosol was measured with the L-ToF-AMS. Its application in the same campaign has been described in Paramonov et al. (2020). It builds on the functionality and characteristics of the high-resolution ToF-AMS (DeCarlo et al., 2006). However, due to the longer time-of-flight chamber, the L-ToF-AMS, has a better resolution (8000 M/ΔM) than the

standard ToF-AMS (2000 M/ΔM in V-mode). Detailed descriptions of the instrument, measurements and data processing are available in other publications (Canagaratna et al., 2007; DeCarlo et al., 2006). In general, the L-ToF-AMS measures the size-resolved, non-refractory composition of submicron aerosols, including organic, sulfate, nitrate, ammonium and chloride. The aerodynamic lens has a 100% transmission range of 75-650 nm (in vacuum aerodynamic diameter; Liu et al. (2007)) and focuses particles into a narrow beam that impacts the surface of a porous tungsten vaporizer heated to 600°C, followed by ionization by a 70eV electron source. Ions are detected by a long time-of-flight mass analyzer (Tofwerk AG). The sample flow of 0.09 l min^{-1} is extracted from an extra suction flow (3 l min^{-1}) that is used to avoid aerosol losses in the inlet line. A PM2.5 cyclone mounted at the inlet removes large particles to avoid clogging the critical orifice (100µm), and before entering the L-ToF-AMS, the samples are dried by a Nafion dryer to keep the RH below 30%.

The L-ToF-AMS data were analyzed using standard ToF-AMS data analysis toolkits (Squirrel V1.61B and PIKA1.21B) using Igor Pro software (V6.37, WaveMetrics Inc.). To calculate mass concentrations an ionization efficiency (IE) was determined using 300 nm, size-selected, dry ammonium nitrate particles, and a relative ionization efficiency (RIE) for ammonium of 3.7 was determined. The default relative ionization efficiency (RIE) values of 1.1, 1.2, 1.3 and 1.4 for nitrate, sulfate, chloride and organics, respectively, were applied. A composition-dependent collection efficiency (CE) was applied based on the principles proposed by Middlebrook et al. (2012).

We also added the following text to the discussion on Figure 4 (old Figure 3b) to Section 3.2 "Comparison to meteorology and aerosol properties" to give more information about the measured organics:

The non-refractory organic components measured by the AMS include the commonly observed primary organic aerosol (POA) and oxygenated organic aerosol (OOA).

Figure 1: It would be useful to show an averaged spectrum per month overlaid on the data in each panel.

With monthly averaging, the variability of the spectra within one month and also the characteristic spectral shape is no longer visible. As this Figure is meant to show the daily/monthly variability and characteristic concentrations and spectral shapes throughout the full year of measurements, we have decided to keep the Figure as is.

Figure 2: The data in panel a are redundant from Figure 1. Suggest omitting and just keeping panel b.

We think it is reasonable to keep panel (a) in Figure 2, as the representation on a time axis allows easier peak identification in the INP concentrations and highlights the seasonal variability and trends.

For the "bulge" which is more pronounced in the heated versus unamended INP spectra for the summer samples, why would this be? There should be some discussion as to why this feature is more prominent when the samples were heated, and why this would occur only for samples collected during the summer.

This is a very interesting point. So far, the "bulge" is only an observation, for which we do not yet have a concrete explanation. We want to show what we observed, which may also be a basis for further studies and measurement campaigns that could directly be initiated with the objective to explain this observation.

Because n_s is shown earlier on than page 11, the calculation should be provided in the methods.

Thanks for this comment. We have added the following section to the Methods:

INAS densities were calculated as described in Eq. (2) in Ullrich et al. (2017), where ice number concentrations are normalized by the aerosol surface area concentration. Assuming that every INP triggers the formation of one ice crystal, the ice number concentrations are equal to the INP concentrations, which are determined by the INSEKT measurements. The aerosol surface area concentrations are derived from continuous size distribution measurements of the PM10 atmospheric aerosol at SMEARII. Details on the size distribution measurements are given in the following section.

Like the introduction, the conclusions are brief and somewhat limited. The "bigger picture" should be reiterated for context of the measurements, and perhaps some discussion on what the authors recommend for the next step and future work.

We agree that the conclusion needed improvements – thanks for this comment. We now set our study in the context of the "bigger picture" and have added suggestions for further work:

As INPs strongly influence precipitation formation and cloud evolution, a description of INPs in weather forecast models is crucial. This study shows that the ice nucleation activity in the atmosphere is highly variable depending on the surrounding conditions. Therefore, it is important to investigate INP concentrations and INP types in different characteristic locations on Earth to establish an overall picture of the global INP abundance and variability. For investigating long-term variability, continuous long-term observations are needed to get a profound insight on the ice nucleation activity at a specific site with a good statistics accounting for the difficulties and uncertainties in INP measurements. With this study, we provide a first step to this overall picture by characterizing the INP population abundant in a remote location in the boreal forest. With continuous aerosol filter sampling for more than one year, we provide the first observation of a clear seasonal cycle, which seems to be dominated by the abundance biogenic aerosol. As in this remote environment, biogenic aerosols seem to play an important role, in other areas, the INP population might be dominated by other species. For further studies, we suggest to conduct further continuous long-term measurements of INPs at different locations on Earth, like anthropogenic influenced locations or deserts. Measurements with a higher time resolution might be useful to investigate relations to meteorological events like precipitation and frontal passages in more detail.

References:

Augustin, S., Wex, H., Niedermeier, D., Pummer, B., Grothe, H., Hartmann, S., Tomsche, L., Clauss, T., Voigtländer, J., Ignatius, K. and Stratmann, F.: Immersion freezing of birch pollen washing water, Atmos. Chem. Phys., 13(21), 10989–11003, doi:10.5194/acp-13-10989-2013, 2013.

Canagaratna, M. R., Jayne, J. T., Jimenez, J. L., Allan, J. D., Alfarra, M. R., Zhang, Q., Onasch, T. B., Drewnick, F., Coe, H., Middlebrook, A., Delia, A., Williams, L. R., Trimborn, A. M., Northway, M. J., DeCarlo, P. F., Kolb, C. E., Davidovits, P. and Worsnop, D. R.: Chemical and microphysical characterization of ambient aerosols with the aerodyne aerosol mass spectrometer, Mass Spectrom. Rev., 26(2), 185–222, doi:10.1002/mas.20115, 2007.

Christner, B. C., Morris, C. E., Foreman, C. M., Cai, R. and Sands, D. C.: Ubiquity of biological ice nucleators in snowfall, Science (80-.)., 319(5867), 1214, doi:10.1126/science.1149757, 2008.

Creamean, J. M., Suski, K. J., Rosenfeld, D., Cazorla, A., DeMott, P. J., Sullivan, R. C., White, A. B.,

Ralph, F. M., Minnis, P., Comstock, J. M., Tomlinson, J. M. and Prather, K. A.: Dust and biological aerosols from the Sahara and Asia influence precipitation in the Western U.S, Science (80-.)., 340(6127), 1572–1578, doi:10.1126/science.1227279, 2013.

DeCarlo, P. F., Kimmel, J. R., Trimborn, A., Northway, M. J., Jayne, J. T., Aiken, A. C., Gonin, M., Fuhrer, K., Horvath, T., Docherty, K. S., Worsnop, D. R. and Jimenez, J. L.: Field-deployable, high-resolution, time-of-flight aerosol mass spectrometer, Anal. Chem., 78(24), 8281–8289, doi:10.1021/ac061249n, 2006.

Hader, J. D., Wright, T. P. and Petters, M. D.: Contribution of pollen to atmospheric ice nuclei concentrations, Atmos. Chem. Phys., 14(11), 5433–5449, doi:10.5194/acp-14-5433-2014, 2014.

Hartmann, M., Blunier, T., Brügger, S. O., Schmale, J., Schwikowski, M., Vogel, A., Wex, H. and Stratmann, F.: Variation of Ice Nucleating Particles in the European Arctic Over the Last Centuries, Geophys. Res. Lett., 46(7), 4007–4016, doi:10.1029/2019GL082311, 2019.

Hoose, C., Kristjánsson, J. E. and Burrows, S. M.: How important is biological ice nucleation in clouds on a global scale?, Environ. Res. Lett., 5(2), 1–7, doi:10.1088/1748-9326/5/2/024009, 2010.

Liu, P. S. K., Deng, R., Smith, K. A., Williams, L. R., Jayne, J. T., Canagaratna, M. R., Moore, K., Onasch, T. B., Worsnop, D. R. and Deshler, T.: Transmission Efficiency of an Aerodynamic Focusing Lens System: Comparison of Model Calculations and Laboratory Measurements for the Aerodyne Aerosol Mass Spectrometer, Aerosol Sci. Technol., 41(8), 721–733, doi:10.1080/02786820701422278, 2007.

Middlebrook, A. M., Bahreini, R., Jimenez, J. L. and Canagaratna, M. R.: Evaluation of composition-dependent collection efficiencies for the Aerodyne aerosol mass spectrometer using field data, Aerosol Sci. Technol., 46(3), 258–271, doi:10.1080/02786826.2011.620041, 2012.

Möhler, O., DeMott, P. J., Vali, G. and Levin, Z.: Microbiology and atmospheric processes: The role of biological particles in cloud physics, Biogeosciences, 4(6), 1059–1071, doi:10.5194/bg-4-1059-2007, 2007.

Morris, C. E., Georgakopoulos, D. G. and Sands, D. C.: Ice nucleation active bacteria and their potential role in precipitation, J. Phys. IV JP, 121, 87–103, doi:10.1051/jp4:2004121004, 2004.

Murray, B. J., O'Sullivan, D., Atkinson, J. D. and Webb, M. E.: Ice nucleation by particles immersed in supercooled cloud droplets, Chem. Soc. Rev., 41(19), 6519–6554, doi:10.1039/c2cs35200a, 2012.

O'Sullivan, D., Murray, B. J., Ross, J. F., Whale, T. F., Price, H. C., Atkinson, J. D., Umo, N. S. and Webb, M. E.: The relevance of nanoscale biological fragments for ice nucleation in clouds, Sci. Rep., 5, 1–7, doi:10.1038/srep08082, 2015.

O'Sullivan, D., Adams, M. P., Tarn, M. D., Harrison, A. D., Vergara-Temprado, J., Porter, G. C. E., Holden, M. A., Sanchez-Marroquin, A., Carotenuto, F., Whale, T. F., McQuaid, J. B., Walshaw, R., Hedges, D. H. P., Burke, I. T., Cui, Z. and Murray, B. J.: Contributions of biogenic material to the atmospheric ice-nucleating particle population in North Western Europe, Sci. Rep., 8(1), 1–9, doi:10.1038/s41598-018-31981-7, 2018.

Paramonov, M., Drossaart Van Dusseldorp, S., Gute, E., Abbatt, J. P. D., Heikkilä, P., Keskinen, J., Chen, X., Luoma, K., Heikkinen, L., Hao, L., Petäjä, T. and Kanji, Z. A.: Condensation/immersion mode ice-nucleating particles in a boreal environment, Atmos. Chem. Phys, 20, 6687–6706, doi:10.5194/acp-20-6687-2020, 2020.

Perring, A. E., Schwarz, J. P., Baumgardner, D., Hernandez, M. T., Spracklen, D. V., Heald, C. L., Gao, R. S., Kok, G., McMeeking, G. R., McQuaid, J. B. and Fahey, D. W.: Airborne observations of regional variation in fluorescent aerosol across the United States, J. Geophys. Res. Atmos., 120(3), 1153–1170, doi:10.1002/2014JD022495, 2015.

Pratt, K. A., Demott, P. J., French, J. R., Wang, Z., Westphal, D. L., Heymsfield, A. J., Twohy, C. H., Prenni, A. J. and Prather, K. A.: In situ detection of biological particles in cloud ice-crystals, Nat. Geosci., 2(6), 398–401, doi:10.1038/ngeo521, 2009.

Prenni, A. J., Petters, M. D., Kreidenweis, S. M., Heald, C. L., Martin, S. T., Artaxo, P., Garland, R. M., Wollny, A. G. and Pöschl, U.: Relative roles of biogenic emissions and Saharan dust as ice nuclei in the Amazon basin, Nat. Geosci., 2(6), 402–405, doi:10.1038/ngeo517, 2009.

Šantl-Temkiv, T., Lange, R., Beddows, D., Rauter, U., Pilgaard, S., Dall'osto, M., Gunde-Cimerman, N., Massling, A. and Wex, H.: Biogenic Sources of Ice Nucleating Particles at the High Arctic Site Villum Research Station, Environ. Sci. Technol., 53(18), 10580–10590, doi:10.1021/acs.est.9b00991, 2019.

Savage, N., Krentz, C., Könemann, T., Han, T. T., Mainelis, G., Pöhlker, C. and Huffman, J. A.: Systematic characterization and fluorescence threshold strategies for the Wideband Integrated Bioaerosol Sensor (WIBS) using size resolved biological and interfering particles, Atmos. Meas. Tech. Discuss., 10, 4279–4302, 2017.

Schmale, J., Henning, S., Henzing, B., Keskinen, H., Sellegri, K., Ovadnevaite, J., Bougiatioti, A., Kalivitis, N., Stavroulas, I., Jefferson, A., Park, M., Schlag, P., Kristensson, A., Iwamoto, Y., Pringle, K., Reddington, C., Aalto, P., Äijälä, M., Baltensperger, U., Bialek, J., Birmili, W., Bukowiecki, N., Ehn, M., Fjæraa, A. M., Fiebig, M., Frank, G., Fröhlich, R., Frumau, A., Furuya, M., Hammer, E., Heikkinen, L., Herrmann, E., Holzinger, R., Hyono, H., Kanakidou, M., Kiendler-Scharr, A., Kinouchi, K., Kos, G., Kulmala, M., Mihalopoulos, N., Motos, G., Nenes, A., O'Dowd, C., Paramonov, M., Petäjä, T., Picard, D., Poulain, L., Prévôt, A. S. H., Slowik, J., Sonntag, A., Swietlicki, E., Svenningsson, B., Tsurumaru, H., Wiedensohler, A., Wittbom, C., Ogren, J. A., Matsuki, A., Yum, S. S., Myhre, C. L., Carslaw, K., Stratmann, F. and Gysel, M.: Collocated observations of cloud condensation nuclei, particle size distributions, and chemical composition, Sci. Data, 4(1), 1–27, doi:10.1038/sdata.2017.3, 2017.

Schnell, R. C. and Vali, G.: World-wide source of leaf-derived freezing nuclei, Nature, 246(5430), 212–213, doi:10.1038/246212a0, 1973.

Schrod, J., Thomson, E. S., Weber, D., Kossmann, J., Pöhlker, C., Saturno, J., Ditas, F., Artaxo, P., Clouard, V., Saurel, J.-M., Ebert, M., Curtius, J., and Bingemer, H. G.: Long-term INP measurements from four stations across the globe, Atmos. Chem. Phys. Discuss., https://doi.org/10.5194/acp-2020-667, in review, 2020.

Stopelli, E., Conen, F., Morris, C. E., Herrmann, E., Bukowiecki, N. and Alewell, C.: Ice nucleation active particles are efficiently removed by precipitating clouds, Sci. Rep., 5, 1–7, doi:10.1038/srep16433, 2015.

Stopelli, E., Conen, F., Morris, C. E., Herrmann, E., Henne, S., Steinbacher, M. and Alewell, C.: Predicting abundance and variability of ice nucleating particles in precipitation at the high-altitude observatory Jungfraujoch, Atmos. Chem. Phys., 16(13), 8341–8351, doi:10.5194/acp-16-8341-2016, 2016.

Stopelli, E., Conen, F., Guilbaud, C., Zopfi, J., Alewell, C. and Morris, C. E.: Ice nucleators, bacterial cells and Pseudomonas syringae in precipitation at Jungfraujoch, Biogeosciences, 14(5), 1189–1196, doi:10.5194/bg-14-1189-2017, 2017.

Tobo, Y., Prenni, A. J., Demott, P. J., Huffman, J. A., McCluskey, C. S., Tian, G., Pöhlker, C., Pöschl, U. and Kreidenweis, S. M.: Biological aerosol particles as a key determinant of ice nuclei populations in a forest ecosystem, J. Geophys. Res. Atmos., 118(17), 10100–10110, doi:10.1002/jgrd.50801, 2013.

Tobo, Y., Adachi, K., DeMott, P. J., Hill, T. C. J., Hamilton, D. S., Mahowald, N. M., Nagatsuka, N., Ohata, S., Uetake, J., Kondo, Y. and Koike, M.: Glacially sourced dust as a potentially significant source of ice nucleating particles, Nat. Geosci., 12(April), 253–258, doi:10.1038/s41561-019-0314-x, 2019.

Ullrich, R., Hoose, C., Möhler, O., Niemand, M., Wagner, R., Höhler, K., Hiranuma, N., Saathoff, H. and Leisner, T.: A new ice nucleation active site parameterization for desert dust and soot, J. Atmos. Sci., 74(3), 699–717, doi:10.1175/JAS-D-16-0074.1, 2017.

Vogel, F.: First field application of a mobile expansion chamber to measure ice nucleating particles, Karlsruhe Insitute of Technology, Karlsruhe, Germany, 2018.

Wex, H., Huang, L., Zhang, W., Hung, H., Traversi, R., Becagli, S., Sheesley, R. J., Moffett, C. E., Barrett, T. E., Bossi, R., Skov, H., Hünerbein, A., Lubitz, J., Löffler, M., Linke, O., Hartmann, M., Herenz, P. and Stratmann, F.: Annual variability of ice-nucleating particle concentrations at different Arctic locations, Atmos. Chem. Phys., 19(7), 5293–5311, doi:10.5194/acp-19-5293-2019, 2019.

Response to the interactive comment by Referee #3:

We thank referee #3 for his or her thoughtful comments and feedback. Please find below our responses and suggestions for the manuscript revision, with the referee comments in black, our answers in red, and suggested changes or additions to the manuscript in blue.

In the manuscript titled “The seasonal cycle of ice-nucleating particles linked to the abundance of biogenic aerosol in boreal forests”, Schneider et al. describe results from a year-long measurement campaign of ice nucleating particles (INPs) over a forested site in Finland. The data are unique and provide an additional constraint for INPs present over a boreal environment, which are of value to the aerosol-cloud interaction community. I have several comments, most of which I think can be addressed by the authors and I hope to support the publication of this manuscript once these comments have been adequately addressed.

SECTION 1 INTRO The introduction is concise and has room to address two current missing items: 1) a description of the goal of the manuscript or study; and 2) because one of the main deliverables of this paper is parameterized INP concentrations at this location, it is important to describe the physical mechanisms that INPs may be generated locally or other regional aerosol sources that may impact the INP populations - this is important in creating a physically-based parameterization that may one day be expanded to modeling studies.

We agree with the referee that the paper would benefit from a stronger definition of the objective of the study. Therefore, we have added a description of the objectives of this study at the end of the introduction:

The main objective of this study is to investigate and describe the variability and seasonal trends in INP concentrations and INP temperature spectra in a boreal forest environment. The absence of anthropogenic and/or dust aerosol sources in the boreal region motivates the additional investigation of biogenic ice nucleation activity and reveals the relevance of boreal forest areas as an important INP source. The comprehensive instrumentation provided at the measurement site at the SMEARII station allows comparisons between INP measurements with simultaneous measurements of many meteorological variables. These measurements are complemented by measurements characterizing the sampled aerosol number concentrations, size distributions and chemical compositions in order to elucidate the potential origin and nature of the INPs. Heat treatments of the suspensions prior to INP analysis also help identifying the nature of INPs. We aim to improve the parameterizations describing atmospheric INP concentrations in the boreal forest by considering seasonal dependences in the formulations. Finally, this study provides motivation for further continuous long-term studies of INP in different environments across the globe.

General information about the characteristic aerosol particle population is already given in the introduction. Here, we state that boreal forests are generally far from anthropogenic or dust sources, which consequently are not expected to contribute to the generation of boreal INPs. As the main source of aerosol particle in boreal forest areas appeared to be the forest itself, it is also likely, that the INP populations are mainly influenced and generated by this source. As we present indication for abundant biogenic particles in the INP population, this expectation is underlined. We cannot give more precise description on INP generation processes in the boreal forest, as we did not directly measure the nature of the INP in our samples. Of course, different biogenic aerosol particles are also

generated differently, but in general, we state the forest with its vegetation as the main INP source, releasing biogenic particles like pollen and fungal spores e.g. through wind dispersion.

SECTION 2 METHODS The methods describing measurements of INPs is quite thorough.
I would like the authors to expand on the uncertainty description for INPs - it is not clear where the systematic error percentages were derived. Were blanks collected?

Thanks for this suggestion. We have added a more detailed description of the determination of the systematic errors to Section 2.2 "INSEKT":

A systematic error due to the preparation process and flow measurements is added. Applying a simple linear error propagation to the formulas given in Vali (1971) and inserting the error-containing parameters like the pipetted suspension volumes and the flow rate systematic errors of 4% for the undiluted suspension, 5% for the first dilution step, 8% for the third dilution step and 11% for the fourth step, are calculated. The systematic error increases with each dilution step because the additional pipetting step adds uncertainty.

In the following sentence, it is mentioned that blank filters have also been collected and the resulting INP temperature spectra have been subtracted from the INP temperature spectra of the "normal" samples.

The inlet for the "additional instrumentation" was heated and "RH remains below 40%"
– how does this compare to the inlet used for the INP filter collections? Without knowing the exact RH at this site, I suspect RH can get quite high and may increase collection efficiencies of large particles.

Thanks for this comment, this is a good point to consider. We do not expect the collection efficiency to be impacted by the relative humidity. However, it is possible that the measured surface area distribution is somehow shifted, which is a common problem when using different inlets. This adds uncertainty to the INAS densitiy parameterization. Currently, we are not able to quantify this uncertainty, but it is important to be aware of the potential bias. It is important to note that the INSEKT is only measuring ice-nucleating particles, which are not soluble.

For the other measurements, there seems to be a few missing details: - What exactly was measured by the L-ToF-AMS? What sizes are detectable by this measurement? - Was the WIBS connected to a similar inlet as the other instruments? Where large super micron particles measurable? Could the authors include a comparison between the scattering particle size distribution measured from the WIBS and the APS data?

We agree with the referee that the paper would benefit from a more detailed explanation on the additional instrumentation used for this study. For both instruments, the WIBS and the L-Tof-AMS, we added a more detailed description, which addresses your questions and also the associated questions of the other referees.

We added a more detailed description on the WIBS instrument to Section 2.3. "Additional Instrumentation at SMEARII":

The WIBS-NEO (Droplet Measurement Technologies, Longmont, CO, USA) is a bioaerosol sensor that provides information on the fluorescence properties, size and asphericity ratio of individual aerosol

particles. It operates with an inlet flow of 0.3 l min^{-1} and detects particles with diameters between 500 nm and 30 µm. From 11 March 2018 to 2 April 2018, the WIBS was located about 50m from the aerosol filter sampling line used for the INP analysis. There, it was attached to a total aerosol inlet, which is characterized in Vogel (2018). On 3 April 2018, the WIBS was moved and installed directly next to the filter sampling line and attached to a PM10 inlet, which is described in Schmale et al. (2017). For the WIBS data analysis, particles from 0.5 µm to 10 µm were considered. To analyse the fluorescence of the particles, the WIBS sensor utilizes two xenon flashlamps as excitation light sources (optically filtered at wavelengths of 280 nm and 370 nm) and two emission detection channels (wavelength bands 310 – 400 nm and 420 – 650 nm). Optical size information is acquired utilizing elastic scattering from a continuous wave laser with a wavelength of 635 nm and a photomultiplier tube located orthogonally with respect to the laser. The excitation pulses are fired into the sample volume at different times and both detection channels record the emission(s) from both excitations, leading to three distinguishable excitation-emission combinations (the 370 nm light saturates the 310 – 400 nm detection channel and therefore does not provide any information). Thus, the fluorescence can be divided into 7 unique fluorescence groups based on the excitation-emission wavelength pairs and their combinations, after Perring et al. (2015) and Savage et al. (2017): A (only FL1: excitation 280 nm, emission 310 – 400 nm), B (only FL2: excitation 280 nm, emission 420 – 650 nm), C (only FL3: excitation 370 nm, emission 420 – 650 nm), AB (FL1 + FL2), BC (FL2 + FL3), AC (FL1 + FL3) and ABC (FL1 + FL2 + FL3).

The WIBS performs an empty-chamber background signal check every 8 hours, during which the excitation pulses are fired into the optical chamber without any present particles. The background check collects a multitude of emission intensities that form a baseline for particle fluorescence. In this study, a particle is considered fluorescent, if the associated emission peak intensity is larger than $FT + 9\sigma$. FT is the mean value of the forced trigger intensities and σ is their standard deviation.

A more commonly used method would be to compare the emission peak intensity to $FT + 3\sigma$. However, some non-biological particle types such as wood smoke, African dust and black carbon are weakly fluorescent and therefore might satisfy the lower threshold value, leading to an overestimation of biological particle concentration. Furthermore, the stricter threshold only marginally affects the detection efficiency of biological particles, because they tend to have stronger fluorescence (Savage et al., 2017). More detailed descriptions on the WIBS are also available in Savage et al. (2017) and Perring et al. (2015).

We also added the following text to the description on Figure 4 (old Figure 3b) to Section 3.2 "Comparison to meteorology ad aerosol properties" to explain the characteristic of the different excitation-emission wavelengths pairs:

The time series of the number concentration of particles with a fluorescence signal in other fluorescence groups is shown in the Appendix in Fig. A2. In this Figure, the strongest seasonal increase in the transition period from winter to summer is observed in the group ABC. Consequently, this fluorescent group correlates best with the measured INP concentrations (see Figure 4). The characteristics of each fluorescence group are comprehensively investigated and reported in Savage et al. (2017), who examined the fluorescence emissions of different types of pollen, fungi, bacteria, biofluorophores, dust, HULIS (humic-like substances), PAH (polycyclic aromatic hydrocarbons), soot and brown carbon. Using the $FT + 9\sigma$ threshold for defining a particle as fluorescent, nearly all dust and HULIS types show no fluorescence signal at all. Some of the soot and brown carbon types only show weak signals in A, and B, BC and A, respectively. Nearly all of the bacteria types show fluorescence only in group A. The fluorescence of fungal spores are also mainly detected in group A, but also in AB and ABC. The investigated biofluorophores show mainly fluorescence in the groups BC (Riboflavin, NAD), A (Pyridoxamine), AB (Tryptophan) and ABC (Ergosterol). PAHs show fluorescence

mostly in groups ABC and A. Finally, most pollen types show fluorescence in groups ABC and AB. Some pollen types also show a fluorescence signal in groups A and B.

We also adjusted the discussion on the comparison of WIBS data to INP in the same Section as follows:

Such a correlation is also supported by the peaks of pollen and PBAP concentrations observed in snow-free periods in spring and in autumn, and by the increases of the organic aerosol mass concentration and fluorescent particle numbers of group ABC observed in spring. According to the study of Savage et al. (2017), we assume particles of fluorescence group ABC to be mainly pollen, particles containing PAH or Ergosterol, or fungal spores. ~~Fluorescent particles are expected to be primarily of biological origin except for a few percent, which could arise from non-biological materials (Pöhlker et al., 2012; Savage et al., 2017).~~

We also added a more detailed description on the L-ToF-AMS instrument to Section 2.3. "Additional Instrumentation at SMEARII":

The size-resolved chemical composition of ambient aerosol was measured with the L-ToF-AMS. Its application in the same campaign has been described in Paramonov et al. (2020). It builds on the functionality and characteristics of the high-resolution ToF-AMS (DeCarlo et al., 2006). However, due to the longer time-of-flight chamber, the L-ToF-AMS, has a better resolution (8000 M/ΔM) than the standard ToF-AMS (2000 M/ΔM in V-mode). Detailed descriptions of the instrument, measurements and data processing are available in other publications (Canagaratna et al., 2007; DeCarlo et al., 2006). In general, the L-ToF-AMS measures the size-resolved, non-refractory composition of submicron aerosols, including organic, sulfate, nitrate, ammonium and chloride. The aerodynamic lens has a 100% transmission range of 75-650 nm (in vacuum aerodynamic diameter; Liu et al. (2007)) and focuses particles into a narrow beam that impacts the surface of a porous tungsten vaporizer heated to 600°C, followed by ionization by a 70eV electron source. Ions are detected by a long time-of-flight mass analyzer (Tofwerk AG). The sample flow of 0.09 l min^{-1} is extracted from an extra suction flow (3 l min^{-1}) that is used to avoid aerosol losses in the inlet line. A PM2.5 cyclone mounted at the inlet removes large particles to avoid clogging the critical orifice (100µm), and before entering the L-ToF-AMS, the samples are dried by a Nafion dryer to keep the RH below 30%.

The L-ToF-AMS data were analyzed using standard ToF-AMS data analysis toolkits (Squirrel V1.61B and PIKA1.21B) using Igor Pro software (V6.37, WaveMetrics Inc.). To calculate mass concentrations an ionization efficiency (IE) was determined using 300 nm, size-selected, dry ammonium nitrate particles, and a relative ionization efficiency (RIE) for ammonium of 3.7 was determined. The default relative ionization efficiency (RIE) values of 1.1, 1.2, 1.3 and 1.4 for nitrate, sulfate, chloride and organics, respectively, were applied. A composition-dependent collection efficiency (CE) was applied based on the principles proposed by Middlebrook et al. (2012).

We also added the following text to the discussion on Figure 4 (old Figure 3b) to Section 3.2 "Comparison to meteorology ad aerosol properties" to give more information about the measured organics:

The non-refractory organic components measured by the AMS include the commonly observed primary organic aerosol (POA) and oxygenated organic aerosol (OOA).

WIBS vs. APS: We have included a new Figure in the Appendix (Figure A3) showing the size distributions measured with the APS/DMPS (red) and the WIBS (blue) from 11 March 2018 to 13 May 2018. In each panel, one size distribution per month is highlighted to better show the agreement between WIBS and APS/DMPS measurements.
A description of this Figure has been added to section 2.3 "Additional Instrumentation at SMEARII":

Daily size distributions measured by the DMPS and APS combination are compared with the size distributions measured by the WIBS from 11 March 2018 to 13 May 2018 and are shown in Figure A3. Note, that the WIBS only measures particles larger than 0.5 µm. In summer, WIBS tends to measure slightly more particles with diameters larger than about 3 µm compared to the APS. However, the size distributions agree well for the other time periods and the smaller size ranges.

SECTION 3 RESULTS AND DISCUSSION Figure 1 is nearly impossible to read, consider expanding this figure to take up the full page and also increase font sizes for the axes.

We have increased the size of the axis description in Figure 1.

L200-204 – are the increases in INPs, organic aerosol, and fluorescent particles statistically significant? I'm not sure I would consider the organic and fluorescent particle concentrations to demonstrate "clear increases".

We agree that the increase in organic and fluorescent particle concentrations are not as pronounced as the increase in INP concentration. We have therefore reformulated the description:

Both, the organic aerosol mass concentration measured by L-ToF-AMS and the number concentration of PM10 fluorescent particles measured by WIBS, tend to increase ~~show clear increases~~ during the transition period from winter to summer (Fig. 4a and b).

Figure 3 – It looks as though the INP data are smoothed significantly in Figure 3a. This is especially clear when one compared the subfigure (Figure 3b) with the rest of the timeline. what kind of curve is fit to the INP data in Figure 3a? If there is no curve, why is it so smoothed? The daily data or monthly averages as points with standard deviations would be a better, more clear, way of visualizing the data.

INP data are represented as monthly averages in Figure 3a, as are the other data (NPF events, pollen and other PBAP). We have adapted the suggestion to not draw a smoothed line, but to draw points of the averaged INP concentrations with the standard deviation as error bars. Thanks for this suggestion!

L208 – This section is title" Comparison to meteorology and aerosol properties", yet only temperature and snow cover are compared. Are there other ambient variables that are correlated, for example relative humidity & winds? It is possible that relative humidity or winds may impact emissions?

Thanks for this comment. Other referees are also interested in comparisons with other meteorological variables, and therefore we have extended Figure 4 (in the new version, this is Figure 5) by including three additional panels showing the time series of RH (Fig. 5c), wind speed (Fig. 5d) and precipitation (Fig. 5e) and have ajusted the description accordingly. We have included the following section in the manuscript:

Figure 5c shows the comparison of the INP time series with the time series of relative humidity (RH) measured 35 m above ground. Over the entire time period, no clear relationship between RH and INP concentrations is observed. For a shorter time period from June 2018 to September 2018, there seems to be some correlation of the INP concentration with the RH, during which the peaks in INP concentration in June corresponds to a RH peak. In Figure 5d, we compare the time series of INP

concentrations with the time series of wind speed measured 34 m above the ground, which is also above the forest canopy. A relationship between measured INP concentrations and wind speed is not observed. In Figure 5e, the time series of INP concentration is compared to the occurrence of precipitation. Although other studies like Prenni et al. (2013), Huffman et al. (2013) and Iwata et al. (2019) report increasing INP concentrations during and after rain events in forested sites, we do not consistently observe this behavior. In this respect, increased INP concentrations are observed only during two of the strongest precipitation events in June and September 2018. However, it should be noted that in the cited studies INP concentrations were measured with higher time resolutions from minutes to hours. Huffman et al. (2013) reported increased INP and biological particle concentrations during rain events and up to one day after rain events. With our sampling (and therefore averaging) time of 24 hours or more, rain-induced enhancements of INP concentrations may have been missed. Therefore, this type of sampling strategy may not be appropriate to deterministically link INP concentrations with rain events.

Finally, when considering the full time period of this study, we did not find clear correlations of the INP concentrations with other parameters like the relative humidity, the wind speed or precipitation events. We do not exclude that the INP concentrations measured in the boreal forest are influenced by precipitation events for the whole year. However, our sampling set up is not appropriate to investigate the relationship more precisely.

L258 – While heating does remove a significant portion of the ice nucleation activity, I think it is important for the authors to also acknowledge that the heat-resistant residual is still associated with significant INP numbers. That is, the INP population is not just heat-labile and may not be entirely biological. I think the way the manuscript is currently written indicates that all INPs are biological, but that is not supported by Figure 5, where there are still significant INPs remaining after heating the samples.

Thanks for this comment. As the INP concentrations are significantly reduced after heat-treatment (about two orders of magnitude lower), we concluded that the majority of INPs in our samples are heat-sensitive, what indicates biogenic origin. However, we agree that this does not mean that **all** INPs have to be of biogenic origin. We therefore choose not state that **all** INPs are biogenic, but that the **majority** seems to be of biogenic origin or that boreal forest INP populations **seem to be dominated** by biogenic particles. To address this more clearly in the manuscript, we have added the following text to Section 3.3 “Heat treatment tests”:

As a significant number of residual heat-resistant INPs is still remaining after heat treatment, this indicates that not all measured INPs are associated with heat-labile biogenic materials. However, the majority of the INP population seems to be dominated by heat-labile materials, which is shown by the systematic shift in INP-temperature spectra.

L272 – “: : : as they do not include seasonal dependencies.” – this is not necessarily the case. Seasonal variability in INP abundances is accounted for by being linked to aerosol amount (in these cases n500 or nFBAP), which have seasonal variability.

That is correct, thank you. We have removed the second part of this sentence:

The predictions of DeMott et al. (2010) and Tobo et al. (2013) overestimate INP concentrations especially in wintertime~~, as they do not include seasonal dependencies~~.

L267 - I understand the WIBS was used to determine the fluorescent biological aerosol particles (FBAPs); How does this method compare to the UV-APS used in the Tobo et al. (2013) study? Given the number of uncertainties associated with measuring fluorescent measurements, can the authors describe the possible differences between the UV-APS and WIBS and how that would impact the performance of the Tobo et al. (2013) parameterization? Also, how does the Boreal forest in this study differ from that measured in Tobo et al. (2013)?

In general, the UV-APS operates with only one light source (excitation wavelength of 355 nm) and one detection channel (wavelength range of 420-575 nm), which reduces the classification power compared to WIBS. The excitation wavelengths of WIBS are 280nm and 370nm, with detection channels at 310 – 400 nm and 420 – 650 nm and thus the wavelengths of the two instruments also do not agree. For the application of the Tobo et al. (2013) parameterization, we used the WIBS data with excitation wavelength of 370nm and detection channel of 420 – 650nm (FL3), as this comes closest to the set-up of the UV-APS used in Tobo et al. (2013). Besides the elastic light scattering and fluorescence, the UV-APS measures the Aerodynamic particle size (which WIBS does not). Further, UV-APS does not perform any scheduled background "empty chamber" fluorescence check, instead it must be manually checked and calibrated using manual laser power and PMT gain adjustments. Furthermore, the UV-APS is discontinued and TSI no longer supports the instrument.

Concerning the forest around the measurement sites, both are dominated by pine trees and are far from anthropogenic sources. In both studies, it is assumed that the abundant aerosol population is mainly influenced by the forest and emissions from the vegetation. Differences are that the location in Tobo et al. (2013) is in Colorado, America and therefore at lower latitude than the Finnish forest. The dominant pine species in this lower latitudes is ponderosa pine. The Finnish forest is dominated by a different pine species called Scots pine.

Finally, potential differences in the Tobo et al. (2013) and our study, which could impact and explain the performance of the Tobo et al. (2013) parameterization, are the different wavelengths used in the UV-APS and the WIBS, the different latitudes, the different pine species or simply the season in which the measurements have been conducted. The parameterization in Tobo et al. (2013) is based on measurements conducted in the North American monsoon season from July to August 2011. The HyICE-2018 campaign took place from March to May 2018. In this time period, we do not observe a relation of INP concentrations to FL3 fluorescent particle concentrations. It cannot be excluded that this relation becomes stronger in the summer months, as it is observed in Tobo et al. (2013).

Figure 6 – I think it would be helpful to mention that only data from the HyICE-2018 period were possible to use in the Tobo et al. (2013) (2) parameterization and therefore that panel has fewer points.

Thanks for this suggestion. We have added the following text to Section 3.4 Parameterizations:

Note for the application of the Tobo et al., (2013) parameterization using FBAP concentrations, only data from the HyICE-2018 time period could be used, as the fluorescence measurements from the WIBS are only available in this period. Therefore, the number of data points in Fig. 7c is lower than in the other panels.

L295 – Should clearly state that this parameterization is based on ground-level ambient temperature, not "ambient temperature". If T is described as ambient temperature, a model will implement this as

the temperature predicted at any level, which I do not think is the intention. Additionally, while I understand the impressive correlation between
INP and ambient temperature is inviting for a parameterization, I caution the authors in publishing this as an INP parameterization given that it is highly specific to this location and has not been tested for other years, or is not really supported by a physical mechanism.
For example, aerosol-based INP parameterizations have a physical mechanism
– an aerosol particle that is seasonally variable with an assumed ice nucleation density.
The second parameterization presented in this paper has more physical meaning, linking INP abundance to the physical process of snow melting and exposed surface emissions. Without a clear physical basis for a "ground-level temperature-based" parameterization, I would recommend removing this.

The "ground-level temperature-based" parameterization is an empirical description of the INP concentration at ground level. It is not a theory, which tries to describe the physical mechanisms and processes behind the observed INP. Thus, this parameterization is not an explanation of the complex processes that result in observed INP occurrences. This formulation can still be useful as a technical basis for atmospheric models, which could help to improve the representation of atmospheric INP concentration by using the ground-level ambient temperature. The models will not manage to describe the real physical processes behind aerosol particle behaviors as this is very complex and any model cannot resolve the involved time scales. We therefore suggest this parameterization to technically describe INP concentrations in models and to test it and develop it in further studies.

We added "ground-level" to all passages where we discuss the ambient air temperature to make clear, that we do not use ambient air temperature in other higher altitudes. Thanks for this comment!

L311 – What is T in this equation?

Thanks for this question. T is the activation temperature of the ice-nucleating particles. As this explanation is missing in the manuscript, we have added the following text right after Eq. (2):

[…], where T is the activation temperature of INPs.

References:

Canagaratna, M. R., Jayne, J. T., Jimenez, J. L., Allan, J. D., Alfarra, M. R., Zhang, Q., Onasch, T. B., Drewnick, F., Coe, H., Middlebrook, A., Delia, A., Williams, L. R., Trimborn, A. M., Northway, M. J., DeCarlo, P. F., Kolb, C. E., Davidovits, P. and Worsnop, D. R.: Chemical and microphysical characterization of ambient aerosols with the aerodyne aerosol mass spectrometer, Mass Spectrom. Rev., 26(2), 185–222, doi:10.1002/mas.20115, 2007.

DeCarlo, P. F., Kimmel, J. R., Trimborn, A., Northway, M. J., Jayne, J. T., Aiken, A. C., Gonin, M., Fuhrer, K., Horvath, T., Docherty, K. S., Worsnop, D. R. and Jimenez, J. L.: Field-deployable, high-resolution, time-of-flight aerosol mass spectrometer, Anal. Chem., 78(24), 8281–8289, doi:10.1021/ac061249n, 2006.

DeMott, P. J., Prenni, A. J., Liu, X., Kreidenweis, S. M., Petters, M. D., Twohy, C. H., Richardson, M. S., Eidhammer, T. and Rogers, D. C.: Predicting global atmospheric ice nuclei distributions and their impacts on climate, Proc. Natl. Acad. Sci. U. S. A., 107(25), 11217–11222, doi:10.1073/pnas.0910818107, 2010.

Heald, C. L. and Spracklen, D. V.: Atmospheric budget of primary biological aerosol particles from

fungal spores, Geophys. Res. Lett., 36(9), doi:10.1029/2009GL037493, 2009.

Hoose, C., Kristjánsson, J. E. and Burrows, S. M.: How important is biological ice nucleation in clouds on a global scale?, Environ. Res. Lett., 5(2), 1–7, doi:10.1088/1748-9326/5/2/024009, 2010.

Huffman, J. A., Prenni, A. J., Demott, P. J., Mason, R. H., Huffman, J. A., Prenni, A. J., Demott, P. J., Pöhlker, C., Mason, R. H., Robinson, N. H., Fröhlich-Nowoisky, J., Tobo, Y., Després, V. R., Garcia, E., Gochis, D. J., Harris, E., M ¨ Uller-Germann, I., Ruzene, C., Schmer, B., Sinha, B., Day, D. A., Andreae, M. O., Jimenez, J. L., Gallagher, M., Kreidenweis, S. M., Bertram, A. K. and Pöschl, U.: High concentrations of biological aerosol particles and ice nuclei during and after rain, Atmos. Chem. Phys, 13, 6151–6164, doi:10.5194/acp-13-6151-2013, 2013.

Iwata, A., Imura, M., Hama, M., Maki, T., Tsuchiya, N., Kunihisa, R. and Matsuki, A.: Release of highly active ice nucleating biological particles associated with rain, Atmosphere (Basel)., 10(10), 1–13, doi:10.3390/atmos10100605, 2019.

Liu, P. S. K., Deng, R., Smith, K. A., Williams, L. R., Jayne, J. T., Canagaratna, M. R., Moore, K., Onasch, T. B., Worsnop, D. R. and Deshler, T.: Transmission Efficiency of an Aerodynamic Focusing Lens System: Comparison of Model Calculations and Laboratory Measurements for the Aerodyne Aerosol Mass Spectrometer, Aerosol Sci. Technol., 41(8), 721–733, doi:10.1080/02786820701422278, 2007.

Middlebrook, A. M., Bahreini, R., Jimenez, J. L. and Canagaratna, M. R.: Evaluation of composition-dependent collection efficiencies for the Aerodyne aerosol mass spectrometer using field data, Aerosol Sci. Technol., 46(3), 258–271, doi:10.1080/02786826.2011.620041, 2012.

Paramonov, M., Drossaart Van Dusseldorp, S., Gute, E., Abbatt, J. P. D., Heikkilä, P., Keskinen, J., Chen, X., Luoma, K., Heikkinen, L., Hao, L., Petäjä, T. and Kanji, Z. A.: Condensation/immersion mode ice-nucleating particles in a boreal environment, Atmos. Chem. Phys, 20, 6687–6706, doi:10.5194/acp-20-6687-2020, 2020.

Perring, A. E., Schwarz, J. P., Baumgardner, D., Hernandez, M. T., Spracklen, D. V., Heald, C. L., Gao, R. S., Kok, G., McMeeking, G. R., McQuaid, J. B. and Fahey, D. W.: Airborne observations of regional variation in fluorescent aerosol across the United States, J. Geophys. Res. Atmos., 120(3), 1153–1170, doi:10.1002/2014JD022495, 2015.

Prenni, A. J., Tobo, Y., Garcia, E., DeMott, P. J., Huffman, J. A., McCluskey, C. S., Kreidenweis, S. M., Prenni, J. E., Pöhlker, C. and Pöschl, U.: The impact of rain on ice nuclei populations at a forested site in Colorado, Geophys. Res. Lett., 40(1), 227–231, doi:10.1029/2012GL053953, 2013.

Savage, N., Krentz, C., Könemann, T., Han, T. T., Mainelis, G., Pöhlker, C. and Huffman, J. A.: Systematic characterization and fluorescence threshold strategies for the Wideband Integrated Bioaerosol Sensor (WIBS) using size resolved biological and interfering particles, Atmos. Meas. Tech. Discuss., 10, 4279–4302, 2017.

Schmale, J., Henning, S., Henzing, B., Keskinen, H., Sellegri, K., Ovadnevaite, J., Bougiatioti, A., Kalivitis, N., Stavroulas, I., Jefferson, A., Park, M., Schlag, P., Kristensson, A., Iwamoto, Y., Pringle, K., Reddington, C., Aalto, P., Äijälä, M., Baltensperger, U., Bialek, J., Birmili, W., Bukowiecki, N., Ehn, M., Fjæraa, A. M., Fiebig, M., Frank, G., Fröhlich, R., Frumau, A., Furuya, M., Hammer, E., Heikkinen, L., Herrmann, E., Holzinger, R., Hyono, H., Kanakidou, M., Kiendler-Scharr, A., Kinouchi, K., Kos, G., Kulmala, M., Mihalopoulos, N., Motos, G., Nenes, A., O'Dowd, C., Paramonov, M., Petäjä, T., Picard, D., Poulain, L., Prévôt, A. S. H., Slowik, J., Sonntag, A., Swietlicki, E., Svenningsson, B., Tsurumaru, H., Wiedensohler, A., Wittbom, C., Ogren, J. A., Matsuki, A., Yum, S. S., Myhre, C. L., Carslaw, K., Stratmann, F. and Gysel, M.: Collocated observations of cloud condensation nuclei, particle size distributions, and chemical composition, Sci. Data, 4(1), 1–27, doi:10.1038/sdata.2017.3, 2017.

Tobo, Y., Prenni, A. J., Demott, P. J., Huffman, J. A., McCluskey, C. S., Tian, G., Pöhlker, C., Pöschl, U. and Kreidenweis, S. M.: Biological aerosol particles as a key determinant of ice nuclei populations in a

forest ecosystem, J. Geophys. Res. Atmos., 118(17), 10100–10110, doi:10.1002/jgrd.50801, 2013.

Vali, G.: Quantitative evaluation of experimental results on the heterogeneous freezing nucleation of supercooled liquids, J. Atmos. Sci., 28(3), 402–409, doi:10.1175/1520-0469(1971)028<0402:qeoera>2.0.co;2, 1971.

Vogel, F.: First field application of a mobile expansion chamber to measure ice nucleating particles, Karlsruhe Insitute of Technology, Karlsruhe, Germany, 2018.

Wright, T. P., Hader, J. D., McMeeking, G. R. and Petters, M. D.: High relative humidity as a trigger for widespread release of ice nuclei, Aerosol Sci. Technol., 48(11), i–v, doi:10.1080/02786826.2014.968244, 2014.

The seasonal cycle of ice-nucleating particles linked to the abundance of biogenic aerosol in boreal forests

Julia Schneider[1], Kristina Höhler[1], Paavo Heikkilä[2], Jorma Keskinen[2], Barbara Bertozzi[1], Pia Bogert[1], Tobias Schorr[1], Nsikanabasi Silas Umo[1], Franziska Vogel[1], Zoé Brasseur[3], Yusheng Wu[3], Simo Hakala[3], Jonathan Duplissy[3,7], Dmitri Moisseev[3], Markku Kulmala[3], Michael P. Adams[4], Benjamin J. Murray[4], Kimmo Korhonen[5], Liqing Hao[5], Erik S. Thomson[6], Dimitri Castarède[6], Thomas Leisner[1], Tuukka Petäjä[3], and Ottmar Möhler[1]

[1]Institute of Meteorology and Climate Research, Karlsruhe Institute of Technology, Karlsruhe, Germany
[2]Aerosol Physics Laboratory, Physics Unit, Faculty of Engineering and Natural Sciences, Tampere University, Tampere, Finland
[3]Institute for Atmospheric and Earth System Research/Physics, Faculty of Science, University of Helsinki, Helsinki, Finland
[4]Institute for Climate and Atmospheric Science, School of Earth and Environment, University of Leeds, Leeds, UK
[5]Department of Applied Physics, University of Eastern Finland, Kuopio, Finland
[6]Department of Chemistry and Molecular Biology, Atmospheric Science, University of Gothenburg, Gothenburg, Sweden
[7]Helsinki Institute of Physics, University of Helsinki, Helsinki, Finland

Correspondence to: Ottmar Möhler (ottmar.moehler@kit.edu)

Abstract. Ice-nucleating particles (INPs) trigger the formation of cloud ice crystals in the atmosphere. Therefore, they strongly influence cloud microphysical and optical properties, as well as precipitation and the life cycle of clouds. Improving weather forecasting and climate projection requires an appropriate formulation of atmospheric INP concentrations. This remains challenging, as the global INP distribution and variability depend on a variety of aerosol types and sources, and neither their short-term variability nor their long-term seasonal cycles are well covered by continuous measurements. Here, we provide the first year-long set of observations with a pronounced INP seasonal cycle in a boreal forest environment. Besides the observed seasonal cycle in INP concentrations with a minimum in wintertime and maxima in early and late summer, we also provide indications for a seasonal variation in the prevalent INP type. We show that the seasonal dependency of INP concentrations and prevalent INP types is most likely driven by the abundance of biogenic aerosol. As current parameterizations do not reproduce this variability, we suggest a new parameterization approach, which considers the seasonal variation of INP concentrations. For this, we use the ground-level ambient air temperature as a proxy for the season which affects the source strength of biogenic emissions and by that the INP abundance over the boreal forest areas. Furthermore, we provide new INP parameterizations based on the Ice Nucleation Active Surface Site (INAS) approach, which specifically describes the ice nucleation activity of boreal aerosols particles prevalent in different seasons. Our results characterize the boreal forest as an important but variable INP source and provide new perspectives to describe these new findings in atmospheric models.

1 Introduction

Cloud processes are of particular importance for the evolution of weather and climate, as they regulate the global distribution of precipitation and influence Earth's radiative budget (Hoose and Möhler, 2012; Murray et al., 2012). Ice-nucleating particles (INPs) trigger the formation of ice crystals in clouds (Pruppacher and Klett, 2010), and therefore influence cloud microphysical and optical properties, as well as the lifetimes of mixed-phase and ice clouds (Hoose and Möhler, 2012). However, cloud processes remain highly uncertain in weather forecasting and climate projections (Boucher et al., 2013), also due to a lack of understanding of the critical parameters that predict atmospheric INP concentrations. The proportion of aerosol particles, which can act as INPs generally increases with decreasing temperature, as the free energy barrier to nucleation is reduced. Early parameterizations therefore linked INP or primary ice formation in clouds solely to temperature without any link to aerosol properties (Cooper, 1986; Fletcher, 1962; Meyers et al., 1992). More recent studies suggest a dependence of the INP number

concentration on aerosol concentrations in specific size ranges (DeMott et al., 2010; Tobo et al., 2013), air mass origin (McCluskey et al., 2018) and rain events (Huffman et al., 2013; Iwata et al., 2019; Prenni et al., 2013, Stopelli et al., 2015, (Stopelli et al., 2017)). Others suggest aerosol type-specific descriptions (Harrison et al., 2019; Ullrich et al., 2017; Wilson et al., 2015), e.g. by linking the ice nucleation ability of the aerosol type to the aerosol surface area (Harrison et al., 2019; Ullrich et al., 2017). Due to the abundance of diverse atmospheric INP types distributed over the globe, it is not possible to find a direct dependence of INPs on a single parameter, which could be used to describe and predict primary ice formation processes. Long-range transport of aerosol particles as well as local sources and sinks influence INP populations and are potentially in flux due to both anthropogenic and natural influences like seasonal cycles. To examine the impact of seasonal changes on the INP population, continuous long-term measurements are necessary, but currently lacking. Only a few studies report atmospheric INP data collected in different seasons and resolve seasonal trends. (Hartmann et al., 2019; Schrod et al., 2016; Tobo et al., 2019; Wex et al., 2019), Hartmann et al. (2019) report INP concentrations from the past 500 years derived from ice core samples collected at two Arctic sites. These measurements do not show a long-term trend of INP concentrations over their multiyear period, but the variability within a year is observed to be large. They do suggest indications that biological INPs contribute to Arctic INP populations throughout the past centuries, for example the general shape of the INP spectra and high INP concentrations at relatively high temperatures are typically associated with biological materials. Although they did not find a statistically significant seasonal variation, they assume that it is likely that the strength of local biological particle sources is enhanced during a particular time of the year influencing the INP variability. However, due to the time resolution and dating uncertainty a seasonal relation could not be explicitly shown. Tobo et al. (2019) also report INP concentrations measured at an Arctic station in Svalbard in July 2016 and March 2017, which show seasonal changes with enhanced values in summertime. Tobo et al. (2019) link these enhanced concentrations to the emission of high-latitude dust from glacial outwash plains. Šantl-Temkiv et al. (2019) report INP measurements from the Arctic in spring 2015 and spring and summer 2016 and also show higher INP concentrations in summer than in spring, which they also associate with biological aerosol and biogenic compounds. In another study of pan-Arctic INP, Wex et al. (2019) report INP concentrations from four Arctic stations for different time periods and time resolutions measured between 2012 and 2016. At all locations, the highest observed INP concentrations are recorded in the summer months from June to September. The nature of the INPs was not explicitly determined, but high INP concentrations observed at high activation temperatures indicate a contribution from biogenic material. Wex et al. (2019) suggest potential INP source regions mainly on open land and open water. Stopelli et al. (2015) presents INP concentrations measured from snow samples collected at the Jungfraujoch on a few days per month in the period from December 2012 to September 2013. Here, INP concentrations are again higher in the summer months. Based on this dataset, a model to predict INP concentrations at the Jungfraujoch was established by Stopelli et al. (2016) and validated using several precipitation samples collected between May and October 2014. The dataset from 2014 shows a completely different seasonal pattern than the 2012/2013 dataset with the lowest values during summer and maxima in May and October. The authors suggest these maxima are related to a Saharan dust event and a cold front passage. Schrod et al. (2020) describe a global network of four INP sampling stations, at a range of northern hemisphere latitudes, where atmospheric aerosol samples were collected on substrates for two years from September 2014. The substrates were analysed for deposition and condensation mode INPs using the FRIDGE isothermal static diffusion chamber (Schrod et al., 2020). The Schrod et al. (2020) results do not yield a clear seasonality but instead show that short-term variability overwhelms long term trends. That observation may not, however, represent the full picture of INP in those locations. The short sampling times (low volumes, 1 hr per day) and/or colder activation temperatures may serve to maximize sampling variability and mask any potential biological signal (Schrod et al. 2020). To-date these studies present the first observations and indications of the seasonal variability of INP concentrations, addressing the need for more long-term INP observations. None of these studies presents a comprehensive analysis of continuously recorded INP data for a full seasonal cycle at one location without interruptions. Moreover, the focus of most of the previous studies except for the Schrod et al. (2020) study was especially at Arctic INPs. In this study, we present

a long-term record of INP measurements for more than a full seasonal cycle at a location in the Finnish boreal forest. The boreal forest ecosystem is one interesting environment for such long-term observations, as INP measurements in these areas are currently lacking. Boreal environments are characterized by meteorological conditions, vegetation and radiation budgets with strong seasonal trends and a clear annual cycle. Boreal forests cover 15 million square kilometres, representing one-third of all forested land (Tunved et al., 2006). They are generally far from anthropogenic and dust sources and are characterized by high biogenic aerosol concentrations (Kulmala et al., 2013; Spracklen et al., 2008; Tunved et al., 2006). The vegetation in boreal forests emits primary biological aerosol particles (PBAPs) and biogenic volatile organic compounds (BVOCs), which are prone to form secondary organic aerosol (SOA) (Spracklen et al., 2008), and collectively constitute 'biogenic aerosol'. PBAPs are directly derived from biological organisms, for example spores, pollen, fungi and leaf litter, and are distinct from SOA particles that form via new particle formation (NPF) and grow in size by multicomponent condensation (Ehn et al., 2014; Kulmala et al., 2013). BVOCs are integral as precursors for the NPF events, which are frequently observed in boreal forests (Kulmala et al., 1998, 2001). The frequency of NPF events shows a seasonal variability with a bimodal distribution of peak frequencies in spring and in autumn (Dall'Osto et al., 2018; Kulmala et al., 2001; Nieminen et al., 2014). A similar seasonal trend is observed in PBAP concentrations (Manninen et al., 2014; Schumacher et al., 2013). Several biogenic aerosol types have been shown to have atmospherically relevant ice-nucleating abilities (Augustin et al., 2013; Creamean et al., 2013; Hader et al., 2014; Möhler et al., 2007; Morris et al., 2004; O'Sullivan et al., 2015, 2018; Pratt et al., 2009; Schnell and Vali, 1973) especially at temperatures above -15°C (Christner et al., 2008; Murray et al., 2012). Although the contribution of biogenic INPs to the total global INP abundance is thought to be rather low (Hoose et al., 2010), biogenic aerosol may contribute substantially at regional scales where biological aerosol sources are important. For example, Tobo et al. (2013), Prenni et al. (2009) and O'Sullivan et al. (2018) have observed biogenic aerosol in the INP populations of the forested environments in Colorado, in the Amazon basin and in rural areas in Northern Europe. Furthermore, Pratt et al. (2009) and Creamean et al. (2013) showed that biological particles were frequently present in ice crystal and precipitation residues measured over the western United States and suggested that these particles play a key role in cloud ice formation. In a study about Swedish and Czech birch pollen, Augustin et al. (2013) reported the ice-nucleation activity of sampled macromolecules and formulated new parameterizations for the heterogeneous nucleation rates of two different ice-active macromolecules. However, in general, measuring and parameterizing the IN ability of biogenic particles has proven to be difficult for several reasons. For accurate biogenic INP model simulations, it is critical to understand the global distribution of biogenic INP, their source strength and their aerosolization and atmospheric transport mechanisms (O'Sullivan et al., 2018). It remains unresolved how the microphysical and chemical properties of biogenic aerosol may change during transport processes in the atmosphere. In field studies, which attempt to address these deficiencies, it remains difficult to identify biogenic aerosol particles and to separate them from non-biogenic particles (Möhler et al., 2007). Moreover, there are many biogenic species with a range of properties, which complicate comparisons and generalized parameterizations. ~~(Augustin et al., 2013; Creamean et al., 2013; Hader et al., 2014; Möhler et al., 2007; Morris et al., 2004; O'Sullivan et al., 2015, 2018; Pratt et al., 2009; Schnell and Vali, 1973), especially at temperatures above -15°C (Christner et al., 2008; Murray et al., 2012). Although their contribution to the total global INP abundance is thought to be rather low (Hoose et al., 2010), biogenic aerosol may contribute substantially at regional scales where biological aerosol sources are important. For example, Tobo et al. (2013), Prenni et al. (2009) and O'Sullivan et al. (2018) have observed biogenic aerosol in the INP populations of the forested environments in Colorado, in the Amazon basin and in rural areas in Northern Europe.~~

To address this difficulties in a first approach, we systematically measured INP concentrations at the Station for Measuring Ecosystem-Atmosphere Relations SMEARII (Hari and Kulmala, 2005), which is located in the Finnish boreal forest (61° 50' 50.685"N, 24° 17' 41.206"E, 181 m a.m.s.l.). As the nearest city (Tampere) is located about 60 km west-southwest from the station (Sogacheva et al., 2008) the prevalent aerosol population is mainly influenced by the forest. The boreal forest around the SMEARII station is dominated by Scots pine trees (Hari and Kulmala, 2005). In summer 2018, the canopy height of pines

at SMEARII was determined to be 21.8 m. An extensive set of permanent measurements at the SMEARII contributes to a well-characterized picture of the site including meteorological as well as general aerosol-related information, which are available on the open research data portal AVAA (Junninen et al., 2009). The first comprehensive ice nucleation campaign at SMEARII called HyICE-2018 took place from February 2018 to June 2018. First results from HyICE-2018 are published in Paramonov et al. (2020), who show INP measurements with a continuous flow diffusion chamber (CFDC) during the first part of the HyICE-2018 campaign from 19 February 2018 to 2 April 2018. Here, we present the results of filter-based INP measurements, which provide a continuous record from 11 March 2018 to 13 May 2018 with a consistent time resolution of 24 hours. After these two intensive sampling months during the HyICE-2018 campaign, the INP measurements were continued until 31 May 2019 with a time resolution of mostly 48 hours or 72 hours, and only in a few cases with sample time intervals of up to 144 hours. By this, we obtained a continuous long-term record of INP temperature spectra from 11 March 2018 to 31 May 2019. The main objective of this study is to investigate and describe the variability and seasonal trends in INP concentrations and INP temperature spectra in a boreal forest environment. The absence of anthropogenic and/or dust aerosol sources in the boreal region motivates the additional investigation of biogenic ice nucleation activity and reveals the relevance of boreal forest areas as an important INP source. The comprehensive instrumentation provided at the measurement site at the SMEARII station allows comparisons between INP measurements with simultaneous measurements of many meteorological variables. These measurements are complemented by measurements characterizing the sampled aerosol number concentrations, size distributions and chemical compositions in order to elucidate the potential origin and nature of the INPs. Heat treatments of the suspensions prior to INP analysis also help identifying the nature of INPs. We aim to improve the parameterizations describing atmospheric INP concentrations in the boreal forest by considering seasonal dependences in the formulations. Finally, this study provides motivation for further continuous long-term studies of INP in different environments across the globe.

2 Methods

~~We systematically measured INP concentrations at the Station for Measuring Ecosystem-Atmosphere Relations SMEARII (Hari and Kulmala, 2005), which is located in the Finnish boreal forest (61° 50' 50.685"N, 24° 17' 41.206"E, 181 m a.m.s.l.). As the nearest city (Tampere) is located about 60 km west-southwest from the station (Sogacheva et al., 2008) the prevalent aerosol population is mainly influenced by the forest. An extensive set of permanent measurements at the SMEARII contributes to a well-characterized picture of the site including meteorological as well as general aerosol-related information, which are available on the open research data portal AVAA (Junninen et al., 2009). The first comprehensive ice nucleation campaign at SMEARII called HyICE-2018 took place from February 2018 to June 2018. First results from HyICE-2018 are published in Paramonov et al. (2020), who show INP measurements with a continuous flow diffusion chamber (CFDC) during the first part of the HyICE-2018 campaign from 19 February 2018 to 2 April 2018. In this paper, we present the results of filter-based INP measurements, which provide a continuous record from 11 March 2018 to 13 May 2018 with a consistent time resolution of 24 hours. After these two intensive sampling months during the HyICE-2018 campaign, the INP measurements were continued until 31 May 2019 with a time resolution of mostly 48 hours or 72 hours, and only in a few cases with sample time intervals of up to 144 hours. By this, we obtained a continuous long-term record of INP temperature spectra from 11 March 2018 to 31 May 2019.~~

2.1 Aerosol filter sampling

Ambient aerosol particles were collected on 47 mm Whatman nuclepore track-etched polycarbonate membrane filters with a pore size of 0.2 µm. The filter sampling line and the filter holder are made of stainless steel and were installed in a cottage in

the forest, with a rooftop PM10 inlet connected to the other sampling components installed indoors. The inlet height is approximately 4.6 m above ground and therefore approximately 17.2 m below the forest canopy. A vacuum pump in combination with a critical orifice ensured a constant sampling flow rate of about 11 std l min^{-1}. Because the PM10 inlet provides a precise 10 µm cut-off size for a flow rate of about 16 std l min^{-1}, it is possible that larger particles have also been collected. However, the deviation of total aerosol number and surface concentration from the PM10 concentrations is < 1%~~, as it is shown in the Appendix Fig. A1a~~. We therefore refer to PM10 number concentration and PM10 surface concentration, when comparing the INP concentrations and calculating INAS (Ice Nucleation Surface Site) densities. Filters were pre-cleaned with 10% H_2O_2 and rinsed with deionized water that was passed through a 0.1 µm Whatman syringe filter, before being dried for use in sampling. After sampling, the filters were stored in sterile petri dishes, wrapped in aluminium foil and frozen until the sample were analysed for their INP content.

2.2 INSEKT

The INP content of the collected aerosol samples was quantified using the INSEKT (Ice Nucleation Spectrometer of the Karlsruhe Institute of Technology) method described in Schiebel (2017). The INSEKT is based on an ice spectrometer developed at the Colorado State University, which is described in Hill et al. (2016). INSEKT measures INP concentration as a function of activation temperature in the immersion freezing mode between about 247 K and 268 K. For the INP analysis, the collected aerosol particles are washed from the filter membranes by immersion in 8 ml of nanopure water, which was passed through a 0.1 µm Whatman syringe filter. The sample solution was spun on a rotator for approximately 20 min, and subsequently the aerosol suspension is diluted with 15- and 225-, or 10- and 100-fold volumes of filtered nanopure water. Small volumes of 50 µl are pipetted into two 96-well PCR plates. The wells are partitioned into different groups, including a group for the undiluted suspensions, the two diluted samples, and for the filtered nanopure water that serves to determine background freezing levels. Filter handling and suspension preparation always occurs in a clean flow cabinet using tweezers, which have been pre-cleaned in the same manner as the filter membranes. The filled PCR plates are then placed into the INSEKT instrument, which consists of two aluminium blocks, each with openings for holding a 96 well PCR plate. The aluminium blocks are connected to a chiller (LAUDA Proline RP 890), which pumps ethanol cooling liquid through the aluminium blocks at a constant cooling rate of 0.25 K min^{-1}. Eight evenly distributed temperature sensors measure the temperature distribution inside the blocks with a 2 Hz resolution. The aluminium blocks are placed in a PVC box insulated with 2 cm of Armaflex insulation material. The upper part of the PVC box is equipped with an antireflection and depolarized glass pane covering the PCR plates and preventing contamination from the ambient air. In order to avoid condensation on the glass the interior of the PVC box and the upper side of the glass pane are continuously flushed with particle free synthetic air at a constant flow rate of about 80 l h^{-1}. A camera with a 60 cm focal distance detects brightness changes in the small suspension volumes that are related to freezing during the cooling process. LabView software is used to control and monitor the cooling rate, temperature and brightness changes. Using this setup the frozen fraction of the small aerosol suspension volumes are determined as a function of temperature. From the fraction frozen, the INP concentration per standard litre of sampled air is calculated, binned on a 0.5 K grid and corrected by the background from the filtered nanopure water, using the procedure described in Vali (1971). Error is estimated by determination of 95% confidence intervals using the Wilson score interval (Wilson, 1927) in the form described by Agresti and Coull (1998). Data points with a ratio of upper to lower confidence interval higher than 8 are considered insignificant and neglected. A systematic error due to the preparation process and flow measurements is added. Applying a simple linear error propagation on the formulas given in Vali (1971) and inserting the error-containing parameters like the pipetted suspension volumes and the flow rate~~,~~ systematic errors of~~with~~ 4% for the undiluted suspension, 5% for the first dilution step, 8% for the third dilution step and 11% for the fourth step, are calculated~~ if needed~~. The systematic error increases with each dilution step because the additional pipetting step adds uncertainty. In

addition, INP concentrations derived from handling blank filters, which were collected without flowing air through the membranes, are subtracted.

Heat treatment tests of the collected aerosol samples provide additional information about the heat sensitivity of the containing INPs and have been applied in various previous INP studies (Hill et al., 2016; O'Sullivan et al., 2018; Wilson et al., 2015). For these tests, a test tube filled with 2 ml of the aerosol suspension is kept in boiling water for approximately 20 min. Afterwards, the treated sample is analysed with the INSEKT in the same way as previously described. INAS densities were calculated as described in Eq. (2) in Ullrich et al. (2017), where ice number concentrations are normalized by the aerosol surface area concentration. Assuming that every INP triggers the formation of one ice crystal, the ice number concentrations are equal to the INP concentrations, which are determined by the INSEKT measurements. The aerosol surface area concentrations are derived from continuous size distribution measurements of the PM10 atmospheric aerosol at SMEARII. Details on the size distribution measurements are given in the following section.

2.3 Additional Instrumentation at SMEARII

For characterizing the sampled aerosol particles further, atmospheric aerosol size distributions were continuously measured with a Differential Mobility Particle Sizer (DMPS). The covered size range was 3 nm - 1000 nm in electrical equivalent diameter with 10 min time resolution (Aalto et al., 2001) with a closed loop flow arrangement (Jokinen and Mäkelä, 1997). The instrument was operated following guidelines from Aerosols, Trace Gases, and Clouds Research Infrastructure (ACTRIS) (Wiedensohler et al., 2012). The aerosol sample was taken from 8 m height inside the canopy through a total suspended particle (TSP) inlet. The super-micron aerosol size distribution was determined with a TSI Aerodynamic Particle Sizer (APS) model 3321 for the size range 0.5 - 10 µm in aerodynamic diameter. The sample was drawn through a vertical sampling line to avoid particle losses. The inlet is at a height of 6 m above the ground and consists of a total suspended particle inlet (Digitel Inc.). The inlet was heated to 40°C to prevent condensation and to ensure that fog droplets are evaporated and the RH remains below 40 %.

The intense measurement period during the HyICE-2018 campaign also provides additional aerosol instrumentation, like a long time-of-flight aerosol mass spectrometer (L-ToF-AMS) to measure the aerosol chemical composition and a wideband integrated bioaerosol sensor (WIBS-NEO) ~~(Kaye et al., 2000; Savage et al., 2017)~~ to derive information about biogenic fluorescent aerosol particles. The WIBS-NEO (Droplet Measurement Technologies, Longmont, CO, USA) is a bioaerosol sensor that provides information on the fluorescence properties, size and asphericity ratio of individual aerosol particles. It operates with an inlet flow of 0.3 l min^{-1} and detects particles with diameters between 500 nm and 30 µm. From 11 March 2018 to 2 April 2018, the WIBS was located about 50m from the aerosol filter sampling line used for the INP analysis. There, it was attached to a total aerosol inlet, which is characterized in Vogel (2018). On 3 April 2018, the WIBS was moved and installed directly next to the filter sampling line and attached to a PM10 inlet, which is described in Schmale et al. (2017). For the WIBS data analysis, particles from 0.5 µm to 10 µm were considered. To analyse the fluorescence of the particles, the WIBS sensor utilizes two xenon flashlamps as excitation light sources (optically filtered at wavelengths of 280 nm and 370 nm) and two emission detection channels (wavelength bands 310 – 400 nm and 420 – 650 nm). Optical size information is acquired utilizing elastic scattering from a continuous wave laser with a wavelength of 635 nm and a photomultiplier tube located orthogonally with respect to the laser. The excitation pulses are fired into the sample volume at different times and both detection channels record the emission(s) from both excitations, leading to three distinguishable excitation-emission combinations (the 370 nm light saturates the 310 – 400 nm detection channel and therefore does not provide any information). Thus, the fluorescence can be divided into 7 unique fluorescence groups based on the excitation-emission wavelength pairs and their combinations, after Perring et al. (2015) and Savage et al. (2017): A (only FL1: excitation 280 nm, emission 310 – 400 nm), B (only FL2: excitation 280 nm, emission 420 – 650 nm), C (only FL3: excitation 370 nm, emission 420 – 650 nm),

AB (FL1 + FL2), BC (FL2 + FL3), AC (FL1 + FL3) and ABC (FL1 + FL2 + FL3). The WIBS performs an empty-chamber background signal check every 8 hours, during which the excitation pulses are fired into the optical chamber without any present particles. The background check collects a multitude of emission intensities that form a baseline for particle fluorescence. In this study, a particle is considered fluorescent, if the associated emission peak intensity is larger than $FT + 9\sigma$. FT is the mean value of the forced trigger intensities and σ is their standard deviation. A more commonly used method would be to compare the emission peak intensity to $FT + 3\sigma$. However, some non-biological particle types such as wood smoke, African dust and black carbon are weakly fluorescent and therefore might satisfy the lower threshold value, leading to an overestimation of biological particle concentration. Furthermore, the stricter threshold only marginally affects the detection efficiency of biological particles, because they tend to have stronger fluorescence (Savage et al., 2017). More detailed descriptions on the WIBS are also available in Savage et al. (2017) and Perring et al. (2015).

~~The WIBS provides information about particle size, particle asymmetry and fluorescence emission intensity for particles in the size range 0.5 – 10 µm in diameter. Fluorescence excitation is achieved by two lasers with wavelengths of 280 nm and 360 nm. Two channels record the fluorescence emission in the ranges of 310 nm – 400 nm and 420 nm – 650 nm. A detailed description of the set up and working principle of the L-Tof AMS during the HyICE-2018 campaign can be found in Paramonov et al. (2020).~~ Daily size distributions measured by the DMPS and APS combination are compared with the size distributions measured by the WIBS from 11 March 2018 to 13 May 2018 and are shown in Figure A3. Note, that the WIBS only measures particles larger than 0.5 µm. In summer, WIBS tends to measure slightly more particles with diameters larger than about 3 µm compared to the APS. However, the size distributions agree well for the other time periods and the smaller size ranges. The size-resolved chemical composition of ambient aerosol was measured with the L-ToF-AMS. Its application in the same campaign has been described in Paramonov et al. (2020). It builds on the functionality and characteristics of the high-resolution ToF-AMS (DeCarlo et al., 2006). However, due to the longer time-of-flight chamber, the L-ToF-AMS, has a better resolution (8000 M/ΔM) than the standard ToF-AMS (2000 M/ΔM in V-mode). Detailed descriptions of the instrument, measurements and data processing are available in other publications (Canagaratna et al., 2007; DeCarlo et al., 2006). In general, the L-ToF-AMS measures the size-resolved, non-refractory composition of submicron aerosols, including organic, sulfate, nitrate, ammonium and chloride. The aerodynamic lens has a 100% transmission range of 75-650 nm (in vacuum aerodynamic diameter; Liu et al. (2007)) and focuses particles into a narrow beam that impacts the surface of a porous tungsten vaporizer heated to 600°C, followed by ionization by a 70eV electron source. Ions are detected by a long time-of-flight mass analyzer (Tofwerk AG). The sample flow of 0.09 l min^{-1} is extracted from an extra suction flow (3 l min^{-1}) that is used to avoid aerosol losses in the inlet line. A PM2.5 cyclone mounted at the inlet removes large particles to avoid clogging the critical orifice (100µm), and before entering the L-ToF-AMS, the samples are dried by a Nafion dryer to keep the RH below 30%.

The L-ToF-AMS data were analyzed using standard ToF-AMS data analysis toolkits (Squirrel V1.61B and PIKA1.21B) using Igor Pro software (V6.37, WaveMetrics Inc.). To calculate mass concentrations an ionization efficiency (IE) was determined using 300 nm, size-selected, dry ammonium nitrate particles, and a relative ionization efficiency (RIE) for ammonium of 3.7 was determined. The default relative ionization efficiency (RIE) values of 1.1, 1.2, 1.3 and 1.4 for nitrate, sulfate, chloride and organics, respectively, were applied. A composition-dependent collection efficiency (CE) was applied based on the principles proposed by Middlebrook et al. (2012).

3 Results and Discussion

3.1 INP temperature spectra and time series

All INP temperature spectra measured from 11 March 2018 to 31 May 2019 are shown in Figure 1 in a monthly representation. The INP concentrations range from about 10^{-4} std l^{-1} to 10^{-2} std l^{-1} at the highest and from about 10^{0} std l^{-1} to 10^{2} std l^{-1} at the

lowest temperatures. These concentration values fall within the range of INP concentrations measured during previous globally distributed field studies, which are summarized in Kanji et al., (2017). This indicates that primary ice formation in boreal forest areas is comparable to other regions on Earth, despite the lack of anthropogenic and dust sources. In our study, we observe both INP concentrations and spectral shape to be highly variable from day to day and to show clear seasonal trends. INP temperature spectra in March, December, January and February constitute the lowest of the entirety of INP temperature spectra, whereas the INP temperature spectra with highest INP concentrations are recorded in May and September. Figure 2a depicts the full time series of INP concentrations measured as a function of activation temperature with a time resolution between 24 h and 144 h. The colour contours represent the seasonal cycle of INP concentrations, which are lowest in wintertime from December to March and highest in the summer months, especially during May and September, as it was already observed in Fig. 1. An additional peak is found in the beginning of July. The INP concentrations in the middle temperature range around 257 K show the most distinct seasonal cycle. The variability of INP concentrations at the lower and upper end of the temperature range is less pronounced. Figure 2b shows the time series of INAS densities, which are calculated by normalizing the INP concentration measured by INSEKT with the aerosol surface concentration of atmospheric PM10 aerosol particles derived from DMPS and APS. The INAS densities show the similar seasonal trend and annual variability as the INP concentrations. For comparison, the time series of PM10 aerosol number concentrations and PM10 aerosol surface concentrations are shown in the Appendix Fig. A1~~b~~.

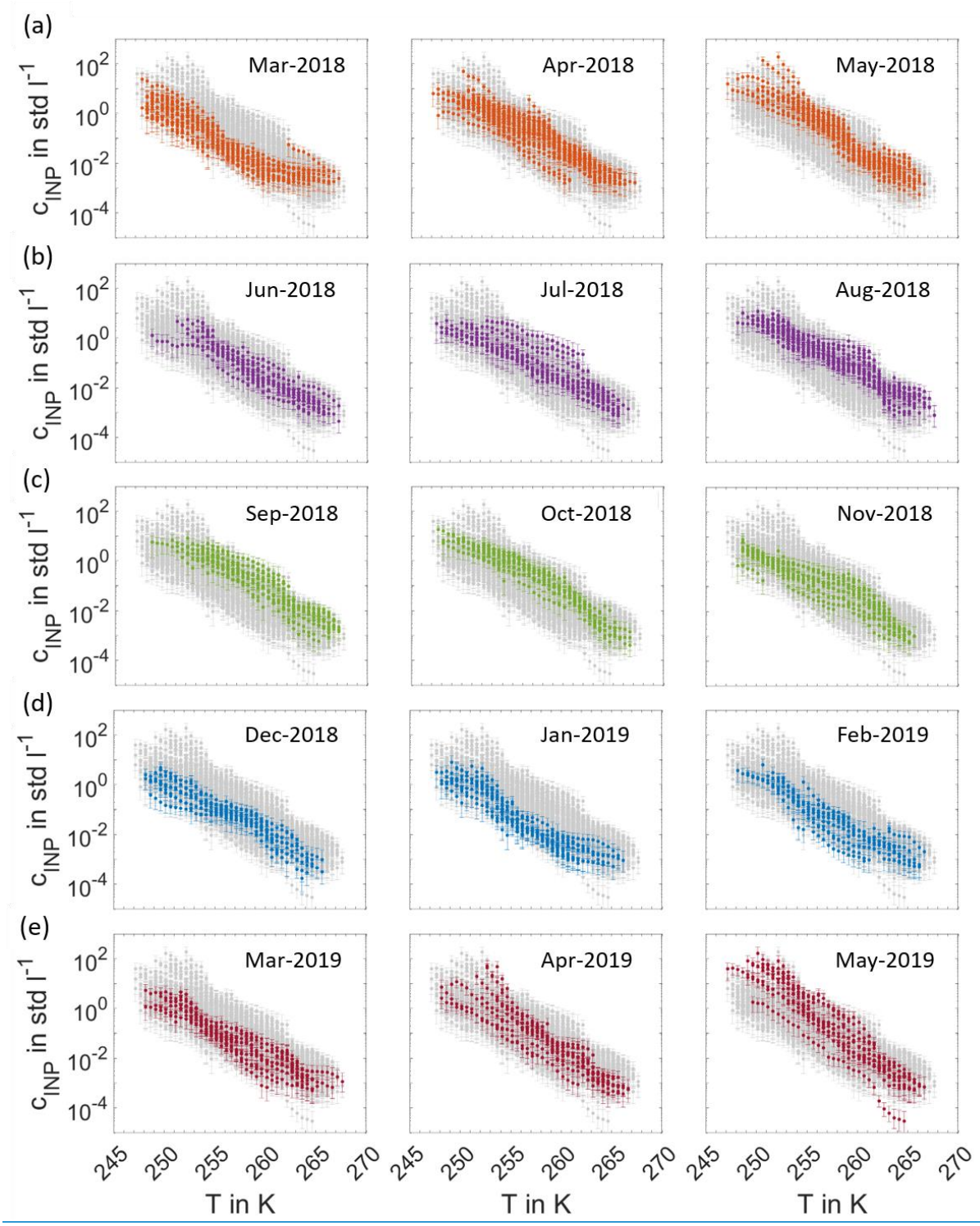
(a)
(b)
(c)
(d)
(e)
Mar-2018
Apr-2018
May-2018
Jun-2018
Jul-2018
Aug-2018
Sep-2018
Oct-2018
Nov-2018
Dec-2018
Jan-2019
Feb-2019
Mar-2019
Apr-2019
May-2019
c_INP in std l^-1
T in K

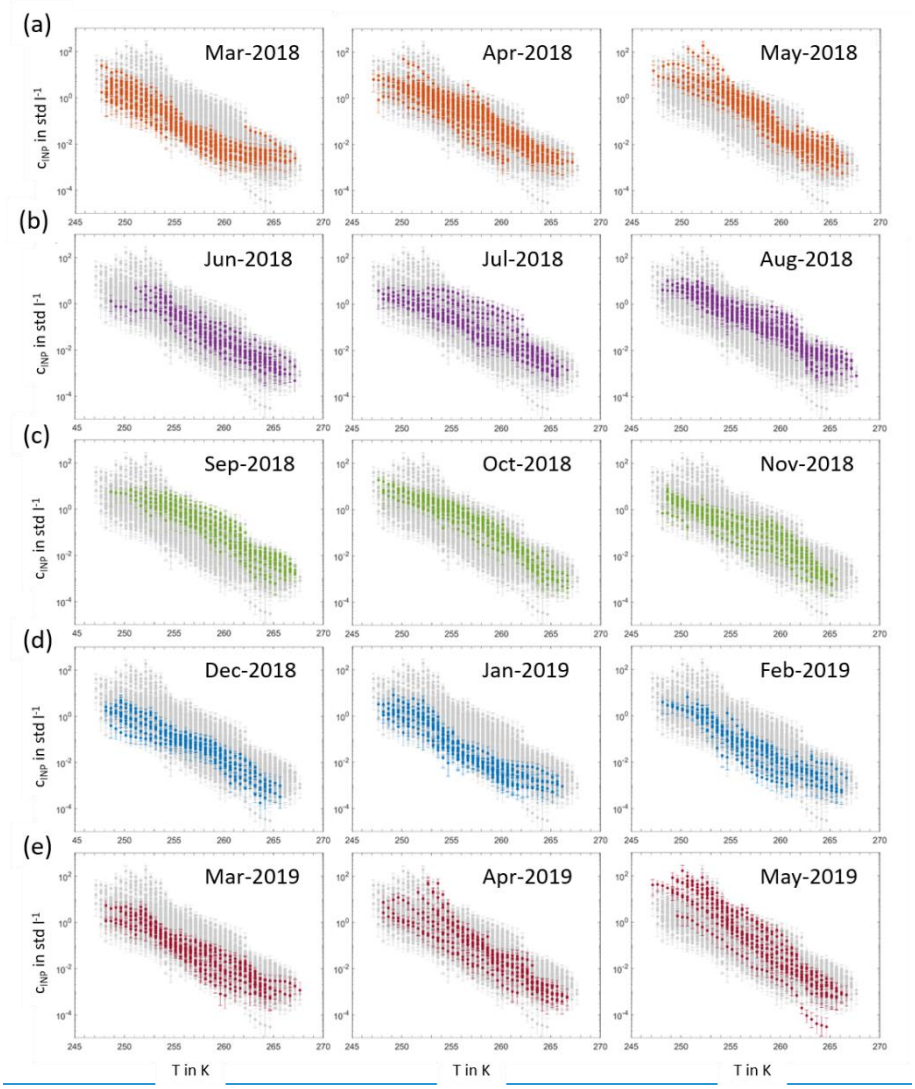

Figure 1: Monthly overview of INP temperature spectra. Each panel shows the entirety of INP temperature spectra measured from 11 March 2018 to 31 May 2019 (grey) with the spectra of the specific month highlighted in colour.

315 ~~Figure 2a depicts the full time series of INP concentrations measured as a function of activation temperature with a time resolution between 24 h and 144 h. The colour contours represent the seasonal cycle of INP concentrations, which are lowest in wintertime from December to March and highest in the summer months, especially during May and September, as it was already observed in Fig. 1. An additional peak is found in the beginning of July. The INP concentrations in the middle temperature range around 257 K show the most distinct seasonal cycle. The variability of INP concentrations at the lower and~~

320 ~~upper end of the temperature range is less pronounced. Figure 2b shows the time series of INAS densities, which are calculated by normalizing the INP concentration measured by INSEKT with the aerosol surface concentration of atmospheric PM10 aerosol particles derived from DMPS and APS. The INAS densities show the similar seasonal trend and annual variability as the INP concentrations. For comparison, the time series of PM10 aerosol number concentrations and PM10 aerosol surface concentrations are shown in the Appendix Fig. A1b.~~

325

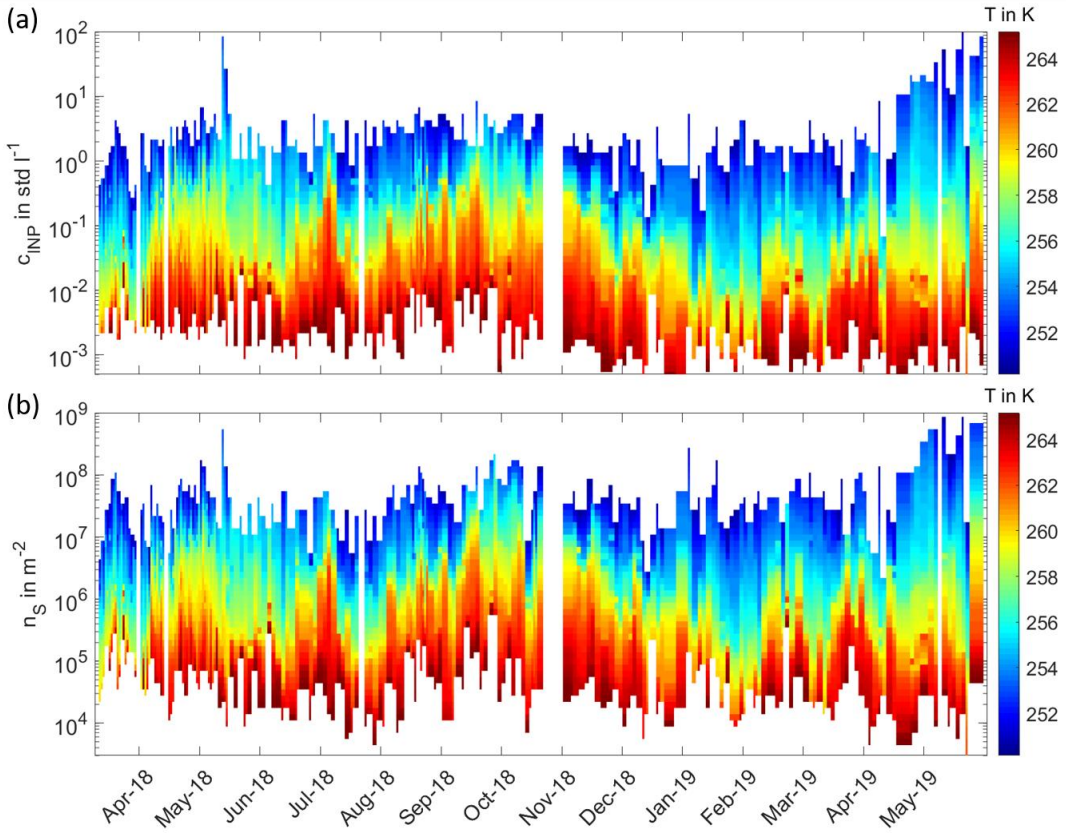

Figure 2: Long term record of INPs from 11 March 2018 to 31 May 2019 in the Finnish boreal forest. Panel (a) shows the time series of INP concentrations c_{INP} with a general temporal resolution between 24h and 144h. The colour code indicates the corresponding activation temperatures in K. In panel (b) the time series auf INAS densities n_S is displayed in the same manner as for the INP concentrations in panel (a).

3.2 Comparison to meteorology and aerosol properties

To investigate factors that influence the abundance of INP and might explain the daily and seasonal variability of INP concentrations, the INP time series are compared with other data sets like meteorological and aerosol data. As the seasonal trends and variability is most pronounced at activation temperatures around 257K, the INP time series at 257 K is used for this comparison. In Fig. 3~~a~~, the monthly averaged INP time series at 257 K is compared with the monthly fraction of NPF event days and snow coverage measured alongside the INP measurements at SMEARII, as well as with the averaged concentrations of pollen and other PBAP. We have defined snow coverage as measured snow depth > 1 cm, where snow depth was measured by a Jenoptik SHM30 snow depth sensor, which is based on an opto-electronic laser distance sensor, in open field about 500m southeast of the aerosol collection area of SMEARII. The analysis of NPF events is based on permanent measurements at SMEARII and was provided by Simo Hakala, University of Helsinki. As there were no simultaneous direct measurements of pollen and other PBAP available for the period of our INP measurements, we compare to pollen and PBAP measured in 2003 and 2004 by Manninen et al. (2014) at SMEARII. Manninen et al. (2014) collected aerosol samples in a Hirst-type volumetric spore trap (Burkard Manufacturing Co. Ltd.; Hirst, 1952), located at SMEARII 3 m above the forest canopy. The trap is driven by a clockwork and collects aerosol particles larger than approximately 3 µm on an adhesive, transparent, plastic tape with a sampling flow rate of approximately 10 l min^{-1}. The analysis of the collected particles was performed according to standard methodology adopted by the Finnish pollen information network and following the principles of the European Aeroallergen Network (www.polleninfo.org/) and Rantio-Lehtimäki et al. (1994). The observed INP peak in spring coincides with the peak in pollen concentrations, whereas the peak in September is found to correlate with enhanced concentrations of other PBAP. Maxima in NPF event fractions are recorded in spring and in autumn, which has also been observed in many previous years back to 1996 (Dall'Osto et al., 2018; Kulmala et al., 2004; Nieminen et al., 2014). Snow-free periods are characterized by relatively high INP concentrations, whereas complete snow cover yields low concentrations. Figure 4~~3~~b shows the INP time

series at 257 K ~~during the~~focussing on the intensive measurement period of the HyICE-2018 campaign from March to May 2018. After a period of rather constant INP concentrations in March, we observe a steady increase of INP concentrations in April, which comes along with the snowmelt period at SMEARII. After the snowmelt, INP concentrations are again on a rather constant but higher level. During the HyICE-2018 period, more comprehensive aerosol characterization was done, including measurements with the~~a~~ L-ToF-AMS and the~~a~~ WIBS shown in Fig. 4a and b. ~~Both, the organic aerosol mass concentration measured by L-ToF-AMS and the number concentration of PM10 fluorescent particles measured by WIBS, show clear increases during the snowmelt period.~~ Here, we define the number concentration of PM10 fluorescent particles as the number concentration of ~~PM10~~ aerosol particles, whose fluorescence emission intensity produces a fluorescent signal in ~~all three laser-channel combinations of WIBS~~the fluorescence group ABC (see Section 2.3 for details on the categorization in fluorescence groups). The time series of the number concentration of particles with a fluorescence signal in other fluorescence groups is shown in the Appendix in Fig. A2. In this Figure, the strongest seasonal increase in the transition period from winter to summer is observed in the group ABC. Consequently, this fluorescent group correlates best with the measured INP concentrations (see Figure 4). The characteristics of each fluorescence group are comprehensively investigated and reported in Savage et al. (2017), who examined the fluorescence emissions of different types of pollen, fungi, bacteria, biofluorophores, dust, HULIS (humic-like substances), PAH (polycyclic aromatic hydrocarbons), soot and brown carbon. Using the $FT + 9\sigma$ threshold for defining a particle as fluorescent, nearly all dust and HULIS types show no fluorescence signal at all. Some of the soot and brown carbon types only show weak signals in A, and B, BC and A, respectively. Nearly all of the bacteria types show fluorescence only in group A. The fluorescence of fungal spores are also mainly detected in group A, but also in AB and ABC. The investigated biofluorophores show mainly fluorescence in the groups BC (Riboflavin, NAD), A (Pyridoxamine), AB (Tryptophan) and ABC (Ergosterol). PAHs show fluorescence mostly in groups ABC and A. Finally, most pollen types show fluorescence in groups ABC and AB. Some pollen types also show a fluorescence signal in groups A and B. Both, the organic aerosol mass concentration measured by the L-ToF-AMS and the number concentration of fluorescent particles measured by WIBS, tend to increase during the transition period from winter to summer (Fig. 4a and b). The number concentration of atmospheric PM10 aerosol presented in Fig. 4c does not show this trend. However, a slight seasonal trend is visible in the PM10 surface concentration (Fig. 4d). The number and surface concentration of PM10 atmospheric aerosol for the whole time period from March 2018 to May 2019 is shown in the Appendix in Fig. A1.

~~Besides a significant correlation of INP concentrations to the snow depth, the ambient air temperature measured in 4 m above ground level also showed a significant correlation.~~ Figure 5~~4~~a depicts ~~the related time series~~the whole time series of INP concentrations in comparison to the measured ground-level ambient air temperature from March 2018 to May 2019~~,~~ which clearly shows the INP time series a~~t 257 K~~ following the course of the ground-level ambient air temperature. Only for ground-level ambient air temperatures about > 15°C, the deviation of the two time series is higher. However, the general seasonal trend in the ground-level ambient air temperature is the same as we observed in the INP time series. Besides a significant correlation of INP concentrations to the ground-level ambient air temperature, the snow depth also showed a significant correlation. Figure 5~~4~~b shows a direct comparison of the INP time series with the measured snow depth. Periods of decreasing INP concentrations clearly overlap with snowmelt periods, whereas an increasing snow depth comes along with increasing INP concentrations. Figure 5c shows the comparison of the INP time series with the time series of relative humidity (RH) measured 35 m above ground. Over the entire time period, no clear relationship between RH and INP concentrations is observed. For a shorter time period from June 2018 to September 2018, there seems to be some correlation of the INP concentration with the RH, during which the peaks in INP concentration in June corresponds to a RH peak. In Figure 5d, we compare the time series of INP concentrations with the time series of wind speed measured 34 m above the ground, which is also above the forest canopy. A relationship between measured INP concentrations and wind speed is not observed. In Figure 5e, the time series of INP concentration is compared to the occurrence of precipitation. Although other studies like Prenni et al. (2013), Huffman et al. (2013) and Iwata et al. (2019) report increasing INP concentrations during and after rain events in

forested sites, we do not consistently observe this behavior. In this respect, increased INP concentrations are observed only during two of the strongest precipitation events in June and September 2018. However, it should be noted that in the cited studies INP concentrations were measured with higher time resolutions from minutes to hours. Huffman et al. (2013) reported increased INP and biological particle concentrations during rain events and up to one day after rain events. With our sampling (and therefore averaging) time of 24 hours or more, rain-induced enhancements of INP concentrations may have been missed. Therefore, this type of sampling strategy may not be appropriate to deterministically link INP concentrations with rain events. In wintertime, complete snow cover seems to suppress biogenic particle emissions, resulting in comparably low INP concentrations. Such a correlation is also supported by the peaks of pollen and PBAP concentrations in snow-free periods in spring and in autumn, and by the increases of the organic aerosol mass concentration and fluorescent particle numbers of group ABC observed in spring. According to the study of Savage et al. (2017), we assume particles of fluorescence group ABC to be mainly pollen, particles containing PAH or Ergosterol, or fungal spores. ~~Fluorescent particles are expected to be primarily of biological origin except for a few percent, which could arise from non-biological materials (Pöhlker et al., 2012; Savage et al., 2017).~~ The non-refractory organic components measured by AMS include the commonly observed primary organic aerosol (POA) and oxygenated organic aerosol (OOA). As the surface concentration of PM10 particles is more sensitive to larger particles, the increase in PM10 surface concentration (see Figure 4d) indicates that the observed seasonal increase may be due to larger particles, which are expected to be mainly of biogenic origin. No day-by-day relation of NPF events and INP peaks are identified, but this is not unexpected given that particles formed during NPF events are initially smaller than 5 nm in diameter and events are more likely when condensation sinks are low (Dada et al., 2017). However, we consider the enhanced NPF event frequency as an indicator of generally higher biological activity in the forest. Enhanced biological activity means more biogenic INP emissions from the vegetation, which agrees with the seasonal dependencies from the previous findings. Any direct impact of NPF events on the boreal forest INP abundance remains uncertain and requires more investigation.

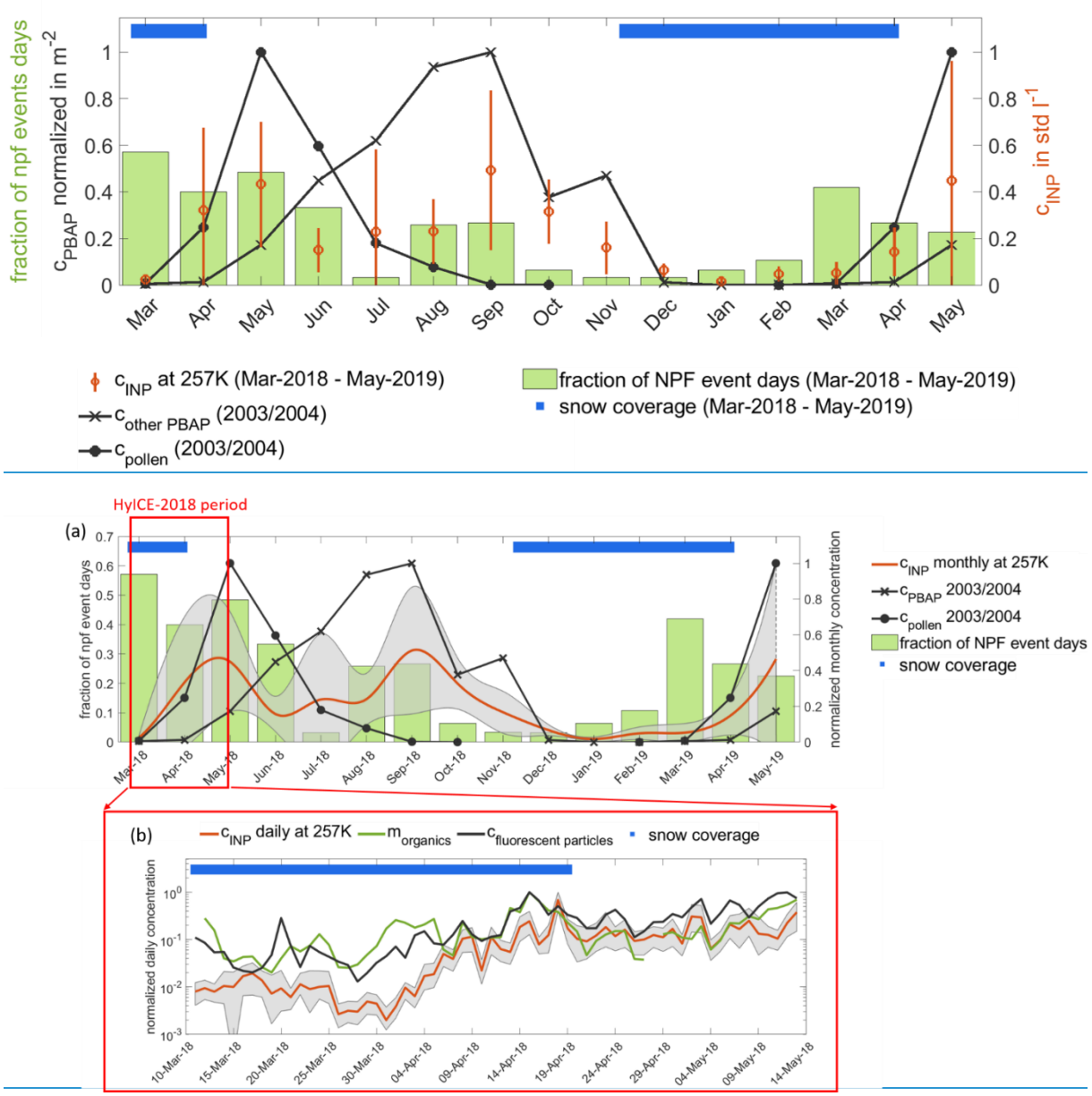

Figure 3: Factors co-varying with INP concentrations. MIn panel (a), monthly averaged INP concentrations at 257 K (red, standard deviation grey shadingin error bars) are compared to the monthly fraction of NPF event days (green bars) from March 2018 to May 2019. Monthly averaged concentrations of PBAP and pollen (black dots and crosses) measured in 2003 and 2004 by Manninen et al. (2014) are additionally displayed. The panel (b) inset shows the HyICE-2018 period including a comparison of daily INP concentrations at 257 K (red, error bar area grey shading) to the mass concentration of organics (green) and to the concentration of fluorescent PM10 aerosol particles with a fluorescence signal in all three WIBS laser-channel-combinations (black). In both panels, The blue bar is indicative of snow coverage.

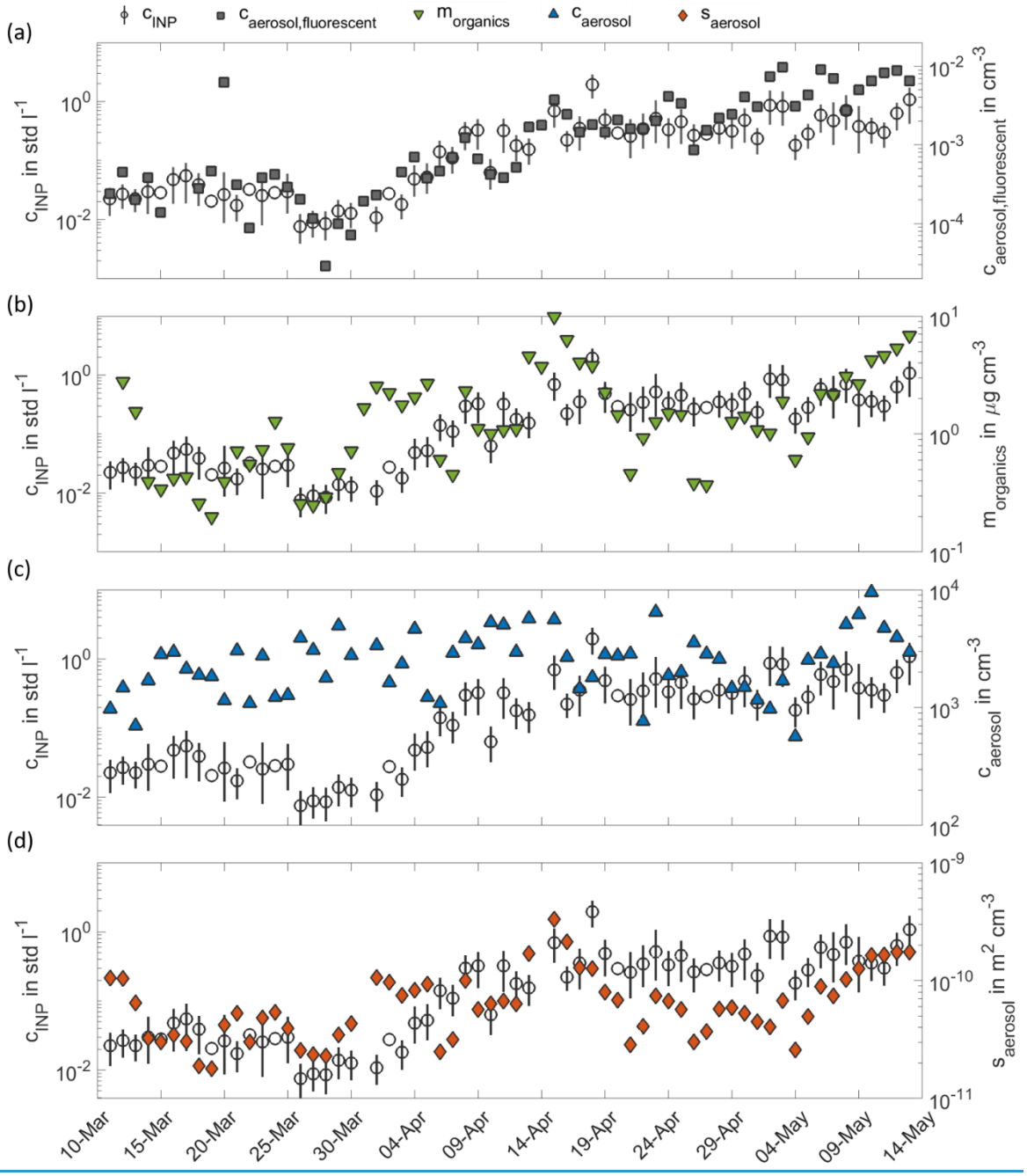

Figure 4: Factors co-varying with INP concentrations in the HyICE-2018 period. In panel (a), INP concentrations at 257 K (circles) are compared to the concentration of fluorescent PM10 aerosol particles with a fluorescence signal in group ABC (grey squares). In panels (b), (c) and (d) the INP concentrations are further compared to the mass concentration of non-refractory organic compounds (green triangles), the number concentration of atmospheric PM10 aerosol (blue triangles) and the surface concentration of atmospheric PM10 aerosol (orange diamonds).

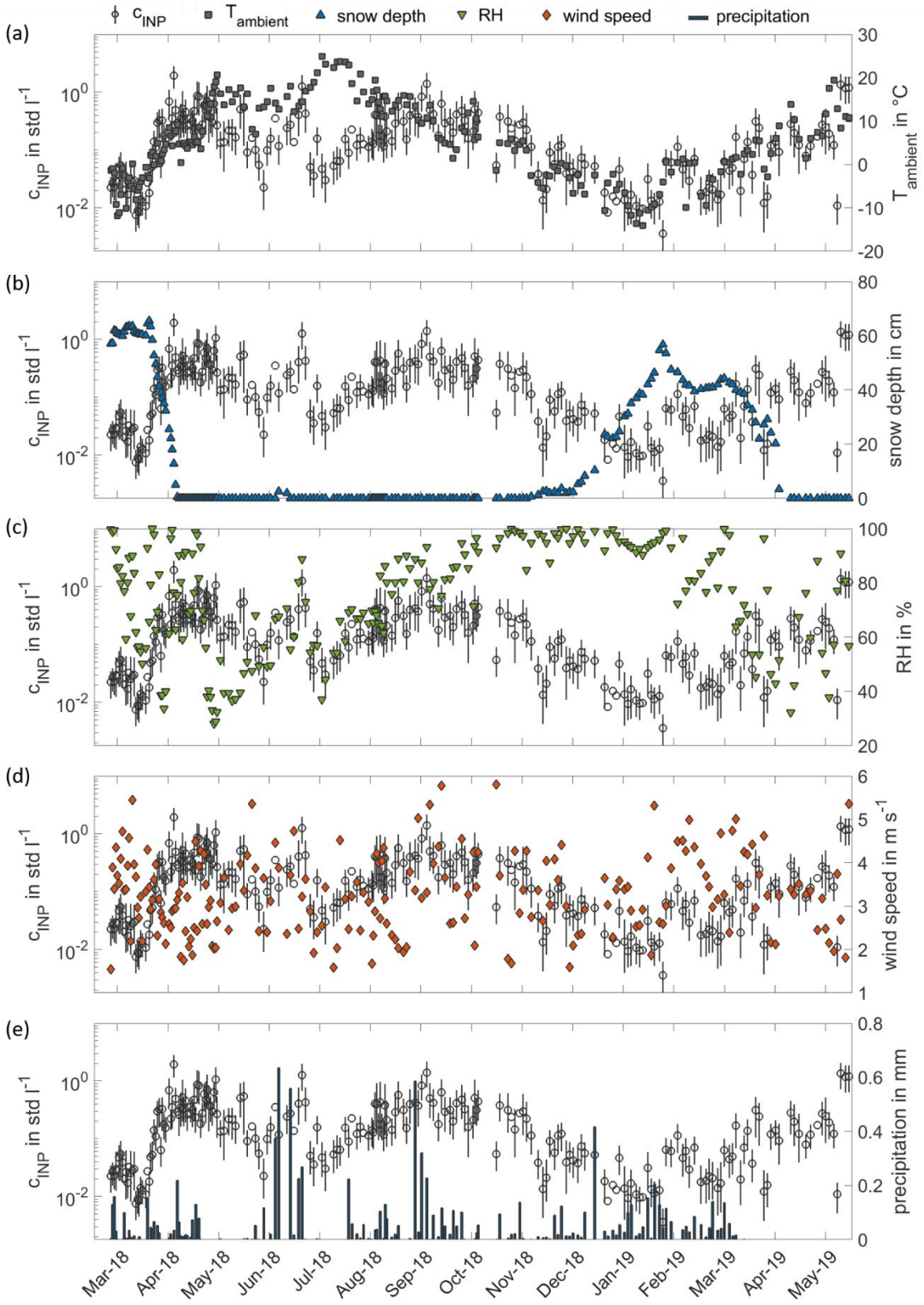
c_INP
T_ambient
snow depth
RH
wind speed
precipitation
(a)
(b)
(c)
(d)
(e)
c_INP in std l^-1
T_ambient in °C
snow depth in cm
RH in %
wind speed in m s^-1
precipitation in mm
Mar-18
Apr-18
May-18
Jun-18
Jul-18
Aug-18
Sep-18
Oct-18
Nov-18
Dec-18
Jan-19
Feb-19
Mar-19
Apr-19
May-19

435

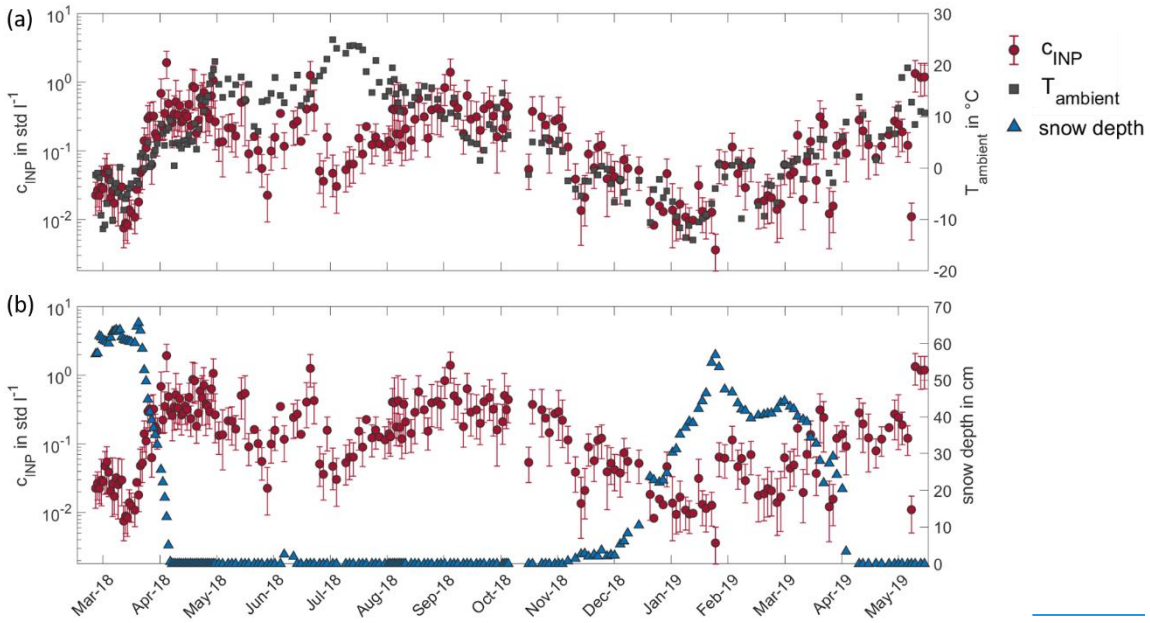

Figure 54: Time series of INP concentrations compared with the time series of ~~ambient air temperature and snow depth~~different meteorological parameters from 11 March 2018 to 31 May 2019. In panel (a), the time series of INP concentrations at 257 K (circles~~red dots~~) is plotted with the ground-level ambient air temperature measured at 4 m above ground level ~~and averaged over the INSEKT filter sampling time intervals from 11 March 2018 to 31 May 2019~~ (grey squares). In panel (b), (c), (d) and (e) the INP concentrations at 257 K are replotted and compared to the measured snow depth~~, also averaged over the INP sampling intervals~~ (blue triangles), the relative humidity measured in 35 m height (green triangles), the wind speed measured in 34 m height (orange diamonds) and precipitation (black bars). All meteorological parameters are averaged over the INSEKT filter sampling time intervals.

3.3 Heat treatment tests

The exemplary INP spectra in Fig. 65 demonstrate that the INP concentrations show an exponential trend with activation temperature (approximately linear shape of the log(c_{INP})-T-spectra) during wintertime, whereas summertime spectra show enhanced concentrations at around 260 K resulting in curvature in the spectra. After heating the INSEKT samples in boiling water for approximately 20 min, the resulting INP spectra are shifted towards lower concentrations by one to two orders of magnitude throughout the temperature range. However, the characteristic bulge in the summertime spectra is conserved or even more pronounced after the heat treatment. The observed shift of INP spectra after heat treatment reveals the presence of heat-labile INP types, which hints to particles of biogenic origin containing ice active proteinaceous material (Hill et al., 2016; Morris et al., 2004). As a significant number of residual heat-resistant INPs is still remaining after heat treatment, this indicates that not all measured INPs are associated with heat-labile biogenic materials. However, the majority of the INP population seems to be dominated by heat-labile materials, which is shown by the systematic shift in INP-temperature spectra. The characteristic differences in the shapes of the INP spectra further indicate that different aerosol types dominate the INP populations in winter- and summertime. These differences are consistent for the observations in 2018 and in 2019, suggesting a systematic seasonal behaviour.

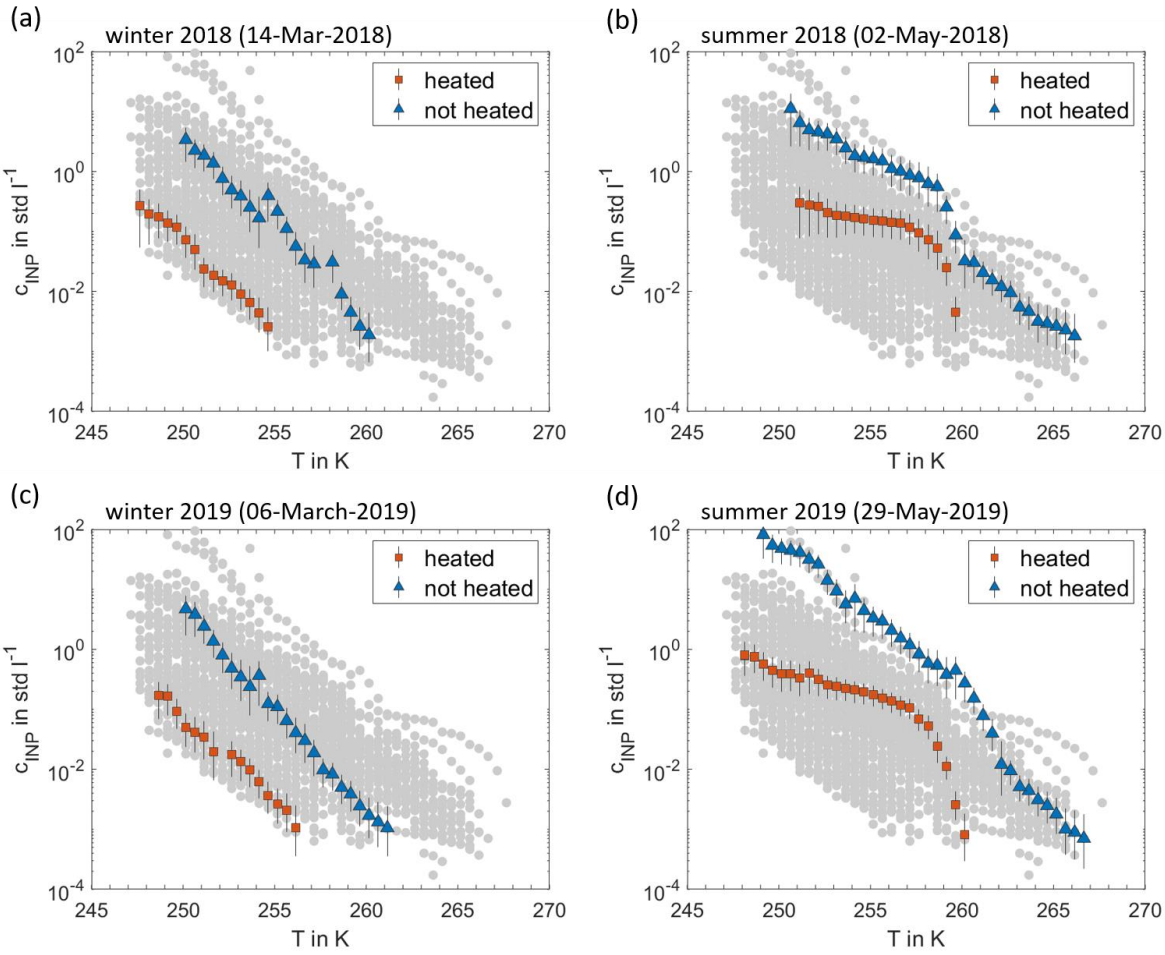

Figure 65: Effect of heat treatments. INP temperature spectra of the non-heated aerosol samples (blue triangles) are compared to the spectra of the heat-treated samples (red squares). Examples of two days in 2018 typical for winter and summer (panels (a) and (b)) and two days in 2019 also typical for winter and summer (panels (c) and (d)) are shown. In each panel, the grey dots display the entirety of non-heated and heat-treated samples.

3.4 Parameterizations

The observations presented in Fig. 1-65 indicate that the INP populations in boreal environments are dominated by biogenic emissions from the vegetation in the forest. We provide evidence that INP concentrations experience a seasonal cycle, which we link to seasonal trends in biogenic aerosol. The observational data we have presented poses new challenges for quantitative INP predictions, as it is essential to incorporate seasonal trends to achieve accurate descriptions. In Fig. 76a-d the measured INP concentrations are plotted versus the INP concentrations predicted by current parameterizations (DeMott et al., 2010; Tobo et al., 2013; Ullrich et al., 2017). DeMott et al. (2010) and Tobo et al. (2013) have developed temperature-dependent parameterizations that use the number concentration of aerosol particles with diameters > 0.5 µm (Fig. 76a and b). Tobo et al. (2013) provide an additional temperature-dependent formulation using the FBAP (fluorescent biological aerosol particle) concentration (Fig. 76c). Ullrich et al. (2017) use the measured aerosol surface area concentration to formulate a temperature-dependent parameterization of the INAS density of mineral dust (Fig. 76d). Among the selected parameterizations, Tobo et al. (2013) reproduce most of the data points by predicting 63% (Fig. 76b) and 80% (Fig. 76c) of the measurements to within one order of magnitude. Note for the application of the Tobo et al., (2013) parameterization using FBAP concentrations, only data from the HyICE-2018 time period could be used, as the fluorescence measurements from the WIBS are only available in this period. Therefore, the number of data points in Fig. 7c is lower than in the other panels. The aerosol-specific parameterization of Ullrich et al. (2017) best matches the temperature trend, but overestimates the measured INP data, reproducing only 23% of the data points to within a factor of 10. This is not surprising, as the boreal forest aerosol is not dominated by mineral dust.

The predictions of DeMott et al. (2010) and Tobo et al. (2013) overestimate INP concentrations especially in wintertime, ~~as they do not include seasonal dependencies~~. These comparisons emphasize the need for a parameterization that accounts for seasonality.

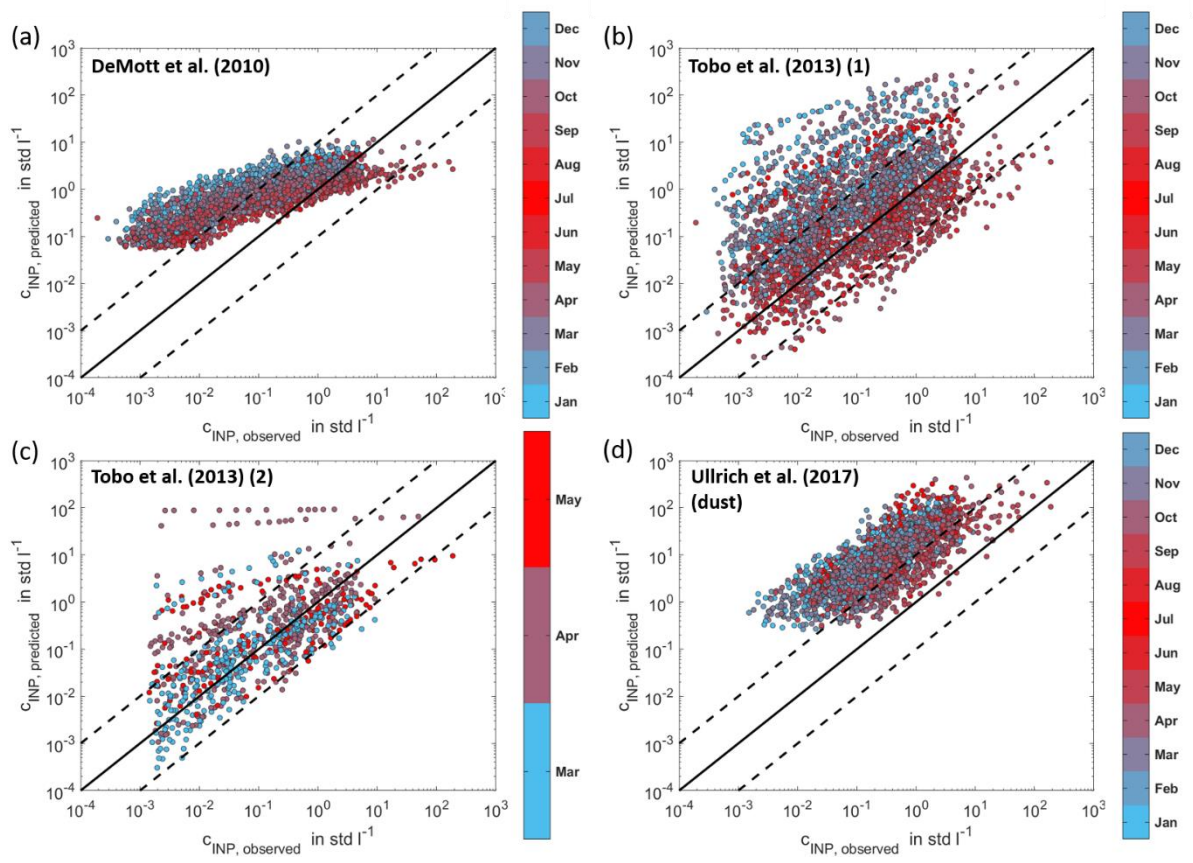

Figure ~~7~~6: Comparisons to INP parameterizations. The measured INP concentrations are compared to INP concentrations predicted by parameterizations from DeMott et al. (2010) (a) and Tobo et al. (2013) (b) both using the number concentration of aerosol particles with diameter > 0.5 µm. Further, the measured concentrations are compared to the predicted concentrations by the second parameterization of Tobo et al.,(2013) using the number concentration of FBAP (c) and to the parameterization by Ullrich et al. (2017) for the temperature-dependent INAS density of mineral dust (d). In Tobo et al. (2013), FBAP concentrations were measured using an excitation wavelength of 355 nm and detecting the fluorescence emission in the range of 420 – 575 nm. The black lines show the 1-1-line (solid) and the 1-10-line and 10-1-line, respectively (dashed).

Given the need to represent seasonality, we suggest two new formulations for describing the seasonal variability of boreal forest INPs. Our first new non-aerosol specific approach assumes that the atmospheric INP concentration is predominantly determined by the boreal forest as the major INP emitting source with a magnitude that naturally changes with the seasons. Using ground-level ambient air temperature averaged over the aerosol filter sampling times as a proxy for the seasonal cycle, the observed INP concentration is quite well overlaid (see Fig. ~~5~~4a). This clear relationship motivates us to use this parameter for formulating the new parameterization. The measured INP temperature spectra between 250 K and 265 K were used to create a least squares fit between the activation temperature T in K and the natural logarithm of INP concentrations c_{INP} in std l^{-1}. This describes the activation behaviour of INPs in temperature space. To account for seasonal dependencies in this formulation, the linear relation between the ground-level ambient air temperature T_{amb} in K and the natural logarithm of the time series of INP concentrations c_{INP} in std l^{-1} was used to establish a prefactor which shifts the parameterized INP temperature spectra to higher or lower INP concentrations depending on the ground-level ambient air temperature. The resulting parameterization is

$$c_{INP} = 0.1 \cdot exp\,(a1 \cdot T_{amb} + a2)\ \cdot exp\,(b1 \cdot T + b2) \qquad (1)$$

with a1 = 0.074 ± 0.006, a2 = -18 ± 2, b1 = -0.504 ± 0.005, b2 = 127 ± 1 and with the activation temperature T and ground-level ambient air temperature T_{amb} in K. This new parameterization is able to reproduce 97.22% of the data to within a factor of 10. 88.21% and 49.79% are reproduced within a factor of 5 and 2, respectively. In Fig. 87a measured INP concentrations are compared to those predicted by the new parameterization underlining the good agreement. With this new approach, we do not directly describe the INP concentration in the atmosphere in a specific environment, as it was common in previous studies (DeMott et al., 2010; Tobo et al., 2013). Rather we have found a way to describe the boreal forest as an important INP emitting source. We suggest this formulation for application in atmospheric models to describe the source concentration of INPs abundant at ground level, which can then be further transported to cloud-relevant altitudes within the models. Here, it needs to be considered that INPs might undergo changes in their size distribution and chemical composition, when they are transported from their source to higher altitudes, which could affect their ice nucleation ability.

Our second formulation is aerosol-specific and describes the ice nucleation efficiency of boreal forest aerosol types using the INAS approach (Ullrich et al., 2017; Vali, 1971). As the seasonal cycle of INAS densities (see Fig. 2b) and the heat test results described earlier (see Fig. 65) indicate a seasonal change in INP types, we suggest specific parameterizations for different seasons. For the INAS density parameterization for boreal forest INPs, an exponential relation as suggested by Ullrich et al. (2017) is assumed and has the form

$$n_S = exp(a1 \cdot T + a2) \quad (2)$$

, where T is the activation temperature of INPs. The INAS density n_S in m^{-2} is calculated by normalizing the measured INP concentration by the total surface area concentration derived from DMPS and APS size distribution data. We adjusted the parameters in Eq. (2) to our measured INAS densities considering the data set in three different periods corresponding to winter, summer and transition periods. The periods are defined by the measured snow depth s (s = 0 cm corresponds to summertime, s > 10 cm corresponds to wintertime and 0 < s ≤ 10 is the transition period.). The new fits yield a1 = -0.543 ± 0.007 and a2 = 154 ± 2 for summertime, a1 = -0.495 ± 0.008 and a2 = 141 ± 2 for wintertime and a1 = -0.49 ± 0.01 and a2 = 140 ± 3 for the transition period. In Fig. 87b the INP concentration calculated with these new parameterizations are compared to the measured concentrations. In summertime 92.57% (79.40%, 41.32%) of the data is reproduced by the INAS density fit within a factor of 10 (5, 2), in wintertime 97.32% (86.30%, 47.80%) and in the transition period 99.11% (95.56%, 56.89%) are reproduced.

4 Conclusions

This study provides a unique dataset of continuously recorded INP concentrations for more than one year at the SMEARII station located in the Finnish boreal forest. The observations illustrate that the boreal forest is an important source of biogenic INPs with resulting concentrations comparable to other environments (Kanji et al., 2017). We observe a clear seasonal cycle of INP concentrations and INP types in the boreal forest and conclude that this cycle is linked to the prevalence of biogenic aerosol particles. We suggest that these particles are primarily particles emitted by the forest vegetation, but are also correlated with the variable biogenic activities in the forest which appear to contribute both to INPs and to NPF. Current parameterizations do not represent the newly observed seasonal INP variability or concentrations. Thus, we suggest two new approaches for formulating and quantifying the annual cycle of INPs over boreal forest areas. The first considers the boreal forest as an aerosol emission source, including INPs, which appears to vary strongly with the seasonal changes. The second formulates season specific INAS parameterizations for boreal forest aerosol particles. The new formulations of both approaches reproduce almost all the data points of our long-term record of INP concentrations to within a factor of 10 and provide a basis for models to assess the global or regional importance of boreal forest INPs. As INPs strongly influence precipitation formation and cloud

evolution, a description of INPs in weather forecast models is crucial. This study shows that the ice nucleation activity in the atmosphere is highly variable depending on the surrounding conditions. Therefore, it is important to investigate INP concentrations and INP types in different characteristic locations on Earth to establish an overall picture of the global INP abundance and variability. For investigating long-term variability, continuous long-term observations are needed to get a profound insight on the ice nucleation activity at a specific site with a good statistics accounting for the difficulties and uncertainties in INP measurements. With this study, we provide a first step to this overall picture by characterizing the INP population abundant in a remote location in the boreal forest. With continuous aerosol filter sampling for more than one year, we provide the first observation of a clear seasonal cycle, which seems to be dominated by the abundance biogenic aerosol. As in this remote environment, biogenic aerosols seem to play an important role, in other areas, the INP population might be dominated by other species. For further studies, we suggest to conduct further continuous long-term measurements of INPs at different locations on Earth, like anthropogenic influenced location or deserts. Measurements with a higher time resolution might be useful to investigate relations to meteorological events like precipitation and frontal passages in more detail.

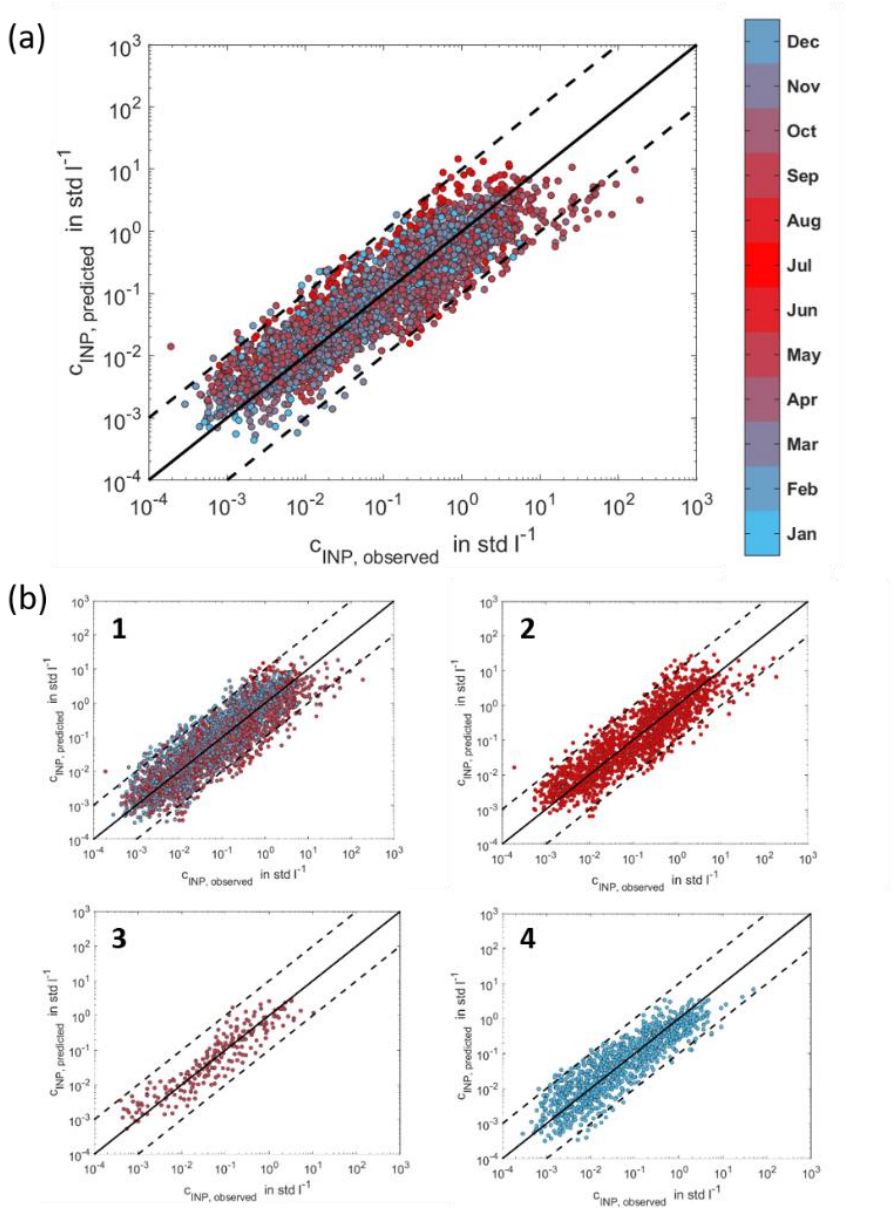

Figure 87: New INP parameterizations for boreal forest INPs. Panel (a) shows INP concentrations predicted by our new parametrization using ground-level ambient air temperature compared to measured INP concentrations colour-coded with the corresponding month. In panel (b), the measurements are compared to the predictions of the new INAS density parametrization.

The four panels show the new INAS parameterization for the boreal forest INP over the whole year (1), only describing summertime INPs (2), the parameterization for the transition period (3) and the formulations for boreal INPs in wintertime (4).

Appendix A

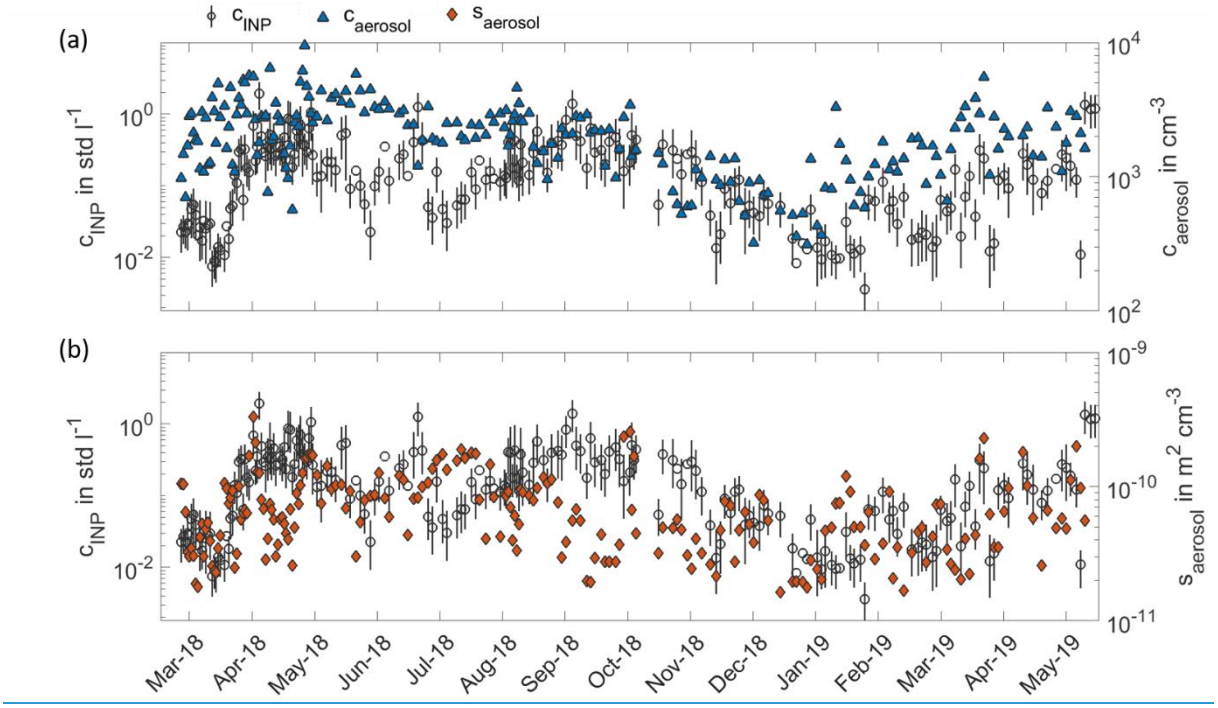

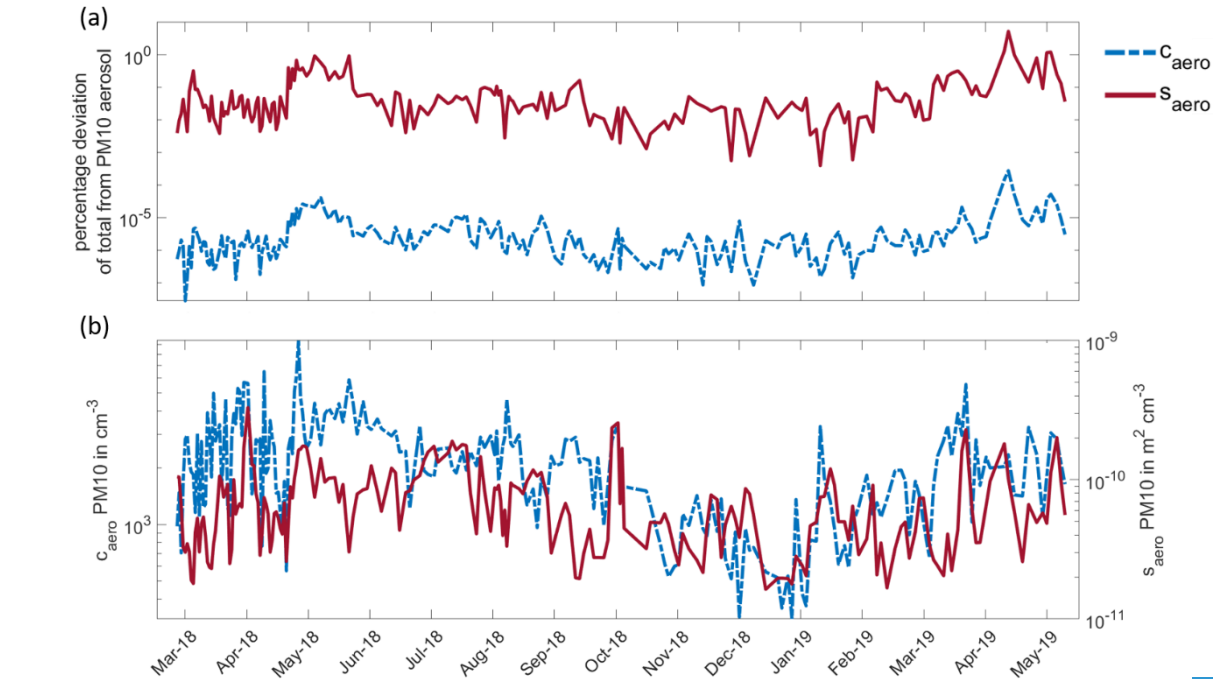

Figure A1. Time series of number and surface concentration of atmospheric PM10 aerosol. Panel (a) shows the number concentration of atmospheric PM10 aerosol particles measured by DMPS and APS (blue triangles) in comparison to the INP time series at 257 K (circles) from 11 March 2018 to 31 May 2019. In panel (b), the time series of PM10 surface concentrations (orange diamonds) is compared to the INP time series for the same time period.

~~**Figure A1. Comparison of PM10 aerosol population to total aerosol population. Panel (a) shows the percentage deviation of the number (blue dashed) and surface area (red solid) concentrations of the total aerosol from the number and surface area concentration only considering PM10 aerosol particles for the time period from 11 March 2018 to 31 May 2019. In panel (b), the time series of PM10 number concentrations (blue dashed) and of PM10 surface area concentration (red solid) are displayed for the same time period.**~~

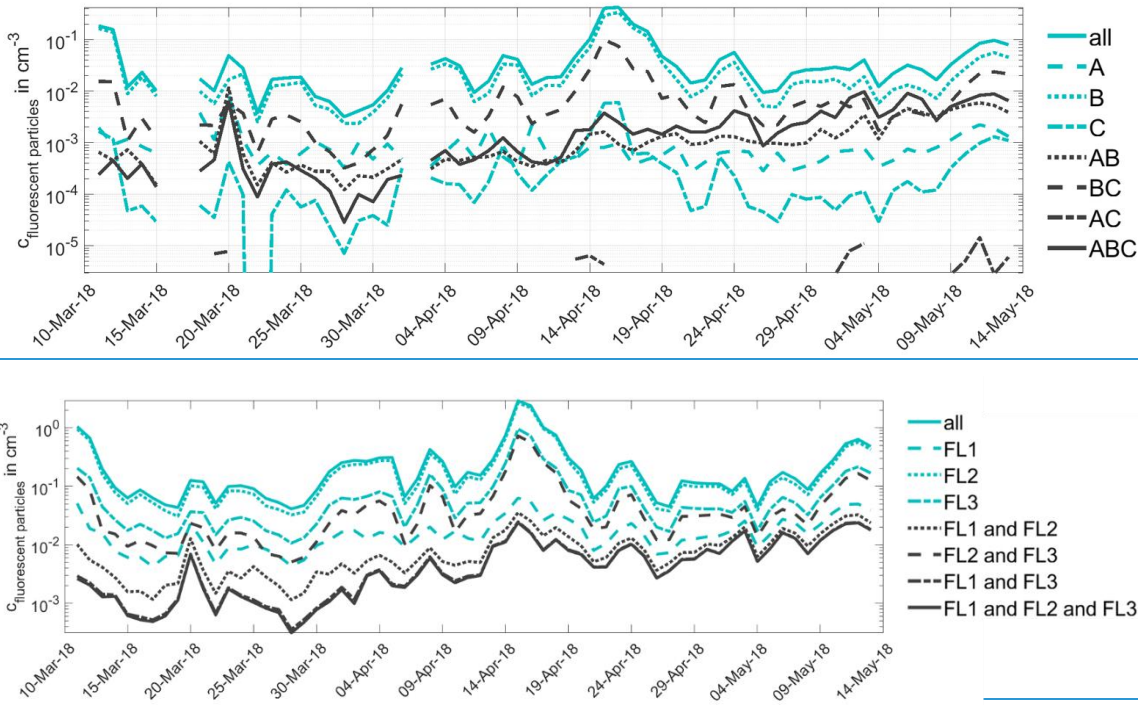

Figure A2: Time series of fluorescent particle number concentrations. The number concentrations of fluorescent particles measured by WIBS in different ~~laser channel combinations~~excitation emission wavelength pair combinations (fluorescence groups) are shown from 11 March 2018 to 13 May 2018. The definition of the different fluorescence groups is based on the categorization given in Savage et al. (2017). A summary of this categorization is given in Section 2.3. ~~(FL1: λ_{ex} = 280 nm, λ_{em} = 310 – 400 nm; FL2: λ_{ex} = 280 nm, λ_{em} = 420 – 650 nm; FL3: λ_{ex} = 370 nm, λ_{em} = 420 – 650 nm).~~

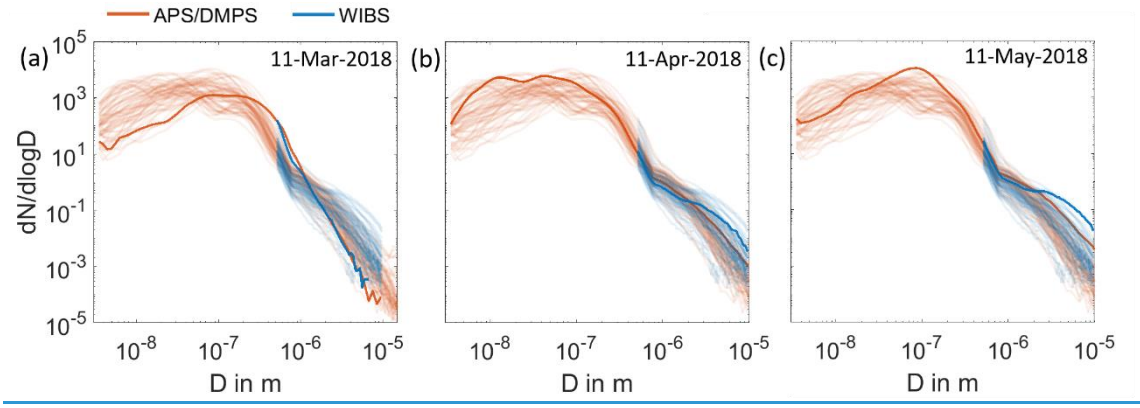

Figure A3: Aerosol size distributions measured by DMPS/APS and WIBS. The daily size distributions of atmospheric aerosol particles measured by DMPS and APS (red) are compared to the daily size distribution of atmospheric aerosol particles measured by WIBS (blue) in the period from 11 March 2018 to 13 May 2018. In each of the panels (a), (b), and (c) one size distribution in March, April and May is highlighted.

Data availability. The measurement data used in this study is available via KITopen data repository under https://doi.org/10.5445/IR/1000120666 (Schneider et al., 2020).

Author contributions. JS wrote this manuscript, did the INP data analysis and part of the filter analysis. KH and OM both strongly supported the analysis and the writing. OM, MK, TP, JD and DM initiated and planned the HyICE-2018 campaign. JS, KH, BB, TS, NSU, FV, PB, PH, ZB, MPA, BJM, EST, DC, KK, YW, DM and JD conducted the measurements within the HyICE-2018 campaign and contributed to the data analysis and the interpretation. PH provided the analysed WIBS data and instrument description. SH provided the analysed NPF event data. LH provided the analysed L-ToF-AMS data and instrument description. JK, TP and TL contributed to the discussion and interpretation of the data and the manuscript writing.

Competing interests. The authors declare no competing interests.

Acknowledgements. This project received funding from the European Union's Horizon 2020 research and innovation programme under grant agreements No 654109 and 739530 and Transnational access via ACTRIS-2 HyICE-2018 TNA project. The work of the KIT Institute for Meteorology and Climate Research (IMK-AAF) was additionally supported through the Research Programm "Atmosphere and Climate (ATMO)" of the Helmholtz Association and by the KIT Technology Transfer Project PINE (N059). The work of University of Helsinki was supported by the Academy of Finland Centre of Excellence in Atmospheric Science (grant no. 307331) and NANOBIOMASS (307537), ACTRIS-Finland (328616), ACTRIS-CF (329274) and Arctic Community Resilience to Boreal Environmental change: Assessing Risks from fire and disease (ACRoBEAR, 334792) Belmont Forum project. In addition, the work of University of Helsinki was financially supported by European Commission through ACTRIS2 (654109) and ACTRIS-IMP (871115) and ACTRIS2 TransNational Access and through integrative and Comprehensive Understanding on Polar Environments (iCUPE, 689443), ERA-NET-Cofund and by University of Helsinki (ACTRIS-HY). BJM and MPA acknowledge the European Research Council, ERC, MarineIce 648661 for funding. PH and JK acknowledge the funding from the Arctic Academy Programme "ARKTIKO" of Academy of Finland under grant No 286558, and PH from the Maj and Tor Nessling Foundation. EST and DC were supported by the Swedish Research Councils, VR (2013-05153) and FORMAS (2017-00564). NSU acknowledges the support of the Alexander von Humboldt Foundation, Germany (1188375).

Janne Levula, Matti Loponen and rest of the technical staff at the SMEARII station are gratefully acknowledged for their efforts during the HyICE-2018 intensive campaign and during the extended filter sampling period. Support by the IMK-AAF technical team in preparing and operating the INP instruments is also gratefully acknowledged.

References

Aalto, P., Hämeri, K., Becker, E. D. O., Weber, R., Salm, J., Mäkelä, J. M., Hoell, C., O'Dowd, C. D., Karlsson, H., Hansson, H., Väkevä, M., Koponen, I. K., Buzorius, G. and Kulmala, M.: Physical characterization of aerosol particles during nucleation events, Tellus, Ser. B Chem. Phys. Meteorol., 53(4), 344–358, doi:10.3402/tellusb.v53i4.17127, 2001.

Agresti, A. and Coull, B. A.: Approximate is better than "Exact" for interval estimation of binomial proportions, Am. Stat., 52(2), 119–126, doi:10.1080/00031305.1998.10480550, 1998.

Augustin, S., Wex, H., Niedermeier, D., Pummer, B., Grothe, H., Hartmann, S., Tomsche, L., Clauss, T., Voigtländer, J., Ignatius, K. and Stratmann, F.: Immersion freezing of birch pollen washing water, Atmos. Chem. Phys., 13(21), 10989–11003, doi:10.5194/acp-13-10989-2013, 2013.

Boucher, O., Randall, D., Artaxo, P., Bretherton, C., Feingold, G., Forster, P., Kerminen, V., Kondo, Y., Liao, H., Lohmann, U., Rasch, P., Satheesh, S., Sherwood, S., Stevens, B., Zhang, X., Qin, D., Plattner, G., Tignor, M., Allen, S., Boschung, J., Nauels, A., Xia, Y., Bex, V., Midgley, P. and Randall, D.: Clouds and Aerosols. In: Climate Change 2013: The Physical Science Basis. Contribution of Working Group I to the Fifth Assessment Report of the Intergovernmental Panel on Climate Change, Cambridge, United Kingdom and New York, NY, USA., 2013.

Canagaratna, M. R., Jayne, J. T., Jimenez, J. L., Allan, J. D., Alfarra, M. R., Zhang, Q., Onasch, T. B., Drewnick, F., Coe, H., Middlebrook, A., Delia, A., Williams, L. R., Trimborn, A. M., Northway, M. J., DeCarlo, P. F., Kolb, C. E., Davidovits, P. and Worsnop, D. R.: Chemical and microphysical characterization of ambient aerosols with the aerodyne aerosol mass spectrometer, Mass Spectrom. Rev., 26(2), 185–222, doi:10.1002/mas.20115, 2007.

Christner, B. C., Morris, C. E., Foreman, C. M., Cai, R. and Sands, D. C.: Ubiquity of biological ice nucleators in snowfall, Science (80-.)., 319(5867), 1214, doi:10.1126/science.1149757, 2008.

Cooper, W.: Ice initiation in natural clouds. Precipitation Enhancement—A Scientific Challenge., Meteor. Monogr. (Am. Meteor. Soc., Boston, MA), 21, 29–32, 1986.

Creamean, J. M., Suski, K. J., Rosenfeld, D., Cazorla, A., DeMott, P. J., Sullivan, R. C., White, A. B., Ralph, F. M., Minnis, P., Comstock, J. M., Tomlinson, J. M. and Prather, K. A.: Dust and biological aerosols from the Sahara and Asia influence precipitation in the Western U.S, Science (80-.)., 340(6127), 1572–1578, doi:10.1126/science.1227279, 2013.

Dada, L., Paasonen, P., Nieminen, T., Mazon, S. B., Kontkanen, J., Peräkylä, O., Lehtipalo, K., Hussein, T., Petäjä, T., Kerminen, V.-M., Bäck, J. and Kulmala, M.: Long-term analysis of clear-sky new particle formation events and nonevents in Hyytiälä, Atmos. Chem. Phys, 17, 6227–6241, doi:10.5194/acp-17-6227-2017, 2017.

Dall'Osto, M., Beddows, D. C. S., Asmi, A., Poulain, L., Hao, L., Freney, E., Allan, J. D., Canagaratna, M., Crippa, M., Bianchi, F., De Leeuw, G., Eriksson, A., Swietlicki, E., Hansson, H. C., Henzing, J. S., Granier, C., Zemankova, K., Laj, P., Onasch, T., Prevot, A., Putaud, J. P., Sellegri, K., Vidal, M., Virtanen, A., Simo, R., Worsnop, D., O'Dowd, C., Kulmala, M. and Harrison, R. M.: Novel insights on new particle formation derived from a pan-european observing system, Sci. Rep., 8(1), 1–11, doi:10.1038/s41598-017-17343-9, 2018.

DeCarlo, P. F., Kimmel, J. R., Trimborn, A., Northway, M. J., Jayne, J. T., Aiken, A. C., Gonin, M., Fuhrer, K., Horvath, T., Docherty, K. S., Worsnop, D. R. and Jimenez, J. L.: Field-deployable, high-resolution, time-of-flight aerosol mass spectrometer, Anal. Chem., 78(24), 8281–8289, doi:10.1021/ac061249n, 2006.

DeMott, P. J., Prenni, A. J., Liu, X., Kreidenweis, S. M., Petters, M. D., Twohy, C. H., Richardson, M. S., Eidhammer, T. and Rogers, D. C.: Predicting global atmospheric ice nuclei distributions and their impacts on climate, Proc. Natl. Acad. Sci. U. S. A., 107(25), 11217–11222, doi:10.1073/pnas.0910818107, 2010.

Ehn, M., Thornton, J. A., Kleist, E., Sipilä, M., Junninen, H., Pullinen, I., Springer, M., Rubach, F., Tillmann, R., Lee, B., Lopez-Hilfiker, F., Andres, S., Acir, I. H., Rissanen, M., Jokinen, T., Schobesberger, S., Kangasluoma, J., Kontkanen, J., Nieminen, T., Kurtén, T., Nielsen, L. B., Jørgensen, S., Kjaergaard, H. G., Canagaratna, M., Maso, M. D., Berndt, T., Petäjä, T., Wahner, A., Kerminen, V. M., Kulmala, M., Worsnop, D. R., Wildt, J. and Mentel, T. F.: A large source of low-volatility secondary organic aerosol, Nature, 506(7489), 476–479, doi:10.1038/nature13032, 2014.

Fletcher, N. H.: The Physics of Rainclouds, Cambridge University Press, Cambridge, UK., 1962.

Hader, J. D., Wright, T. P. and Petters, M. D.: Contribution of pollen to atmospheric ice nuclei concentrations, Atmos. Chem. Phys., 14(11), 5433–5449, doi:10.5194/acp-14-5433-2014, 2014.

Hari, P. and Kulmala, M.: Station for measuring ecosystem-atmosphere relations (SMEARII), Boreal Environ. Res., 10(October), 315–322, doi:10.1007/978-94-007-5603-8_9, 2005.

Harrison, A. D., Lever, K., Sanchez-Marroquin, A., Holden, M. A., Whale, T. F., Tarn, M. D., Mcquaid, J. B. and Murray, B. J.: The ice-nucleating ability of quartz immersed in water and its atmospheric importance compared to K-feldspar, Atmos. Chem. Phys, 19, 11343–11361, doi:10.5194/acp-19-11343-2019, 2019.

Hartmann, M., Blunier, T., Brügger, S. O., Schmale, J., Schwikowski, M., Vogel, A., Wex, H. and Stratmann, F.: Variation of Ice Nucleating Particles in the European Arctic Over the Last Centuries, Geophys. Res. Lett., 46(7), 4007–4016, doi:10.1029/2019GL082311, 2019.

Heald, C. L. and Spracklen, D. V.: Atmospheric budget of primary biological aerosol particles from fungal spores, Geophys. Res. Lett., 36(9), doi:10.1029/2009GL037493, 2009.

Hill, T. C. J., Demott, P. J., Tobo, Y., Fröhlich-Nowoisky, J., Moffett, B. F., Franc, G. D. and Kreidenweis, S. M.: Sources of organic ice nucleating particles in soils, Atmos. Chem. Phys., 16(11), 7195–7211, doi:10.5194/acp-16-7195-2016, 2016.

Hirst, J. M.: An automatic volumetric spore trap, Ann. Appl. Biol., 39(2), 257–265, doi:10.1111/j.1744-7348.1952.tb00904.x, 1952.

Hoose, C. and Möhler, O.: Heterogeneous ice nucleation on atmospheric aerosols: a review of results from laboratory experiments, Atmos. Chem. Phys. Discuss., 12(5), 12531–12621, doi:10.5194/acpd-12-12531-2012, 2012.

Hoose, C., Kristjánsson, J. E. and Burrows, S. M.: How important is biological ice nucleation in clouds on a global scale?, Environ. Res. Lett., 5(2), 1–7, doi:10.1088/1748-9326/5/2/024009, 2010.

Huffman, J. A., Prenni, A. J., Demott, P. J., Mason, R. H., Huffman, J. A., Prenni, A. J., Demott, P. J., Pöhlker, C., Mason, R. H., Robinson, N. H., Fröhlich-Nowoisky, J., Tobo, Y., Després, V. R., Garcia, E., Gochis, D. J., Harris, E., M ¨ Uller-Germann, I., Ruzene, C., Schmer, B., Sinha, B., Day, D. A., Andreae, M. O., Jimenez, J. L., Gallagher, M., Kreidenweis, S. M., Bertram, A. K. and Pöschl, U.: High concentrations of biological aerosol particles and ice nuclei during and after rain, Atmos. Chem. Phys, 13, 6151–6164, doi:10.5194/acp-13-6151-2013, 2013.

Iwata, A., Imura, M., Hama, M., Maki, T., Tsuchiya, N., Kunihisa, R. and Matsuki, A.: Release of highly active ice nucleating biological particles associated with rain, Atmosphere (Basel)., 10(10), 1–13, doi:10.3390/atmos10100605, 2019.

Jokinen, V. and Mäkelä, J. M.: Closed-loop arrangement with critical orifice for DMA sheath/excess flow system, J. Aerosol Sci., 28(4), 643–648, doi:10.1016/S0021-8502(96)00457-0, 1997.

Junninen, H., Lauri, A., Keronen, P., Aalto, P., Hiltunen, V., Hari, P. and Kulmala, M.: Smart-SMEAR: On-line data exploration and visualization tool for SMEAR stations, Boreal Environ. Res., 14(4), 447–457, 2009.

Kanji, Z. A., Ladino, L. A., Wex, H., Boose, Y., Burkert-Kohn, M., Cziczo, D. J. and Krämer, M.: Overview of Ice Nucleating Particles, Meteorol. Monogr., 58, 1.1-1.33, doi:10.1175/amsmonographs-d-16-0006.1, 2017.

Kaye, P. H., Barton, J. E., Hirst, E. and Clark, J. M.: Simultaneous light scattering and intrinsic fluorescence measurement for the classification of airborne particles, Appl. Opt., 39(21), 3738–3745, doi:10.1364/ao.39.003738, 2000.

Kulmala, M., Toivonen, A., Mäkelä, J. M. and Laaksonen, A.: Analysis of the growth of nucleation mode particles observed in Boreal forest, Tellus, Ser. B Chem. Phys. Meteorol., 50(5), 449–462, doi:10.3402/tellusb.v50i5.16229, 1998.

Kulmala, M., Hameri, K., Aalto, P. P., Makela, J. M., Pirjola, L., Nilsson, E. D., Buzorius, G., Rannik, U., Maso, M. D., Seidl, W., Hoffman, T., Janson, R., Hansson, H.-C., Viisanen, Y., Laaksonen, A. and O'Dowd, C. D.: Overview of the international project on biogenic aerosol formation in the boreal forest (BIOFOR), Tellus B, 53(4), 324–343, doi:10.1034/j.1600-0889.2001.530402.x, 2001.

Kulmala, M., Vehkamäki, H., Petäjä, T., Dal Maso, M., Lauri, A., Kerminen, V. M., Birmili, W. and McMurry, P. H.: Formation and growth rates of ultrafine atmospheric particles: A review of observations, J. Aerosol Sci., 35(2), 143–176, doi:10.1016/j.jaerosci.2003.10.003, 2004.

Kulmala, M., Kontkanen, J., Junninen, H., Lehtipalo, K., Manninen, H. E., Nieminen, T., Petäjä, T., Sipilä, M., Schobesberger, S., Rantala, P., Franchin, A., Jokinen, T., Järvinen, E., Äijälä, M., Kangasluoma, J., Hakala, J., Aalto, P. P., Paasonen, P., Mikkilä, J., Vanhanen, J., Aalto, J., Hakola, H., Makkonen, U., Ruuskanen, T., Mauldin, R. L., Duplissy, J., Vehkamäki, H., Bäck, J., Kortelainen, A., Riipinen, I., Kurtén, T., Johnston, M. V., Smith, J. N., Ehn, M., Mentel, T. F., Lehtinen, K. E. J., Laaksonen, A., Kerminen, V. M. and Worsnop, D. R.: Direct observations of atmospheric aerosol nucleation, Science (80-.)., 339(6122), 943–946, doi:10.1126/science.1227385, 2013.

Liu, P. S. K., Deng, R., Smith, K. A., Williams, L. R., Jayne, J. T., Canagaratna, M. R., Moore, K., Onasch, T. B., Worsnop, D. R. and Deshler, T.: Transmission Efficiency of an Aerodynamic Focusing Lens System: Comparison of Model Calculations and Laboratory Measurements for the Aerodyne Aerosol Mass Spectrometer, Aerosol Sci. Technol., 41(8), 721–733, doi:10.1080/02786820701422278, 2007.

Manninen, H. E., Sihto-Nissilä, S. L., Hiltunen, V., Aalto, P. P., Kulmala, M., Petäjä, T., Manninen, H. E., Bäck, J., Hari, P., Huffman, J. A., Huffman, J. A., Saarto, A., Pessi, A. M. and Hidalgo, P. J.: Patterns in airborne pollen and other primary biological aerosol particles (PBAP), and their contribution to aerosol mass and number in a boreal forest, Boreal Environ. Res., 19(September), 383–405, 2014.

McCluskey, C. S., Ovadnevaite, J., Rinaldi, M., Atkinson, J., Belosi, F., Ceburnis, D., Marullo, S., Hill, T. C. J., Lohmann, U., Kanji, Z. A., O'Dowd, C., Kreidenweis, S. M. and DeMott, P. J.: Marine and Terrestrial Organic Ice-Nucleating Particles in Pristine Marine to Continentally Influenced Northeast Atlantic Air Masses, J. Geophys. Res. Atmos., 123(11), 6196–6212,

doi:10.1029/2017JD028033, 2018.

Meyers, M. P., Demott, P. J. and Cotton, W. R.: New primary ice-nucleation parameterizations in an explicit cloud model, J. Appl. Meteorol., 31(7), 708–721, doi:10.1175/1520-0450(1992)031<0708:NPINPI>2.0.CO;2, 1992.

Middlebrook, A. M., Bahreini, R., Jimenez, J. L. and Canagaratna, M. R.: Evaluation of composition-dependent collection efficiencies for the Aerodyne aerosol mass spectrometer using field data, Aerosol Sci. Technol., 46(3), 258–271, doi:10.1080/02786826.2011.620041, 2012.

Möhler, O., DeMott, P. J., Vali, G. and Levin, Z.: Microbiology and atmospheric processes: The role of biological particles in cloud physics, Biogeosciences, 4(6), 1059–1071, doi:10.5194/bg-4-1059-2007, 2007.

Morris, C. E., Georgakopoulos, D. G. and Sands, D. C.: Ice nucleation active bacteria and their potential role in precipitation, J. Phys. IV JP, 121, 87–103, doi:10.1051/jp4:2004121004, 2004.

Murray, B. J., O'Sullivan, D., Atkinson, J. D. and Webb, M. E.: Ice nucleation by particles immersed in supercooled cloud droplets, Chem. Soc. Rev., 41(19), 6519–6554, doi:10.1039/c2cs35200a, 2012.

Nieminen, T., Asmi, A., Aalto, P. P., Keronen, P., Petäjä, T., Kulmala, M., Kerminen, V. M., Nieminen, T. and Dal Maso, M.: Trends in atmospheric new-particle formation: 16 years of observations in a boreal-forest environment, Boreal Environ. Res., 19(September), 191–214, 2014.

O'Sullivan, D., Murray, B. J., Ross, J. F., Whale, T. F., Price, H. C., Atkinson, J. D., Umo, N. S. and Webb, M. E.: The relevance of nanoscale biological fragments for ice nucleation in clouds, Sci. Rep., 5, 1–7, doi:10.1038/srep08082, 2015.

O'Sullivan, D., Adams, M. P., Tarn, M. D., Harrison, A. D., Vergara-Temprado, J., Porter, G. C. E., Holden, M. A., Sanchez-Marroquin, A., Carotenuto, F., Whale, T. F., McQuaid, J. B., Walshaw, R., Hedges, D. H. P., Burke, I. T., Cui, Z. and Murray, B. J.: Contributions of biogenic material to the atmospheric ice-nucleating particle population in North Western Europe, Sci. Rep., 8(1), 1–9, doi:10.1038/s41598-018-31981-7, 2018.

Paramonov, M., Drossaart Van Dusseldorp, S., Gute, E., Abbatt, J. P. D., Heikkilä, P., Keskinen, J., Chen, X., Luoma, K., Heikkinen, L., Hao, L., Petäjä, T. and Kanji, Z. A.: Condensation/immersion mode ice-nucleating particles in a boreal environment, Atmos. Chem. Phys, 20, 6687–6706, doi:10.5194/acp-20-6687-2020, 2020.

~~Pöhlker, C., Huffman, J. A. and Pöschl, U.: Autofluorescence of atmospheric bioaerosols - Fluorescent biomolecules and potential interferences, Atmos. Meas. Tech., 5(1), 37–71, doi:10.5194/amt-5-37-2012, 2012.~~

Perring, A. E., Schwarz, J. P., Baumgardner, D., Hernandez, M. T., Spracklen, D. V., Heald, C. L., Gao, R. S., Kok, G., McMeeking, G. R., McQuaid, J. B. and Fahey, D. W.: Airborne observations of regional variation in fluorescent aerosol across the United States, J. Geophys. Res. Atmos., 120(3), 1153–1170, doi:10.1002/2014JD022495, 2015.

Pratt, K. A., Demott, P. J., French, J. R., Wang, Z., Westphal, D. L., Heymsfield, A. J., Twohy, C. H., Prenni, A. J. and Prather, K. A.: In situ detection of biological particles in cloud ice-crystals, Nat. Geosci., 2(6), 398–401, doi:10.1038/ngeo521, 2009.

Prenni, A. J., Petters, M. D., Kreidenweis, S. M., Heald, C. L., Martin, S. T., Artaxo, P., Garland, R. M., Wollny, A. G. and Pöschl, U.: Relative roles of biogenic emissions and Saharan dust as ice nuclei in the Amazon basin, Nat. Geosci., 2(6), 402–405, doi:10.1038/ngeo517, 2009.

Prenni, A. J., Tobo, Y., Garcia, E., DeMott, P. J., Huffman, J. A., McCluskey, C. S., Kreidenweis, S. M., Prenni, J. E., Pöhlker, C. and Pöschl, U.: The impact of rain on ice nuclei populations at a forested site in Colorado, Geophys. Res. Lett., 40(1), 227–231, doi:10.1029/2012GL053953, 2013.

Pruppacher, H. R. and Klett, J. D.: Microstructure of Atmospheric Clouds and Precipitation, pp. 10–73., 2010.

Rantio-Lehtimäki, A., Viander, M. and Koivikko, A.: Airborne birch pollen antigens in different particle sizes, Clin. Exp. Allergy, 24(1), 23–28, doi:10.1111/j.1365-2222.1994.tb00912.x, 1994.

Šantl-Temkiv, T., Lange, R., Beddows, D., Rauter, U., Pilgaard, S., Dall'osto, M., Gunde-Cimerman, N., Massling, A. and Wex, H.: Biogenic Sources of Ice Nucleating Particles at the High Arctic Site Villum Research Station, Environ. Sci. Technol., 53(18), 10580–10590, doi:10.1021/acs.est.9b00991, 2019.

Savage, N., Krentz, C., Könemann, T., Han, T. T., Mainelis, G., Pöhlker, C. and Huffman, J. A.: Systematic characterization and fluorescence threshold strategies for the Wideband Integrated Bioaerosol Sensor (WIBS) using size resolved biological and interfering particles, Atmos. Meas. Tech. Discuss., 10, 4279–4302, 2017.

Schiebel, T.: Ice nucleation activity of soil dust aerosols, Karlsruhe Institute of Technology, Karlsruhe, Germany., 2017.

Schnell, R. C. and Vali, G.: World-wide source of leaf-derived freezing nuclei, Nature, 246(5430), 212–213, doi:10.1038/246212a0, 1973.

Schmale, J., Henning, S., Henzing, B., Keskinen, H., Sellegri, K., Ovadnevaite, J., Bougiatioti, A., Kalivitis, N., Stavroulas, I., Jefferson, A., Park, M., Schlag, P., Kristensson, A., Iwamoto, Y., Pringle, K., Reddington, C., Aalto, P., Äijälä, M., Baltensperger, U., Bialek, J., Birmili, W., Bukowiecki, N., Ehn, M., Fjæraa, A. M., Fiebig, M., Frank, G., Fröhlich, R., Frumau, A., Furuya, M., Hammer, E., Heikkinen, L., Herrmann, E., Holzinger, R., Hyono, H., Kanakidou, M., Kiendler-Scharr, A., Kinouchi, K., Kos, G., Kulmala, M., Mihalopoulos, N., Motos, G., Nenes, A., O'Dowd, C., Paramonov, M., Petäjä, T., Picard, D., Poulain, L., Prévôt, A. S. H., Slowik, J., Sonntag, A., Swietlicki, E., Svenningsson, B., Tsurumaru, H., Wiedensohler, A., Wittbom, C., Ogren, J. A., Matsuki, A., Yum, S. S., Myhre, C. L., Carslaw, K., Stratmann, F. and Gysel, M.: Collocated observations of cloud condensation nuclei, particle size distributions, and chemical composition, Sci. Data, 4(1), 1–27, doi:10.1038/sdata.2017.3, 2017.

Schneider, J., Höhler, K., Heikkilä, P., Keskinen, J., Bertozzi, B., Bogert, P., Schorr, T., Umo, N. S., Vogel, F., Brasseur, Z., Wu, Y., Hakala, S., Duplissy, J., Moisseev, D., Kulmala, M., Adams, M. P., Murray, B. J., Korhonen, K., Hao, L., Thomson, E. S., Castarède, D., Leisner, T., Petäjä, T., and Möhler, O.: Datasets to: The seasonal cycle of ice-nucleating particles linked to the abundance of biogenic aerosol in boreal forests, KITopen, https://doi.org/10.5445/IR/1000120666, 2020.

Schrod, J., Thomson, E. S., Weber, D., Kossmann, J., Pöhlker, C., Saturno, J., Ditas, F., Artaxo, P., Clouard, V., Saurel, J.-M., Ebert, M., Curtius, J., and Bingemer, H. G.: Long-term INP measurements from four stations across the globe, Atmos. Chem. Phys. Discuss., https://doi.org/10.5194/acp-2020-667, in review, 2020.~~Schrod, J., Bingemer, H. and Curtius, J.: Long Term INP Measurements within the BACCHUS project., 2016.~~

Schumacher, C. J., Pöhlker, C., Aalto, P., Hiltunen, V., Petäjä, T., Kulmala, M., Pöschl, U. and Huffman, J. A.: Seasonal cycles of fluorescent biological aerosol particles in boreal and semi-arid forests of Finland and Colorado, Atmos. Chem. Phys., 13(23), 11987–12001, doi:10.5194/acp-13-11987-2013, 2013.

Sogacheva, L., Saukkonen, L., Nilsson, E. D., Dal Maso, M., Schultz, D. M., De Leeuw, G. and Kulmala, M.: New aerosol particle formation in different synoptic situations at Hyytiälä, Southern Finland, Tellus, Ser. B Chem. Phys. Meteorol., 60(4), 485–494, doi:10.1111/j.1600-0889.2008.00364.x, 2008.

Spracklen, D. V., Bonn, B. and Carslaw, K. S.: Boreal forests, aerosols and the impacts on clouds and climate, Philos. Trans. R. Soc. A Math. Phys. Eng. Sci., 366(1885), 4613–4626, doi:10.1098/rsta.2008.0201, 2008.

Stopelli, E., Conen, F., Morris, C. E., Herrmann, E., Bukowiecki, N. and Alewell, C.: Ice nucleation active particles are efficiently removed by precipitating clouds, Sci. Rep., 5, 1–7, doi:10.1038/srep16433, 2015.

Stopelli, E., Conen, F., Morris, C. E., Herrmann, E., Henne, S., Steinbacher, M. and Alewell, C.: Predicting abundance and variability of ice nucleating particles in precipitation at the high-altitude observatory Jungfraujoch, Atmos. Chem. Phys., 16(13), 8341–8351, doi:10.5194/acp-16-8341-2016, 2016.

Stopelli, E., Conen, F., Guilbaud, C., Zopfi, J., Alewell, C. and Morris, C. E.: Ice nucleators, bacterial cells and Pseudomonas syringae in precipitation at Jungfraujoch, Biogeosciences, 14(5), 1189–1196, doi:10.5194/bg-14-1189-2017, 2017.

Tobo, Y., Prenni, A. J., Demott, P. J., Huffman, J. A., McCluskey, C. S., Tian, G., Pöhlker, C., Pöschl, U. and Kreidenweis, S. M.: Biological aerosol particles as a key determinant of ice nuclei populations in a forest ecosystem, J. Geophys. Res. Atmos., 118(17), 10100–10110, doi:10.1002/jgrd.50801, 2013.

Tobo, Y., Adachi, K., DeMott, P. J., Hill, T. C. J., Hamilton, D. S., Mahowald, N. M., Nagatsuka, N., Ohata, S., Uetake, J., Kondo, Y. and Koike, M.: Glacially sourced dust as a potentially significant source of ice nucleating particles, Nat. Geosci.,

12(April), 253–258, doi:10.1038/s41561-019-0314-x, 2019.

Tunved, P., Hansson, H. C., Kerminen, V. M., Ström, J., Dal Maso, M., Lihavainen, H., Viisanen, Y., Aalto, P. P., Komppula, M. and Kulmala, M.: High natural aerosol loading over boreal forests, Science (80-.)., 312(5771), 261–263, doi:10.1126/science.1123052, 2006.

Ullrich, R., Hoose, C., Möhler, O., Niemand, M., Wagner, R., Höhler, K., Hiranuma, N., Saathoff, H. and Leisner, T.: A new ice nucleation active site parameterization for desert dust and soot, J. Atmos. Sci., 74(3), 699–717, doi:10.1175/JAS-D-16-0074.1, 2017.

Vali, G.: Quantitative evaluation of experimental results on the heterogeneous freezing nucleation of supercooled liquids, J. Atmos. Sci., 28(3), 402–409, doi:10.1175/1520-0469(1971)028<0402:qeoera>2.0.co;2, 1971.

Vogel, F.: First field application of a mobile expansion chamber to measure ice nucleating particles, Karlsruhe Insitute of Technology, Karlsruhe, Germany, 2018.

Wex, H., Huang, L., Zhang, W., Hung, H., Traversi, R., Becagli, S., Sheesley, R. J., Moffett, C. E., Barrett, T. E., Bossi, R., Skov, H., Hünerbein, A., Lubitz, J., Löffler, M., Linke, O., Hartmann, M., Herenz, P. and Stratmann, F.: Annual variability of ice-nucleating particle concentrations at different Arctic locations, Atmos. Chem. Phys., 19(7), 5293–5311, doi:10.5194/acp-19-5293-2019, 2019.

Wiedensohler, A., Birmili, W., Nowak, A., Sonntag, A., Weinhold, K., Merkel, M., Wehner, B., Tuch, T., Pfeifer, S., Fiebig, M., Fjäraa, A. M., Asmi, E., Sellegri, K., Depuy, R., Venzac, H., Villani, P., Laj, P., Aalto, P., Ogren, J. A., Swietlicki, E., Williams, P., Roldin, P., Quincey, P., Hüglin, C., Fierz-Schmidhauser, R., Gysel, M., Weingartner, E., Riccobono, F., Santos, S., Grüning, C., Faloon, K., Beddows, D., Harrison, R., Monahan, C., Jennings, S. G., O'Dowd, C. D., Marinoni, A., Horn, H. G., Keck, L., Jiang, J., Scheckman, J., McMurry, P. H., Deng, Z., Zhao, C. S., Moerman, M., Henzing, B., De Leeuw, G., Löschau, G. and Bastian, S.: Mobility particle size spectrometers: Harmonization of technical standards and data structure to facilitate high quality long-term observations of atmospheric particle number size distributions, Atmos. Meas. Tech., 5(3), 657–685, doi:10.5194/amt-5-657-2012, 2012.

Wilson, E. B.: Probable inference, the law of succession, and statistical inference, J. Am. Stat. Assoc., 22(158), 209–212, doi:10.1080/01621459.1927.10502953, 1927.

Wilson, T. W., Ladino, L. A., Alpert, P. A., Breckels, M. N., Brooks, I. M., Browse, J., Burrows, S. M., Carslaw, K. S., Huffman, J. A., Judd, C., Kilthau, W. P., Mason, R. H., Mcfiggans, G., Miller, L. A., Nájera, J. J., Polishchuk, E., Rae, S., Schiller, C. L., Si, M., Vergara Temprado, J., Whale, T. F., Wong, J. P. S., Wurl, O., Yakobi-Hancock, J. D., Abbatt, J. P. D., Aller, J. Y., Bertram, A. K., Knopf, D. A. and Murray, B. J.: A marine biogenic source of atmospheric ice-nucleating particles, Nature, 525, 234–238, doi:10.1038/nature14986, 2015.

Wright, T. P., Hader, J. D., McMeeking, G. R. and Petters, M. D.: High relative humidity as a trigger for widespread release of ice nuclei, Aerosol Sci. Technol., 48(11), i–v, doi:10.1080/02786826.2014.968244, 2014.